

University of Warwick institutional repository: <http://go.warwick.ac.uk/wrap>

**A Thesis Submitted for the Degree of PhD at the University of Warwick**

<http://go.warwick.ac.uk/wrap/3627>

This thesis is made available online and is protected by original copyright.

Please scroll down to view the document itself.

Please refer to the repository record for this item for information to help you to cite it. Our policy information is available from the repository home page.

# **Gas-Assisted Compression Moulding of Glass Reinforced Polypropylene**

**By**

**Ian Brzeski**

A thesis submitted in partial fulfillment of the requirements for the

Degree of

Doctor of Philosophy in Engineering

University Of Warwick, School of Engineering

July 2009

# Acknowledgments

I am eternally grateful to my supervisor Dr Mark Pharaoh for the continuing support, guidance and teachings throughout the project, even through hard times. Thank you for acknowledging and believing in my potential all those years ago when I was still an undergraduate student. Thank you for bringing me into the family of the IARC materials group and allowing me to experience many happy times. I would like to extend my thanks to Professor Gordon Smith, Dr. Vannessa Goodship and Mr Neil Reynolds for your guidance and support throughout the project, without which, none of this would have been possible.

My thanks also go to the technician staff; Mr Graham Thacker, Mr Gary Arnett, Mr Carl Lobjoit. Thank you for your commitment and knowledge that was vital in many instances during this work.

Special thanks goes to my closest friends: Jess and Stoo, who at times have suffered but managed to keep my motivation up and enabled me to complete this work. They are friendships that will never end.

Thank you to my wonderful girlfriend, Amy, you have showed me continued support, understanding and love that has pushed me and kept my motivation high, right to the end of the thesis.

Most of all I would like to thank my mother and father. I will be forever grateful for all of the opportunities you have given me, and the unwavering support and unconditional love that has always seen me through every hurdle I have ever encountered.

To my brother Simon and his girlfriend Claire who have looked after me very well over the last few years, and have always been there whenever I have needed you.

This thesis is dedicated to my parents and family.

Ian

# Declaration

I declare that all the work described in this thesis was under taken by myself unless otherwise acknowledged in the text and that none of the work has previously been submitted for any academic degree. All sources of quoted information have been acknowledged by means of references.

Ian Brzeski

# Abstract

A new process of combining gas injection with compression moulding was developed and studied in this research work. The process is called Gas Assisted Compression Moulding (or GasComp). The principle is based on the injection of nitrogen gas during a conventional compression moulding cycle. The flow of the material due to the compressive force of the press is assisted by the injection of gas into the centre of the molten material. The gas assists in the flow by coring out the material, reducing the weight by up to 45 percent and increasing the dimensional stability of the component.

Novel glass matt thermoplastic mould tools were designed and developed during the course of the research program for use with the process. These designs were of a flash compression mould tool design with a horizontal clamping face, rather than the conventional positive plug compression mould tool with a vertical shear edge. This created a fixed volume mould tool, which when used in conjunction with a short shot of material, would allow the gas to flow the material to fill the remaining volume.

Several materials were investigated for their suitability with the process. Their characterisation showed that they contained different glass fibre contents and architectures. A material with a short, dispersed glass fibre content of 11 percent proved to consistently contain a significant gas cavity. The glass architecture proved to be the most significant contributing factor in the creation of a successful gas cavity.

The most significant processing parameter in the creation of a large volume cavity proved to be the gas injection delay time. The gas pressure and gas ramp time affected the cavity shape, length and extent of gas fingering.

The shrinkage was reduced in the presence of a gas cavity, along with the visible reduction of sink marks. The presence of other moulding features, such as hesitation marks, gas packing and the change in fibre orientation were also discussed.

# Abbreviations

• ABS	Acrylonitrile-butadiene-styrene
• CAD	Computer Aided Design
• CSM	Chopped Strand Mat
• ELV	End of Life Vehicle
• EU	European Union
• MFR	Melt Flow Rate
• GAIM	Gas Assisted Injection Moulding
• GasComp	Gas Assisted Compression Moulding
• GMT	Glass Mat Thermoplastic
• LFT	Long Fibre Thermoplastic
• PP	Polypropylene
• Re-GMT	Recycled Glass Mat Thermoplastic
• RTC	Rapid Temperature Cycling
• RWT	Residual Wall Thickness
• SGFRT	Short Glass Fibre Reinforced Thermoplastics
• $T_g$	Glass Transition Temperature
• $T_m$	Melting Temperature
• UK	United Kingdom
• UV	Ultra Violet
• XRD	X-Ray Diffraction

# Table of Contents

<b>Acknowledgments</b> .....	<b>ii</b>
<b>Declaration</b> .....	<b>iii</b>
<b>Abstract</b> .....	<b>iv</b>
<b>Abbreviations</b> .....	<b>v</b>
<b>List of Figures</b> .....	<b>x</b>
<b>List of Tables</b> .....	<b>xx</b>
<b>1. Introduction</b> .....	<b>1</b>
<b>1.1. Objectives and Aims</b> .....	<b>4</b>
<b>2. Polymers</b> .....	<b>5</b>
<b>2.1. Elastomers, Thermosets and Thermoplastics</b> .....	<b>7</b>
2.1.1. Molecular Structure .....	9
2.1.2. Glass Transition Temperature .....	11
2.1.3. Polymer Rheology .....	14
2.1.4. Polymer Additives, Fillers and Reinforcement .....	14
<b>2.2. Glass Reinforced Thermoplastic</b> .....	<b>18</b>
2.2.1. Glass Fibre .....	19
2.2.2. Glass Fibre Length .....	22
<b>2.3. Glass Reinforced Polypropylene</b> .....	<b>25</b>
<b>2.4. Glass Mat Thermoplastic</b> .....	<b>26</b>
2.4.1. Manufacture .....	26
2.4.2. Typical Moulding Process .....	31
2.4.3. Physical Properties .....	33
2.4.4. Industrial Applications .....	35
<b>2.5. Long Fibre Thermoplastic</b> .....	<b>36</b>
2.5.1. Manufacture .....	37
2.5.2. Industrial Applications .....	39
<b>2.6. Short Fibre Thermoplastics</b> .....	<b>39</b>
<b>2.7. Recycling Reinforced Polymers</b> .....	<b>40</b>
<b>2.8. Recycled GMT</b> .....	<b>42</b>
<b>2.9. Alternative Reinforced Polymers</b> .....	<b>42</b>

<b>3. Thermoplastic Processing .....</b>	<b>45</b>
<b>3.1. Injection Moulding .....</b>	<b>46</b>
3.1.1. Processing Cycle .....	47
3.1.2. Processing Parameters .....	49
3.1.3. Polymer Flow .....	53
3.1.4. Injection Moulding of Short Glass Fibre Reinforced Thermoplastics .....	57
3.1.5. Injection Moulding of Long Glass Fibre Reinforced Thermoplastics .....	58
<b>3.2. Gas Assisted Injection Moulding .....</b>	<b>60</b>
3.2.1. Gas Injection Stage .....	63
3.2.2. Gas and Polymer Interactions .....	63
3.2.3. Processing Parameters .....	66
3.2.4. Gas Assisted Injection Moulding Of Glass Reinforced Polymers.....	68
3.2.5. Alternatives to Gas Injection .....	69
<b>3.3. Compression Moulding .....</b>	<b>69</b>
3.3.1. Processing Cycle .....	71
3.3.2. Mould Tool.....	74
3.3.3. Glass Mat Thermoplastic Rheology .....	76
<b>4. Literature Review Summary.....</b>	<b>80</b>
<b>5. Methodology .....</b>	<b>81</b>
<b>5.1. Processing Cycle.....</b>	<b>83</b>
<b>5.2. Processing Parameters .....</b>	<b>86</b>
5.2.1. Material.....	87
5.2.2. Press/Mould Tool.....	87
5.2.3. Air Mould Gas Control .....	88
5.2.4. Additional.....	89
5.2.5. Uncontrollable Factors.....	89
<b>6. Investigated Materials .....</b>	<b>90</b>
<b>6.1. Introduction.....</b>	<b>90</b>
<b>6.2. GMT.....</b>	<b>90</b>
<b>6.3. LFT .....</b>	<b>91</b>
<b>6.4. Recycled – GMT .....</b>	<b>91</b>
<b>7. Material Characterisation .....</b>	<b>92</b>
<b>7.1. Material Burn Off.....</b>	<b>92</b>
7.1.1. Results.....	93
<b>7.2. XRD .....</b>	<b>94</b>
<b>7.3. Melt Mass-Flow Rate .....</b>	<b>95</b>
7.3.1. Design of Experiment .....	96

7.3.2.	Experimental Results.....	97
<b>7.4.</b>	<b>Twin Screw Rheometer .....</b>	<b>98</b>
7.4.1.	Design of Experiment .....	99
7.4.2.	Experimental Results.....	99
<b>8.</b>	<b>Project Mould Tool Design .....</b>	<b>100</b>
<b>8.1.</b>	<b>Rib Tool .....</b>	<b>100</b>
8.1.1.	Mould Tool Development.....	103
<b>8.2.</b>	<b>Star Tool .....</b>	<b>104</b>
<b>8.3.</b>	<b>Other Tools.....</b>	<b>105</b>
<b>8.4.</b>	<b>Gas Injection Pins.....</b>	<b>106</b>
8.4.1.	Rib Tool Pins .....	107
8.4.2.	Star Tool Pins .....	108
8.4.3.	Gas Seal.....	111
<b>9.</b>	<b>Moulded Part Characterisation .....</b>	<b>113</b>
<b>9.1.</b>	<b>Microscopy.....</b>	<b>114</b>
<b>9.2.</b>	<b>Indirect Cavity Measurement .....</b>	<b>114</b>
9.2.1.	Water Displacement .....	115
9.2.2.	CAD Model .....	117
9.2.3.	Direct Cavity Volume Water Measurement.....	119
<b>9.3.</b>	<b>Direct Cavity Measurement.....</b>	<b>120</b>
9.3.1.	Hall Effect Probe.....	121
9.3.2.	Digital Linear Vernier Callipers .....	121
<b>9.4.</b>	<b>Part Sectioning .....</b>	<b>122</b>
<b>10.</b>	<b>Effects of Process Parameters .....</b>	<b>124</b>
<b>10.1.</b>	<b>GMT Parameter Scoping Study .....</b>	<b>124</b>
10.1.1.	Results.....	126
10.1.2.	Discussions of GMT Parameter Scoping Study.....	129
<b>10.2.</b>	<b>Effects of Different Material .....</b>	<b>132</b>
10.2.1.	Cavity Structures Produced.....	132
10.2.2.	Discussions of the Effects of Different Material .....	137
<b>10.3.</b>	<b>Effect of Gas Injection Delay Time in Re-GMT .....</b>	<b>139</b>
10.3.1.	Process Parameters Used.....	140
10.3.2.	Results.....	141
10.3.3.	Gas Delay Time Discussion and Conclusions .....	145
<b>10.4.</b>	<b>Effect of Gas Ramp Time Variation with Re-GMT .....</b>	<b>146</b>
10.4.1.	Process Parameters Used.....	146
10.4.2.	Results.....	147
10.4.3.	Gas Ramp in Re-GMT Discussion and Conclusions .....	156

<b>11. Moulding Features.....</b>	<b>156</b>
11.1. Compression Flow of GMT .....	156
11.2. Compression Flow of Re-GMT.....	159
11.3. Re-GMT Flow Due to Gas Pressure.....	164
11.4. Gas Flow Mechanics .....	167
11.5. Hesitation Mark .....	173
11.6. Shrinkage .....	175
11.7. Weight Reduction .....	178
<b>12. Summary of Discussion Points .....</b>	<b>179</b>
12.1. GMT Parameter Scoping Study .....	179
12.2. Suitability of GMT, Re-GMT and LFT for GasComp .....	180
12.3. Effect of Processing Parameters on Re-GMT.....	181
12.4. Tool and Pin Design .....	182
12.5. Moulding Features .....	183
<b>13. Conclusions.....</b>	<b>185</b>
<b>14. Recommendations for Further Work.....</b>	<b>187</b>
<b>15. References .....</b>	<b>188</b>

# List of Figures

Figure 2.1 - Common polymer monomers and structure [4].....	6
Figure 2.2 – Four different polymer chain architectures [2] .....	8
Figure 2.3 - Polymer chain structure, containing crystalline and amorphous phases [2].....	11
Figure 2.4 - Temperature versus volume graph showing first order phase transition for crystalline materials (melting point (A)) and second-order phase transition for amorphous (glass transition point (B)) [7] .....	12
Figure 2.5 - Temperature versus volume graph of a semi-crystalline polymer exhibiting both a glass transition (B) and a melt temperature (A). Solid line denotes melting. Dashed line denotes cooling and the crystalline temperature at the sudden drop in volume. [7].....	13
Figure 2.6 - Fibre reinforced composite strength curve .....	18
Figure 2.7 - Woven fabric glass fibre architecture .....	21
Figure 2.8 - Unidirectional glass fibre architecture .....	21
Figure 2.9 - Random glass fibre architecture .....	22
Figure 2.10 - Manufacture of chopped strand mat (CSM) .....	27
Figure 2.11 - Manufacture of knitted random mat .....	28
Figure 2.12 - Melt impregnation GMT manufacture [9].....	29
Figure 2.13 - Fibre and additive dispersion in slurry deposition composite .....	30
Figure 2.14 - Slurry deposition GMT manufacturing [29].....	31

Figure 2.15 - GMT compression moulding cycle [9] .....	32
Figure 2.16 - Schematic of an automated compression moulding cycle [9] .....	32
Figure 2.17 - Processing GMT with moulding press stops .....	33
Figure 3.1 - Schematic of injection moulding machine (a) shows ram version (b) shows internal reciprocating and rotating screw version [53] .....	47
Figure 3.2 - Polymer flow in injection moulding [56] .....	48
Figure 3.3 - Polymer flow of filling stage by injection moulding [15] .....	54
Figure 3.4 - Drawings of Reynolds die experiments showing stable flow (a) and unstable flow (b,c) due to higher flow rates [63] .....	56
Figure 3.5 - Diagram showing fibre damming at a reduced cross section [9] .....	60
Figure 3.6 - Diagram showing the polymer injection (top), gas injection (middle) and packing stages (bottom) of GAIM [46] .....	62
Figure 3.7 - Growth of entrainment eddies in turbulent flow [64] .....	65
Figure 3.8 - Diagram of typical compression moulding cycle [9] .....	71
Figure 3.9 - Compression moulding tools, positive (a) semi positive (b) flash (c) [53] .....	75
Figure 3.10- Fountain flow and solidification of GMT during compression moulding [9] .....	77
Figure 3.11 - Fibre orientation distribution in compression moulding flow, where $\Psi$ is the fibre count [9] .....	79
Figure 5.1 - Mind map of project progression and methodology .....	82
Figure 5.2 - GasComp process cycle .....	84

Figure 5.3 – Illustration showing the heating of material and placing into open mould tool .....	84
Figure 5.4 - Illustration showing the compression moulding and gas injection stage of moulding process .....	85
Figure 5.5 - Illustration showing the removal of fully moulded part .....	85
Figure 5.6 - Example gas profile .....	86
Figure 7.1 - Photo of Re-GMT burn off.....	93
Figure 7.2 - Photo of LFT burn off .....	93
Figure 7.3 - Photo of GMT 30 percent glass burn off .....	94
Figure 7.4 – Photo of GMT 40 percent glass burn off .....	94
Figure 7.5 - Diagram showing configuration of the twin screw rehometer test rig .....	99
Figure 8.1 - Technical drawing of rib tool .....	102
Figure 8.2 - Photo of rib tool with its side removed, showing upper and lower halves of rib tool with moulded part inside.....	102
Figure 8.3 – Technical drawing with dimensions of part created by the rib tool .....	103
Figure 8.4 - Technical drawing of star tool .....	105
Figure 8.5 - Technical drawing of picture frame tool .....	106
Figure 8.6 - Technical drawing of spoke tool.....	106
Figure 8.7 - Design drawings of brass gas injection pins. A: Straight through B: Four way cross hole C: PTFE sheathed. Arrows denote gas direction.....	109
Figure 8.8 - Cross cut bolt gas injection pin .....	109

Figure 8.9 - Screw down pin and collar gas injection pin design.....	110
Figure 8.10 - Pin and sheath gas injection pin design and assembly.....	111
Figure 8.11 - Mould Seal.....	112
Figure 8.12 – Sectional view of pin assembly with gas seal.....	112
Figure 9.1 - Part orientation in water displacement measurement .....	116
Figure 9.2 - Drawing showing key part measurements .....	118
Figure 9.3- Diagram of cavity measuring points.....	122
Figure 9.4 - Illustrations showing the plane and position of the section cut, used in the analysis of the cavity.....	123
Figure 9.5 - Two halves of a sectioned part shown side by side .....	123
Figure 10.1 - Illustration showing the position of the unsymmetrical gas cavity in	
Figure 10.2.....	126
Figure 10.2 - Picture of unsymmetrical cavity position in GMT .....	127
Figure 10.3 – Photo showing rib tool GMT moulded with parameters 60 bar, 50°C tool temperature and 200°C oven temperature. It contains a smooth cavity and hesitation mark.....	128
Figure 10.4 - Photo of the end of a rib tool GMT moulded with 180 bar, 22°C tool temperature, 230°C oven temperature. It shows a burst hole, with sagged material and a fibrous cavity. ....	129
Figure 10.5 - Table showing the processing parameters of moulding discussed in section 10.2 Effects of Different Material.....	132
Figure 10.6 - Image of a Re-GMT moulding 1. Moulded at 120 bar gas pressure with a 1 second ramp rate and delay time of 1 second .....	133

Figure 10.7 - Image of the top flange of a Re-GMT moulding 1. Moulded at 120 bar gas pressure with a 1 second ramp rate and delay time of 1 second. ....	133
Figure 10.8 - Image of a Re-GMT moulding 2. Moulded at 120 bar gas pressure with a 1 second ramp rate and delay time of 1 second. ....	134
Figure 10.9 - Image of the top flange of a Re-GMT moulding 2. Moulded at 120 bar gas pressure with a 1 second ramp rate and delay time of 1 second. ....	134
Figure 10.10 - Image of a LFT moulding 1. Moulded at 120 bar gas pressure with a 1 second ramp rate and delay time of 1 second. ....	135
Figure 10.11 - Image of the top flange of a LFT moulding 1 – material breakthrough flow is shown at the end of the flange at the bottom of the picture. Moulded at 120 bar gas pressure with a 1 second ramp rate and delay time of 1 second. ....	135
Figure 10.12 - Image of a LFT moulding 2. Moulded at 120 bar gas pressure with a 1 second ramp rate and delay time of 1 second. ....	135
Figure 10.13 - Image of the top flange of a LFT moulding 2. Moulded at 120 bar gas pressure with a 1 second ramp rate and delay time of 1 second. ....	136
Figure 10.14 - Image of a GMT moulding 1. Moulded at 120 bar gas pressure with a 1 second ramp rate and delay time of 1 second. ....	136
Figure 10.15 - Image of top flange of a GMT moulding 1. Moulded at 120 bar gas pressure with a 1 second ramp rate and delay time of 1 second. ....	136
Figure 10.16 - Image of a GMT moulding 2. Moulded at 120 bar gas pressure with a 1 second ramp rate and delay time of 1 second. ....	137
Figure 10.17 - Image of top flange of a GMT Moulding 2. Moulded at 120 bar gas pressure with a 1 second ramp rate and delay time of 1 second. ....	137
Figure 10.18 - Experimental gas profiles with differing delay times.....	140

Figure 10.19 - Cavity volumes with respect to gas delay time of each or rib with an error of $\pm 0.3\text{mm}$ .....	141
Figure 10.20 – Picture of the cavities produced by a 0.5 second delay time.....	142
Figure 10.21 - Picture of the cavities produced by a 1.5 second delay time .....	143
Figure 10.22 - Picture of the cavities produced by a 2.5 second delay time .....	144
Figure 10.23 - Experimental gas ramp time profiles showing the time taken to reach the peak pressure .....	147
Figure 10.24 - Graph showing the peak gas pressure (bar) vs cavity length (mm), with respect to gas ramp time with an error of $\pm 0.1\text{mm}$ on all of the length measurements. ....	148
Figure 10.25 - Photo of moulding with gas profile, 60 bar over 1 second.....	148
Figure 10.26 - Photo of moulding with gas profile, 80 bar over 1 second.....	149
Figure 10.27 - Photo of moulding with gas profile, 60 bar over 5 seconds.....	149
Figure 10.28 - Photo of moulding with gas profile, 80 bar over 5 seconds.....	149
Figure 10.29 - Graph showing the peak gas pressure (bar) vs CAD cavity volume ( $\text{mm}^3$ ), with respect to gas ramp time. CAD Cavity volume has an error of $\pm 0.9\text{mm}$ . ....	150
Figure 10.30 - Graph Showing the gas cavity dimensions for mouldings with a peak gas pressure of 60 bar and ramp time of 1 second. The error for measurements is $\pm 0.1\text{mm}$ . ....	152
Figure 10.31 - Graph Showing the gas cavity dimensions for mouldings with a peak gas pressure of 60 bar and ramp time of 2 seconds. The error for measurements is $\pm 0.1\text{mm}$ . ....	152

Figure 10.32 - Graph Showing the gas cavity dimensions for mouldings with a peak gas pressure of 60 bar and ramp time of 3 seconds. The error for measurements is $\pm 0.1$ mm.....	153
Figure 10.33 - Graph Showing the gas cavity dimensions for mouldings with a peak gas pressure of 60 bar and ramp time of 5 seconds. The error for measurements is $\pm 0.1$ mm.....	153
Figure 10.34 - Graph Showing the gas cavity dimensions for mouldings with a peak gas pressure of 80 bar and ramp time of 1 second. The error for measurements is $\pm 0.1$ mm. ....	154
Figure 10.35 - Graph Showing the gas cavity dimensions for mouldings with a peak gas pressure of 80 bar and ramp time of 2 seconds. The error for measurements is $\pm 0.1$ mm.....	154
Figure 10.36 - Graph Showing the gas cavity dimensions for mouldings with a peak gas pressure of 80 bar and ramp time of 3 seconds. The error for measurements is $\pm 0.1$ mm.....	155
Figure 10.37 - Graph Showing the gas cavity dimensions for mouldings with a peak gas pressure of 80 bar and ramp time of 5 seconds. The error for measurements is $\pm 0.1$ mm.....	155
Figure 11.1 - A cold rib tool GMT moulding at 60 bar over 1 second, with oven temperature of 200°C.....	157
Figure 11.2 - Close up of GMT moulding showing frozen layers, shear layers and central flow layers through a GMT moulding.....	157
Figure 11.3 - Image of a cold rib tool GMT moulding, showing the frozen skin layer and polymer rich area in front of the gas cavity.....	158
Figure 11.4 - Image of a hot rib tool GMT moulding, showing the frozen skin layer and polymer rich area in front of the gas cavity.....	159

Figure 11.5 - Moulding showing section positions and edge of the blank and subsequent compression moulding flow .....	160
Figure 11.6 - Photo of section 9 with the examined section highlighted.....	160
Figure 11.7 - Photo of section 5 with the examined section highlighted.....	160
Figure 11.8 - Photo of section 1 with the examined section highlighted.....	161
Figure 11.9 – Micrograph showing glass orientation at end of top flange of section 9, small white dots denote glass fibre ends, larger white dots denote filler particulates. The flow path is towards the reader. ....	162
Figure 11.10 - Micrograph showing glass orientation at end of top flange of section 5, small white dots denote glass fibre ends, larger white dots denote filler particulates. The flow path is towards the reader. ....	163
Figure 11.11 - Micrograph showing glass orientation at end of top flange of section 1, small white dots glass fibre ends, white lines denote glass fibres rotated to perpendicular to rib direction, larger white dots denote filler particulates. The flow path is towards the reader.....	163
Figure 11.12- Image of slice 13 and the positions of the examined sections .....	164
Figure 11.13 - Micrograph of cavity formation around the rib.....	164
Figure 11.14 - Micrograph of gas cavity beginning to finger up the sidewall.....	165
Figure 11.15 - Photos of sections 1-17 showing cavity shape progression in a rib moulding moulded with 60 bar peak pressure over 1 second .....	166
Figure 11.16 - Image showing top side of a Re-GMT star tool moulding, processed with 100 bar over 0.1 second with a delay time of 0.5 seconds, showing the various stages of material flow and blank position.....	168

Figure 11.17 - Image showing rib side of Re-GMT moulding, processed with 100 bar over 0.1 second with a delay time of 0.5 seconds, showing blank placement effect on material flow .....	169
Figure 11.18 - Radial flow pattern due to gas injection, processed with 100 bar over 4 second with a delay time of 0.5 seconds, showing the progressive flow phases during the moulding cycle .....	170
Figure 11.19 - Image of a Re-GMT rib tool moulding, processed with a peak gas pressure of 120 bar over 1 second ramp rate .....	171
Figure 11.20 - Image of top flange of a Re-GMT Moulding 2 processed with a peak gas pressure of 120 bar over 1 second ramp rate .....	171
Figure 11.21 - Close up of gas flow features; polymer breakthrough and entrainment .....	172
Figure 11.22 - Photo showing symmetrical gas flow in a rib tool moulding .....	173
Figure 11.23 - Image showing packing effect on symmetrical gas flow.....	173
Figure 11.24 - Micrograph showing that no features are present between the upper and lower hesitation marks present on the surface, through the thickness of the top flange. ....	174
Figure 11.25 - Gas cavity length vs part length graph, with a 'no gas length line', denoted by thick red line. Part length tends to increase as cavity length increases denoted by dashed arrow. The error for Gas cavity length and Part length is +- 0.1mm. ....	176
Figure 11.26 - Graph showing the gas cavity length vs part length in mouldings processed with a peak pressure of 80 bar over 1 second ramp time. The error for Gas cavity length and Part length is +-0.1mm.....	177
Figure 11.27 – A sectioned CAD model of Re-GMT star part with a mass of 274g	178

Figure 12.1 - Moulding produced with 60 bar over 1 seconds with a delay time of 1 second .....	182
Figure 12.2- Moulding produced with 80 bar over 1 seconds with a delay time of 1 second .....	182
Figure 12.3- Moulding produced with 60 bar over 5 seconds with a delay time of 1 second .....	182
Figure 12.4 - Moulding produced with 80 bar over 5 seconds with a delay time of 1 second .....	182
Figure 12.5 – Biaxial material flow due to gas pressure .....	184

# List of Tables

Table 2.1 - Fibre reinforcement and properties [14] .....	17
Table 2.2 - Fibre length classification encompassing injection moulding and compression moulding [20] .....	23
Table 2.3 - Physical properties of unfilled, 23 percent glass and 40 percent glass filled polypropylene .....	34
Table 6.1 - Materials glass weight percentage, fibre length, supplied form and manufacturing method .....	90
Table 7.1 - XRD results showing filler percentages.....	95
Table 7.2 - MFR Results .....	98
Table 9.1 - Comparison between, shot volume, CAD model volume and water displacement volume measurements for a full moulding.....	119
Table 10.1 - Taguchi scoping experiment .....	125
Table 10.2 - Taguchi array and experimental plan .....	125
Table 10.3 - Table showing process parameters with changing delay time .....	140
Table 10.4 - Wall thickness and cavity length dimensions of 0.5 secs delay moulding .....	142
Table 10.5 - Wall thickness and cavity length dimensions of 1.5 secs delay moulding .....	143
Table 10.6 - Wall thickness and cavity length dimensions of 2.5 secs delay moulding .....	144
Table 10.7 - Summary of moulding data .....	144

Table 10.8 - Study processing parameters, with varying ramp time and peak pressure ..... 146

Table 10.9 - Table showing the cavity dimensions and the standard deviation of the cavity height, width and overall area at each sampling point ..... 151

# 1. Introduction

Gas Assisted Injection Moulding (GAIM) has been extensively developed since its inception in 1975 by Friedrich Ernst Dipling. Developments such as reverse GAIM cryogenic GAIM, water assisted injection moulding, have shown the worth of coring out a component to reduce weight and the associated processing benefits. In contrast, compression moulding has not developed to the same extent, with clamping systems and automation being some of the biggest developments. The basic process however has not changed in hundreds of years. This research combines elements from both of these polymer processes to create a novel polymer process, used to core out an internal cavity in a glass fibre reinforced thermoplastic component. This process is called Gas Assisted Compression Moulding (GasComp).

Glass filled polymers are structural materials with the ability to be moulded at high production speeds and volumes. Non-reinforced or short fibre reinforced polymers are easily processed using GAIM. Whilst long or continuous fibre polymer composites provide increased strength and stiffness over short fibre polymer composites, they cannot be processed by GAIM, due to the change in fibre length. The wide spread used of polypropylene in industry, low cost and the ease with which it can be compounded with glass fibres of differing lengths, made glass reinforced polypropylene an ideal material for use with GasComp.

The GasComp process looks to combine the benefits of GAIM such as reduced mass, cycle time and part dimensional distortion, with the high production volumes of complex shapes, in long or continuous fibre composites of compression moulding.

This allows the manufacture of structural parts with a reduced mass and material costs and cycle time over a fully solid part. It does this by using the glass fibre processing capability of compression moulding, with the gas assisted stage of GAIM. This gives the potential of producing parts such as load floors, front automotive bumpers or any applications that require good energy absorption with minimal mass. The research will establish some of the potential and limitations of this innovative and novel process which has shown to have potential in real life applications.

A GasComp process cycle involves heating a mass of pre-measured material to its melting point and holding until the material has fully relaxed and is molten. The process uses a short shot technique as used in GAIM, where only 80-90 per cent of a full part, is placed in the mould tool. The molten material is transferred to a mould tool and formed into the desired shape. Instantaneously after the mould tool has fully closed, the gas pressure control module begins the gas injection stage. The gas is delivered to the centre of the molten material via an integral pin in the top half of the mould tool. A gas control unit continually adjusts the gas pressure to reach a preset pressure by a preset time, according to a user set gas profile. The gas is used to further advance the flow of material and create a full part with a cored out centre. The full process cycle is explained in detail, including schematics, in section 5.1

Processing Cycle.

This thesis will set out the research carried out to establish the potential and limitations of the GasComp process, along with investigating how the processing parameters affected the outcome in moulding glass reinforced polypropylene components. It will also determine the boundary parameters for each of the

investigated materials. The interaction between the gas flow and the polymer and glass fibres will be also discussed.

The thesis will follow the following structure:

- Chapters 2 and 3 will review and show the current knowledge and understanding of polymers and polymer composites and how they are currently processed in industry.
- Chapter 4 will highlight the most important findings from the first two chapters.
- Chapters 5 will set out how the process works and the factors that were investigated.
- Chapters 6, 7, 8 and 9 go through the materials and equipment specific to this research and the techniques used to analyse the parts produced in the experiments.
- Chapter 10 sets out and discusses the results and findings of each of the effects of significant processing parameters established during the experimental stage.
- Chapter 11 outlines the main moulding features and effects observed in the research that were not a direct result of the processing parameters discussed in chapter 9.
- Chapter 12 summarises all of the findings of the research and the recommendations of processing parameters and material selection for an ideal moulded component.
- Chapters 13 and 14 conclude the main points of the research and further recommended research for the development and learning of GasComp.

## 1.1. Objectives and Aims

The objectives of this research project are summarised as the following:

- To establish if the gas assisted compression moulding of glass reinforced polypropylene is feasible
- To determine the optimal design for a mould tool for use with the process
- To establish the effects of processing parameters on the ability of the gas to core out glass reinforced materials
- To establish the effect of the glass content and glass architecture on the ability of the gas to core out the material
- To study the flow of the material and gas due to the process
- To investigate the weight reduction and dimensional stability produced by the process

## 2. Polymers

The word polymer is derived from the latin for many (poly) and unit (mer), where the “mer” is the building block of the material - known as a monomer. These monomers are physically linked or molecularly cross-linked together to create the polymer. The most widely used monomers are extracted from crude oil by using high temperatures and pressures to thermally crack the oil. The use of a catalyst allows the process to take place at a low temperature and pressure. The process breaks down long chain hydrocarbons into a multitude of smaller hydrocarbons including methane, ethane, propylene, butadiene and aromatic hydrocarbons. These units can then be linked together or broken down further to create other types of useful building blocks. A process called polymerisation [1] links many monomers (Figure ) together to make a polymer chain .Polymers with a chain of a single type of repeated unit, are known as homopolymers [1, 2]. Polymer chains can however contain two or more different units, bonded together into long chains during polymerisation to create new and useful co-polymers. For example, a polymer consisting of chains entirely of ethylene molecules linked together is a polyethylene homopolymer. The polymer chains are of random length, but do fall within a distribution curve for that process and polymer. The average length of these chains defines the molecular weight of the polymer, which can be used to characterise it as the chain length has a large effect on the physical properties of the polymer such as density, tensile strength and impact resistance. This is due to the increased interaction and entangling of the polymer chains [2, 3] and will be discussed later in the thesis.

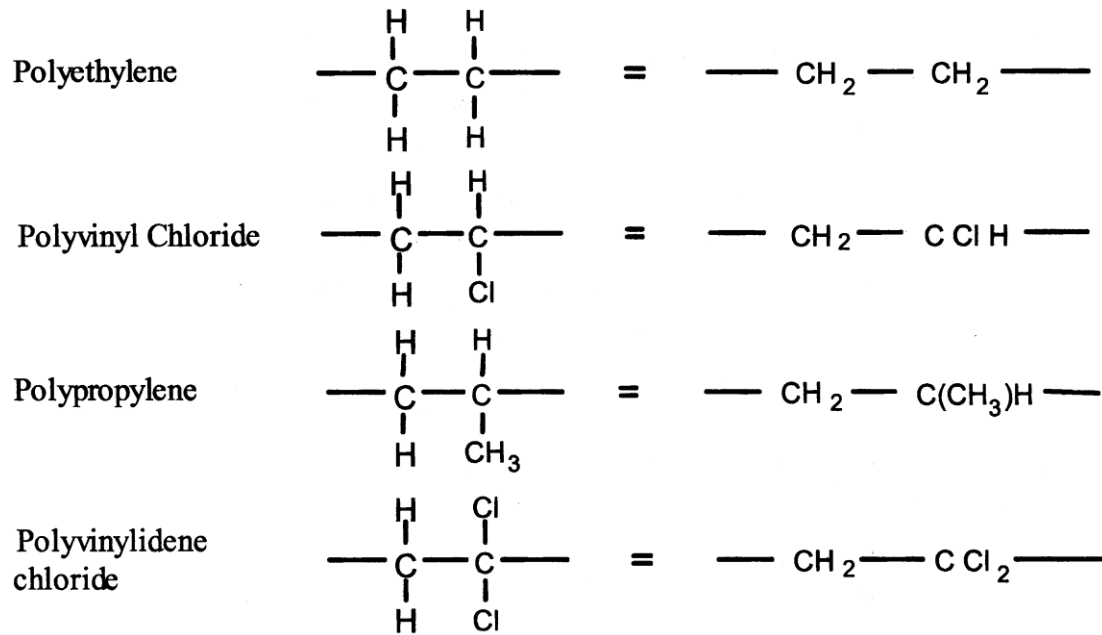


**Figure 2.1 - Common polymer monomers and structure [4]**

Monomers may be synthetic or organic, with the synthetic being the most developed and widely used. The first synthetic, thermosetting polymer was invented by L.H Baekeland in 1906 and was called Bakelite. Since then polymers have become a very important part of everyday life. They are used in a number of industrial sectors, especially in packaging, but also increasingly in structural applications. All polymers exhibit the following common properties [2]:

- Corrosion and chemical resistance
- Low thermal and electrical conductivity
- Ease of manufacture
- Low density
- High specific strength (strength to weight ratio)
- Relatively low cost

## 2.1. Elastomers, Thermosets and Thermoplastics

Polymers can be classed into three categories, determined by their polymeric structure: elastomers, thermosets and thermoplastics.

Elastomers are polymers with highly intertwined and twisted polymer molecules. These chains can be vulcanised which creates physical, three-dimensional, cross-linking bonds between chains. The cross linking however is not on a large-scale as shown in Figure 2.2 (C) taken from Kalpakjian's book "*Manufacturing Engineering and Technology*" [2]. Elastomers have the ability to deform under load but can return to their original shape over a period once the load has been removed. Elastomers are however outside the scope of this research and will not be discussed further.

Thermosets are polymers that create a network of very strong, permanent, cross-linking chemical bonds (Figure 2.2 (d)), that once fully cured cannot be returned to a molten state. The network is more widely spaced and wide spread than locally cross-linking molecules, giving greater strength and stiffness. The most common and well know thermoset is epoxy resin, with a trade name of Araldite. Thermosets are mainly used in high-end performance applications due to the very high specific strength and stiffness and relatively high cost. Other types of thermosetting polymers are polyester, polyvinyl, polyphenolics and polyimides [2]. They each have specific properties such as high toughness, stiffness or chemical resistance that allow them to be used in specific areas. Thermosets are however outside of the scope of this research and will not be discussed further.

Thermoplastic polymers can consist of linear, branched or partially cross-linked chains (Figure 2.2 (a,b,c)), each of which have different interactions with each other giving different physical properties to the polymer. When the polymer is in a relaxed state, there are primary and secondary forces between the molecules. Primary bonds are the chemical links between the atoms themselves. Secondary bonds are non-physical, low force bonds, such as a van der Waals interactions, which are the attraction of two closely spaced molecular objects [2, 5].

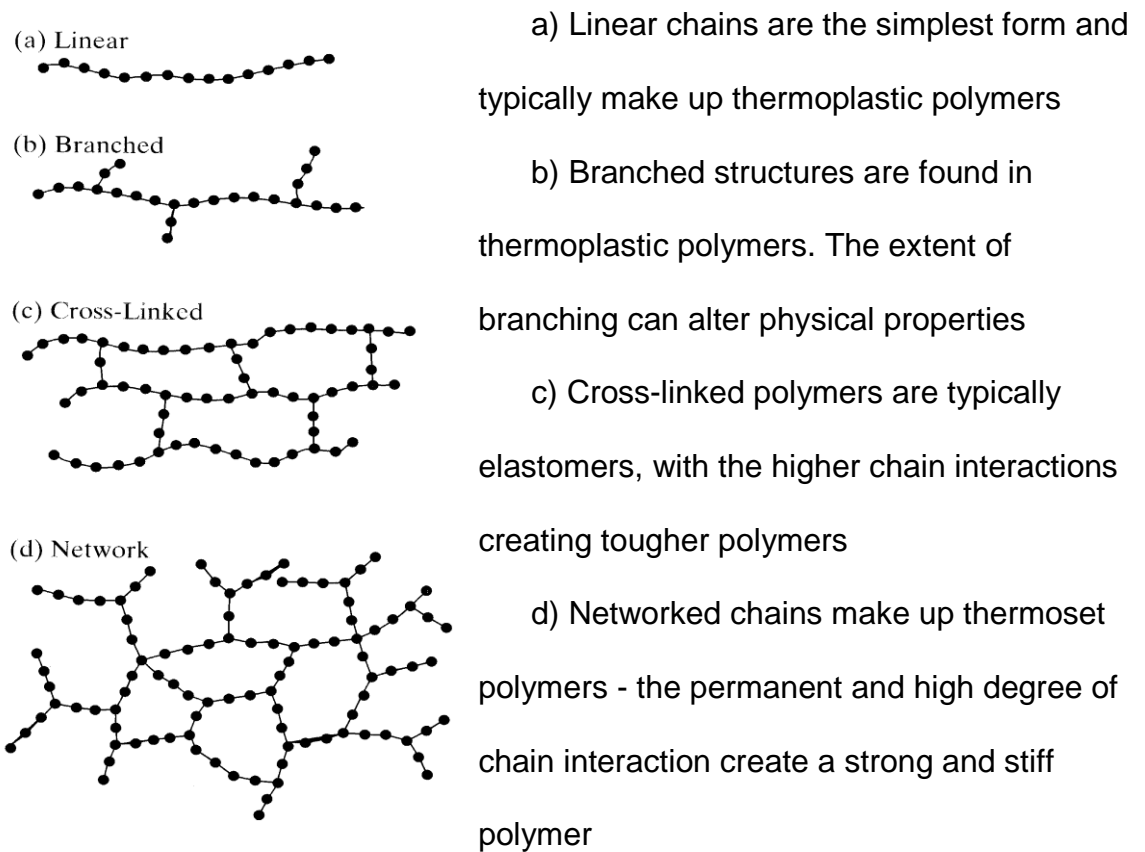


**Figure 2.2 – Four different polymer chain architectures [2]**

When a polymer with linear or branched chains is pulled in a tensile test, the chains begin to straighten and align to the direction of the force, up to a certain point. This point is the point at which the chains can no longer slide or untangle. Linear polymer

chains such as those in polyethylene are in a tangle but can slide easily past each other. A popular analogy of these linear chains is they are like a bowl of spaghetti, which can slide easily around each other but can still loop around each other. A more accurate analogy is to think of the polymer as a pit of snakes in order to incorporate the polymers behaviour with differing temperatures, as snakes are dormant at low temperatures but are active and likely to move at warmer temperatures. Branched chains are akin to a stack of tree branches where smaller branches and leaves jut out from the main branch making them difficult to move past each other, however, there is a large amount of space between them.

There are many types of thermoplastics, some examples are [2]:

- Acrylonitrile-butadiene-styrene (ABS)
- Polyethylene (PE)
- Polystyrene (PS)
- Poly Vinyl Chloride (PVC)
- Polycarbonate (PC)
- Polypropylene (PP)
- Polyamide (PA, Nylon)

### 2.1.1. Molecular Structure

When polymer chains are created, they naturally relax and form together into a preferred structure that is determined by the structure of the chains themselves.

There are several forms that the polymer can contain, a random amorphous structure, a crystalline structure or varying degrees of both (Figure 2.3). Amorphous

regions contain regions of randomly aligned chains, containing no long-range order. Crystalline regions contain long, structured, aligned chains, like a coil of rope. The crystalline alignment is vastly different from the amorphous regions and gives increased stiffness, density and hardness. The degree of change in properties is determined by the level of crystallinity; the higher the crystallinity, the greater the increase in strength and stiffness [2, 6].

Polymers with linear chains will more readily form organized and structured formation, as they do not have polymer molecular chains branching off the main chain; this can stop the chains from packing close to each other.

Through manipulation of the process of creating the polymer molecules, the extent of branching can be controlled which has a direct result on the extent of crystallinity. For example, the polymer molecules of PE can be altered to increase or decrease the amount of branching and therefore extent of crystallinity. With minimised branching, the percentage of crystallinity of PE can be increased to 80-95 percent to create high-density polyethylene (HDPE), giving a polymer that is stiffer, stronger, tougher and less ductile. Low-density polyethylene (LDPE), has a crystallinity of 60-70 percent and is lightweight, flexible and easily mouldable whilst still exhibiting similar base properties such as excellent chemical and water resistance [2].

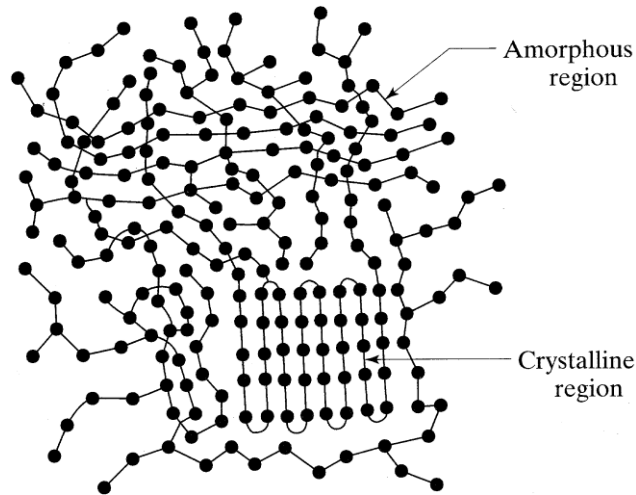
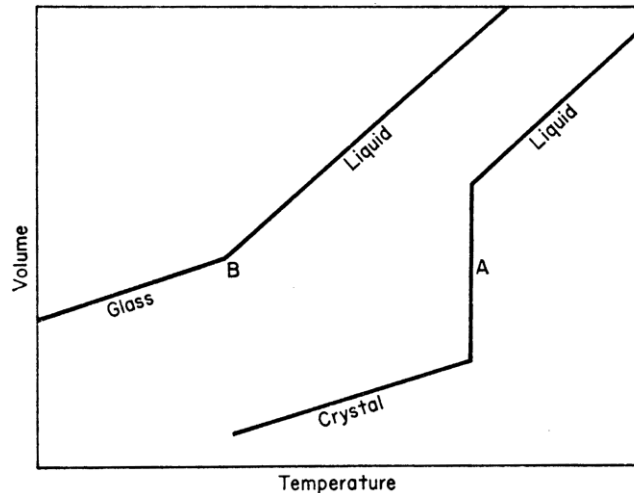


Figure 2.3 - Polymer chain structure, containing crystalline and amorphous phases [2]

### 2.1.2. Glass Transition Temperature

All fully crystalline polymers have a certain and definite temperature at which the ordered structure collapses causing the polymer to melt ( $T_m$ ) (Figure 2.4 point A). It is noted that the crystalline polymer has a first-order phase change, where heat energy is added to the polymer but there is no temperature increase, until all of the crystalline structure has broken down.

Most crystalline polymers contain some degree of amorphous regions. Amorphous polymers do not have a specific melting temperature but rather a narrow temperature range known as the glass transition temperature ( $T_g$ ). During this narrow range, the randomly arranged chains begin to move and slide past each other causing a gradual change in modulus, as well as an increase in volume. This relaxation takes place in a second order phase change, where the temperature continues to rise with heat energy but at a different rate due to a change in heat capacity [6] (Figure 2.4 (B)).



**Figure 2.4 - Temperature versus volume graph showing first order phase transition for crystalline materials (melting point (A)) and second-order phase transition for amorphous (glass transition point (B)) [7]**

As the polymer cools, both fully crystalline and amorphous polymers contract at the same rate as their respective expansion rates, however, semi crystalline polymers do not. The cooling time is critical to the structure and extent of crystallisation, the longer the cooling time the chains have sufficient time to organise into their lowest energy state and hence the most efficient packing formation. If the polymer is cooled quickly then these ordered structures do not have the necessary time to form and can be frozen in their disorganised, spacious state [1].

When the temperature of an amorphous polymer is well below  $T_g$  (Figure 2.4 point B) the polymer is rigid, brittle and hard, but as the polymer approaches the  $T_g$  the polymer becomes soft and pliable, continuously softening until it becomes molten well above the  $T_g$ . As previously mentioned, the chains are likened to a pit of snakes, which are cold blooded and need to be warm to move. If an object were forced through the pit below the  $T_g$ , the snakes would act as a single mass, as they would not have the necessary heat energy to move out of the way. Therefore, the object

either would be stopped by the large mass of snakes or would force its way through them, causing damage. However, once the snakes have warmed up they would be able to move out of the way without being hurt. The snakes would then fall back into their original shape once the object was removed [1].

Semi crystalline polymers like polypropylene (PP) contain both crystalline and amorphous regions and so exhibit both temperature gradients. The amorphous regions begin to move and separate, continuing to soften as the temperature goes through the  $T_g$  (Figure 2.5 (B)). As the crystalline regions begin to melt, the amorphous regions are released from the constraints of the crystalline regions and continue to expand (Figure 2.5 (A)). Once all of the crystalline regions have melted the polymer turns to liquid.

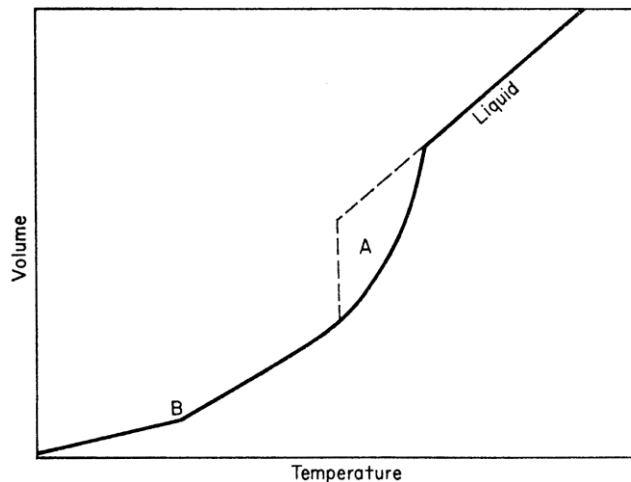


**Figure 2.5 - Temperature versus volume graph of a semi-crystalline polymer exhibiting both a glass transition (B) and a melt temperature (A). Solid line denotes melting. Dashed line denotes cooling and the crystalline temperature at the sudden drop in volume. [7]**

Whether the polymer is crystalline, semi crystalline or amorphous, dictates the heating and cooling cycle used in polymer processing such as injection moulding and

compression moulding. As the polymer cools, it contracts, which in industry is known as shrinkage. This shrinkage, if not properly understood, could cause serious problems with distorted or undersized parts. The cooling rate and characteristics of the process and polymer have a large influence on the shrinkage.

### 2.1.3. Polymer Rheology

Once molten, polymers are predominantly shear thinning non-Newtonian fluids, in that the viscosity decreases as the shear rate increases. However R. Törnqvist, *et al*, discovered that polymers initially act as Newtonian fluids until the shear rate exceeds  $10\text{sec}^{-1}$  after which they exhibit shear thinning properties [8]. This initial phase of Newtonian flow is known as the “Zero Strain Rate Viscosity”, which is the viscosity at very low or no strain rate and is directly linked to the molecular weight of the polymer. Painter and Coleman [1] reported that the greater the molecular weight the greater the Zero Strain Rate Viscosity, as well as affecting the viscosity at higher shear rates. Fillers and additives can also be used to improve the flow and stability (rheology) of the polymer.

### 2.1.4. Polymer Additives, Fillers and Reinforcement

Polymers are rarely used in their pure form, as the polymers do not always have the desired physical properties. Nevertheless, by starting with a polymer that possesses most of the required properties, the characteristics can be easily modified by mixing with certain chemical compounds or reinforcing fibres, to enhance their physical properties. The name “plastic” describes the combination of polymer and any additives and fillers [9], but is typically used interchangeably with the term “polymer”.

According to B. Pukánszky [10], the original aim for these fillers was to bulk out the material, typically accounting for between 30 percent and 70 percent by weight of the final compound, making it cheaper as less of the expensive raw material would be used for the same volume of mixed material [10]. However, these additives were found to enhance the polymers stiffness, heat deflection, fire retardancy, mechanical properties and also reduce cycle times and mould shrinkage. Nevertheless, their main purpose remains to bulk out the material and reduce cost [9]. These filled polymers greatly increased the scope of applications in which polymers could be used and at the “*High Performance Conference 2005*” in Cologne, Germany, Professor Roger Rother “*estimated that about 15 million tonnes of mineral fillers are used in all polymer types worldwide*” [11]. The most common additives used with polypropylene are talc, calcium carbonate ( $\text{CaCO}_3$ ) and glass fibres. The largest overall contributor was carbon black at 2.7 million tonnes annually, which along with silica, are predominantly used as reinforcement in elastomers to increase tensile and tear strength [3]. A large usage for carbon black is to increase wear resistance in tyres so that they last longer on the road. The second largest contributor was calcium carbonate, at 2.3 million tonnes annually, which was originally used a filler to bulk out the material. However B. Pukánszky [10] further commented that Fujiyama and Wakino [12] have proved that by changing the particle size,  $\text{CaCO}_3$  can have a very strong nucleation effect. The nucleation effect causes the onset of crystallisation in the polymer, giving increased physical properties, such as flexural modulus by increasing the proportion of crystalline to amorphous regions. These findings have led to further studies which have found that changes to the particle size, surface

area, surface treatment, shape and the weight percentage used, all have an effect on the polymer's physical properties [13].

Another widely used filler is talc, which is generally accepted to be a nucleation agent. In 1987, talc was the primary filler contained in particulate filled polypropylene [10]. Talc and  $\text{CaCO}_3$  however do not significantly increase the tensile strength, impact strength or toughness. To provide reinforcement it is necessary to use a filler (such as a fibre) which has a larger aspect ratio.

The purpose of fibres is to act as a reinforcement, greatly increasing the strength and stiffness of the polymer since the reinforcement fibres have a far higher stiffness and strength compared to the polymer. When they are combined with a polymer, the fibre allows the polymer to transfer the force more effectively through the material [9]. The effectiveness of the bonding between the polymer and the reinforcement is important for the transference of the force from the polymer to the fibre and hence the performance of the composite. This bond is affected by the degree of wetting out of the reinforcement by the polymer, which is the degree of surface coverage by the polymer on the reinforcement. The perfect composite will always have a complete wet out, where all of the reinforcement will be completely encompassed by polymer. Insufficient adhesion between the polymer and reinforcement can cause stress concentrations around the fibre, causing the polymer around the fibre to fail rather than the fibre itself and consequently, the fibre is cleanly pulled out of the polymer. This failure is called fibre pull out [14]. Additionally, an unbounded area of the reinforcement could allow chemicals to reach and corrode the reinforcement. To prevent chemical attack and allow a good transference of force to the fibre, a

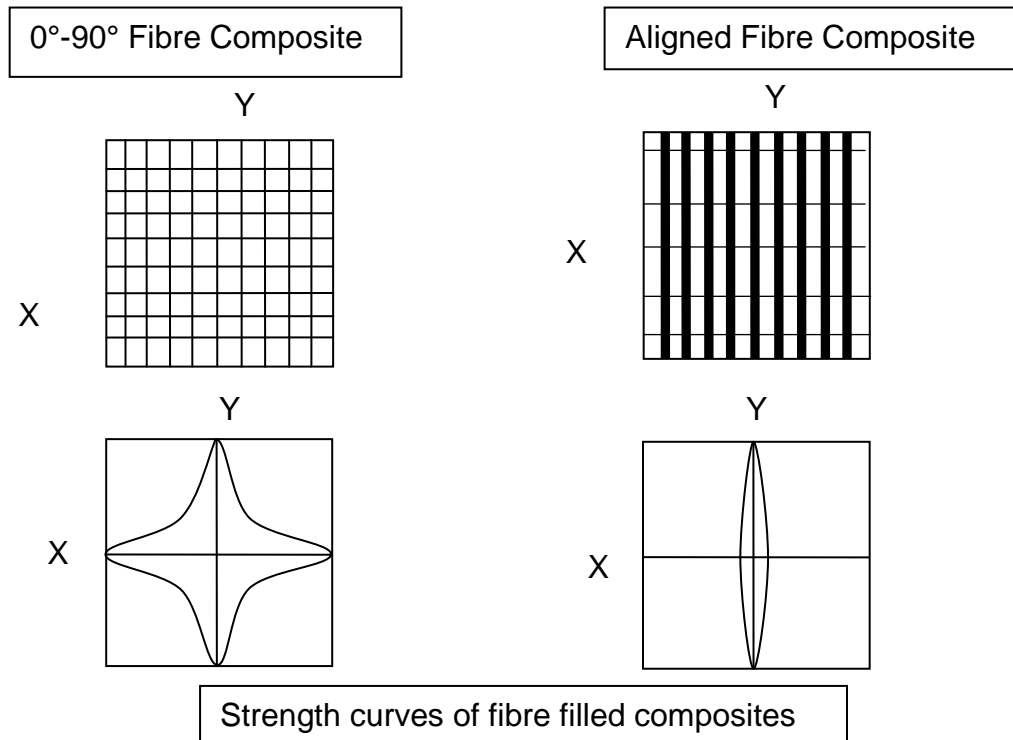
coupling agent or sizing is needed as most polymer systems do not bond well to synthetic reinforcement. The sizing has the ability to bond to both the reinforcement and the polymer giving a strong molecular bond between them [14, 15].

Table 2.1 compares four of the most commonly used fibre reinforcements used in industry, with glass being the most common and boron being the least. Carbon is used extensively in aerospace and motor sport due to its very high specific stiffness.

Fibre reinforcement type		Tensile Strength (MPa)	Elastic Modulus (GPa)	Density (kg/m <sup>3</sup> )	Relative cost
Boron		3500	380	2600	Highest
Carbon	High Strength	3000	275	1900	Low
	High Modulus	2000	415	1900	Low
Glass	E Type	3500	73	2480	Lowest
	S Type	4600	85	2540	Lowest
Kevlar	29	2800	62	1440	High
	49	2800	117	1440	High

**Table 2.1 - Fibre reinforcement and properties [14]**

Fibres are most effective when the fibres are aligned to the direction of the force creating an anisotropic composite material [16, 17]. The composite material needs to be designed with a good knowledge of the force direction and magnitude so that the part can be properly designed [18, 19]. As Figure 2.6 shows, the strength drops off significantly, as the force direction moves off axis to the fibre; the strength then comes from the polymer matrix, which has substantially lower strength and stiffness than the fibre. The manufacturing process significantly affects the orientation and length of the glass fibres and so has to be taken into account at the design process.



**Figure 2.6 - Fibre reinforced composite strength curve**

Glass fibres are the most common reinforcement fibre due to the low cost and ease of manufacture, along with the good specific strength. For this reason, glass fibres will be investigated in greater detail, all other fibres are out of the scope of this research.

## 2.2. Glass Reinforced Thermoplastic

Glass Reinforced Polymers (GRP) is a large group of composite materials that encompasses thermoset and thermoplastic polymers, consisting of a matrix, which is the resin or polymer and the reinforcement which, in this group, is glass fibre. They are increasingly being used in many industries due to their high specific strength as well as other physical properties. There are a very wide range of options available,

allowing the GRP to be tailored to the exact specifications required by means of matrix, fillers, additives, colourants and fibres. Reinforcement fibres can be between 0 percent and 70 percent by weight of the composite. However, as thermoset polymers are outside the scope of this research, only glass reinforced thermoplastics will be discussed further.

Glass reinforced thermoplastics can be manufactured in a sheet or powder/pellet/granule form by extrusion or other forming techniques such as melt impregnation and slurry deposition and will be discussed at a later stage.

### 2.2.1. Glass Fibre

Three types of glass fibre are manufactured with different chemical compositions. These give different properties but with slightly varying cost. The three types are:

- E-Glass - calcium aluminoborosilicate - the cheapest and most widely used glass fibre.
- S-Glass - magnesia-aluminosilicate – a higher strength and stiffness at a higher cost.
- E-CR Glass – specifically manufactured to have increased acid and alkali resistance.

Glass fibres can come in different formats, two of which are:

- Rovings – strands of 1000 filaments bundled into a continuous length.

- Chopped strands – rovings that have been chopped into a certain size specific to that application.

These formats can be combined directly with a raw polymer, or can be processed further into mats or fabrics that can then be combined with a polymer, to create a glass reinforced composite. Three types of glass mat architecture are:

- Woven – continuous rovings are woven into a desired pattern to create a fabric, typically used with thermoset polymers.
- Unidirectional – typically continuous strands are aligned in a single direction, some strands may be off alignment either incidentally through processing or purposely to give off axis strength or to keep the majority of fibres aligned.
- Random – can be continuous rovings, but are typically chopped strands that are placed in random orientations.

Woven mats can come in a very structured, continuous fabric with a range of different fibres and weaves. (Figure 2.7). Each fibre and weave has an advantage in a particular area and so can be tailored to a specific application. The fibres are generally 0-90° to the direction of the fabric but can be +/- 45° to the fabric. The weave direction depends on the anticipated load direction, as +/- 45° weaves are good for torsional rigidity in circular parts.

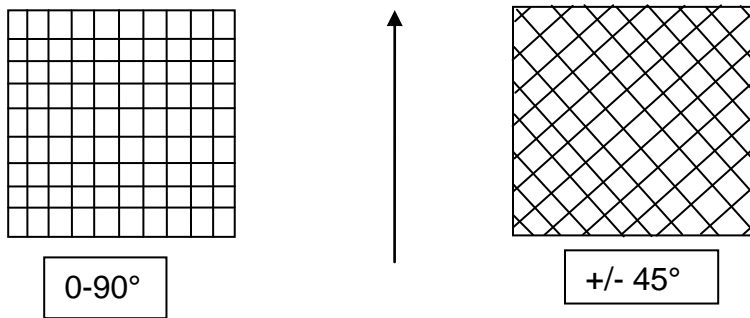
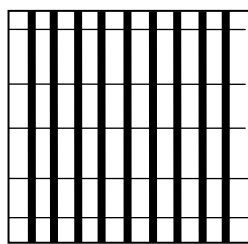
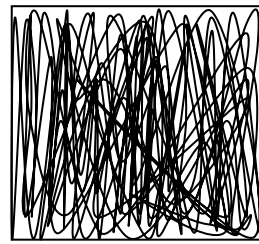


**Figure 2.7 - Woven fabric glass fibre architecture**

Unidirectional glass mats have all or a large majority of the fibres aligned in one direction (Figure 2.8). This can either be a knitted fabric, where small bundles of fibres are used to hold the main fibres in place, or part of a thermoplastic composite sheet. The greatest advantage that unidirectional fibres give over woven and random mats is that it is the most efficient way of withstanding large forces whilst keeping the weight to a minimum. Since unidirectional glass filled materials have a good specific strength in the direction of the fibres it is essential to understand where the forces are being applied.



Unidirectional Fabric



Pseudo aligned extruded mat

**Figure 2.8 - Unidirectional glass fibre architecture**

Random mats contain discontinuous glass fibres, with little or no directionality (Figure 2.9). They can however be needled so that it forms a 3D fabric with some glass fibres running in the Z-plane. The random placement and alignment, gives the composite

an isotropic property. Although the strength of the mat is not as high as woven or unidirectional mats the ability to carry loads in any direction, make it favourable to strengthen a polymer where low forces could be applied at random. Applications such as car door handles or shielding panels are particular examples where the glass mat is there to improve the mechanical properties of the polymer, rather than be the main constituent of the material.

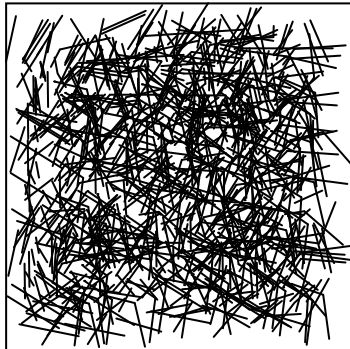


**Figure 2.9 - Random glass fibre architecture**

### 2.2.2. Glass Fibre Length

The glass lengths in GRPs can vary greatly, from 0.1mm to continuous fibre lengths that run the length of the part, but are classed as short, long and continuous (Table 2.2) The classification of short and long fibres does however vary with the process. Due to the mould tool geometry and high shear rates of injection moulding, fibre lengths greater than 25mm are rare. For this reason, long fibres are generally classed between 1mm and 25mm. Compression moulding however is able to process continuous fibre lengths. The shortest fibre lengths that are typically compression moulded are between 10mm and 25mm, with typical lengths between 25mm and 50mm. The properties of the moulded part are largely determined by the aspect ratio of the glass fibres and so the length, as well as sizing, architecture and

weight fraction of the material, determines the processing route that is taken. As the glass length and weight fraction increase, the mechanical properties of the composite increase up to a limit. However, only certain processes will allow the use of certain glass lengths and loadings and these will be discussed at a later stage.

<b>Fibre Classification</b>	<b>Approximate Aspect Ratio</b>	<b>Approximate Fibre Length</b>
Short	10-100	<1mm
Long	100-10000	1-25mm
Continuous	10000-∞	>25mm

**Table 2.2 - Fibre length classification encompassing injection moulding and compression moulding [20]**

Thomason states that it is not only the length but also the diameter, and so the aspect ratio of the fibre, that determines the physical properties of the composite [20]. In this report, short fibres with different aspect ratios (L/D ratio) were mechanically tested and compared against long glass reinforced and unreinforced polypropylene moulded parts. It was stated that the thinner diameter short fibre gave better strength and impact resistance than thicker fibres of the same length. However, the long fibres had a higher modulus, tensile and flexural strength, notched and un-notched impact performance than the short fibre composite. This shows that the aspect ratio of the fibres along with their concentration is critical in the reinforcement provided by the fibres.

Short fibres are primarily used in thermoplastic composites, but are also used with thermoset materials such as Sheet Moulding Compound (SMC) and Bulk Moulding Compound (BMC). Short fibres significantly improve the physical properties, whilst increasing the viscosity. They do not significantly affect the shear rate rheology of the

polymer. In thermoplastic processes, the fibres decrease mould shrinkage and help to create a more isotropic cooling rate by keeping the polymer in contact with the relatively cold mould for longer. Uneven cooling will cause sections of the part to crystallise sooner than others, creating internal stresses and distortion. The short fibres can cause increased mould wear at high weight fractions, as there is a greater chance of the glass fibre ends encountering the mould surface.

Increasing the length of fibres gives improved strength, stiffness and impact resistance [21, 22] up to a particular length after which other effects such as fibre interactions and inter fibre bending, begin to degrade tensile strength. However due to the stiffening action of the fibres, the elongation properties of the composite decrease with increasing fibre length. The fibres hinder the polymers ability to deform and prevent the molecules aligning before failure. Thomason [23] concluded that, for polypropylene, a glass length greater than 8mm gives the best compromise for tensile strength, modulus and impact resistance.

Thomason and Groenewoud [24] also concluded that the thermal coefficient of expansion was directly influenced by the length and concentration in both in-plane and out of plane directions. Long fibres give a compromise of good mouldability whilst exhibiting increased strength, stiffness and impact resistance compared to short fibres.

Glass-reinforced polymers have been used to great success in a wide range of areas, including automotive, aerospace, construction, marine, sport and recreational industries. As stated previously, this research will concentrate on thermoplastics and due to the popularity and success of glass fibre reinforced polymers this research will

concentrate on glass-reinforced thermoplastics and more specifically, glass reinforced polypropylene (GRPP).

## **2.3. Glass Reinforced Polypropylene**

Glass reinforced polypropylene combines two of the cheapest materials in their field, creating a composite that can be easily moulded whilst having a high enough specific strength to be classed as an engineering polymer [4] by being able to carry significant loads. This makes the composite material very popular with the automotive industry, which is the largest consumer of glass-reinforced polymer.

A market survey carried out in 2007 by Ceresana Research, showed that polypropylene had an estimated global market of 45 million tonnes [25, 26].

Polypropylene is one of the cheapest polymers, having excellent mouldability [4], making it suitable for use in high volume processes such as extrusion and injection moulding. Polypropylene can be easily re-processed at any point in the production cycle, greatly reducing the overall cost of raw materials and manufacturing, as less virgin material needs to be used. This ability to be reprocessed continues for the rest of the polymers life, making it easily recyclable, which is becoming more important as raw materials are finite and become more expensive. With correct processing, polypropylene can have an excellent surface finish, which with excellent recyclability, is another large incentive for automotive companies as aesthetics are very important when selling cars. The body of the new Smart “Fortwo” is made entirely of polypropylene [26, 27], making a change from other polymers formally used for this application, such as a co-polymer of polycarbonate.

## 2.4. Glass Mat Thermoplastic

Glass Mat Thermoplastic, or GMT as it is commonly known in industry, is typically a woven or random mat of continuous glass fibres, impregnated with a mixture of additives and pure polypropylene. The flexural stiffness, tensional and flexural strength increase linearly with increasing glass fibres weight percentage. However high glass content and length has the drawbacks of a lower flow rate and other rheological properties that limit viable part manufacturing processes. Through choices in additives and raw material selection at the manufacturing stage, it is possible to customise and create a wide range of materials each with specific properties such as high flow or high strength, fire retardancy and UV protected composite in different colours. This flexibility is one of the key benefits of using glass-filled thermoplastics in many applications.

### 2.4.1. Manufacture

GMT is manufactured using various techniques such as slurry deposition, similar to the paper making process and mat impregnation, where glass mats and sheets of molten polypropylene are compressed together. The glass fibres are typically supplied with a “sizing” or primer on the surface of the fibres that enables the polypropylene to adhere to the glass fibres far more effectively than clean fibres.

When optimised for a given polymer, this sizing has been shown by Thomason, J. L., *et al.* [28] to significantly increase the impact resistance and other physical properties of the composite.

### 2.4.1.1. Glass Fibre Mat Reinforcement

The glass fibre reinforcement for GMT comes in three forms: chopped up glass fibres, Chopped Strand Mat (CSM) (Figure 2.10) or a knitted random mat (Figure 2.11). Chopped glass fibres are supplied loose, in a range of lengths depending on the need. CSM is constructed by placing chopped glass strands onto a conveyor belt, a temporary binder is sprayed on, the mat is passed through a double belt press and then gathered into a large roll (Figure 2.10). A knitted random mat has long chopped or continuous fibres that are knitted into a 3 dimensional mat, 5-8mm thick, by a reciprocating needling machine. This glass mat can then be used in producing GMT via melt impregnation.

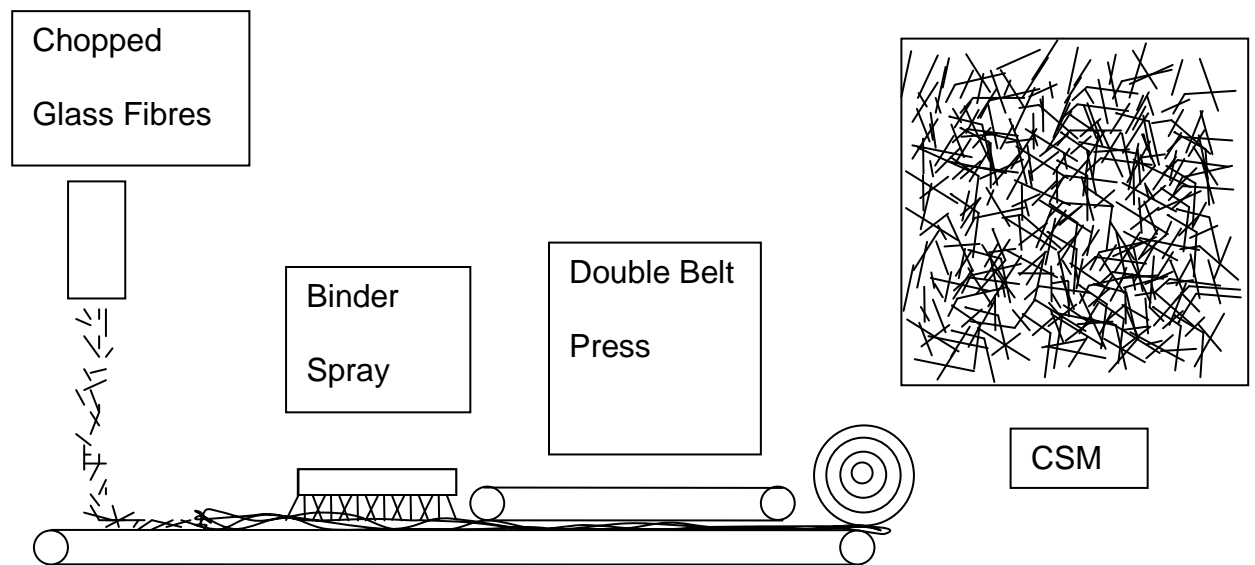


Figure 2.10 - Manufacture of chopped strand mat (CSM)

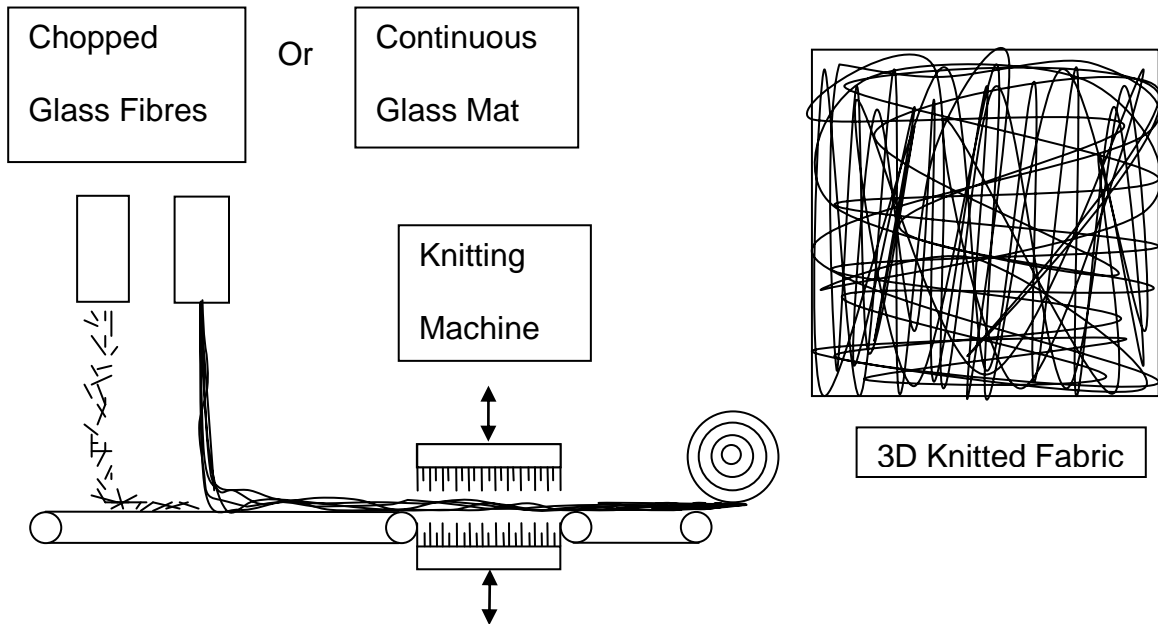


Figure 2.11 - Manufacture of knitted random mat

#### 2.4.1.2. Mat Impregnation

Mat impregnation is the main way of producing GMT, starting with 2-3 layers of knitted glass mat or a CSM, each layer being 5-8mm thick. Hot rollers compress these mats into a molten polymer core, impregnating the mats with polymer and ensuring a full wet-out of the glass fibres. The partially consolidated GMT is then passed between two cool rollers setting the polymer and reducing the mat thickness from 15-20mm to 2-5mm. The sheet is then cut to the appropriate blank size ready for transport. The whole process is depicted by a schematic (Figure 2.12) created by Davis *et al* [9].

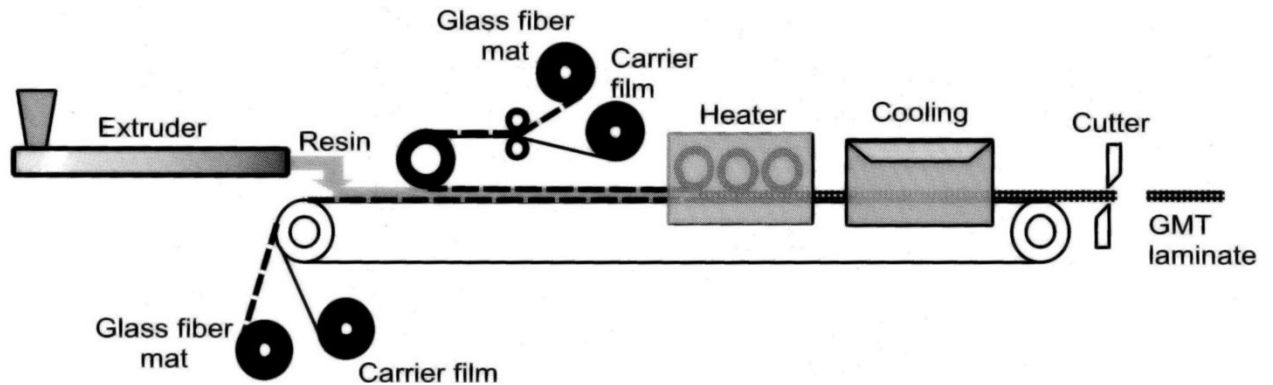


Figure 2.12 - Melt impregnation GMT manufacture [9]

In the final stages of manufacturing, the composite is compressed to around 20 percent of its original size prior to cooling, creating internal stresses. When the GMT is heated ready for processing, all the internal stresses contained in the glass mat are released causing the GMT to loft, or spring back, which occurs to the greatest extent in the Z-plane (thickness), since this is where the largest compression occurs in the manufacturing process. This lofting has to be considered when calculating the blank size, as the increased volume would cause blanks that would fit well into a mould before heating, to over fill after heating. The lofting increases the void content in the composite, creating an insulating effect to the centre of the material, which again has to be considered in the material heating stage. Lofting can be used to an advantage, as it creates a low-density material whilst retaining some properties of a fully consolidated material such as good wear and impact resistance. The high void content gives good soundproofing and thermal insulation, whilst still allowing the part to be used in a semi structural role.

### 2.4.1.3. Slurry Deposition

The alternative process to manufacture GMT is to use slurry deposition, where short chopped glass fibres, polymer and any additives that are required are added to a

water and detergent or solvent base. This is rapidly mixed into a fine foam consistency, comparable to shaving foam. The foam is drawn through a series of vacuum conveyer belts and a hot air oven, to drive off the water and solvent. The heat from the oven then melts the polymer, allowing it to co-mingle with the additives and glass fibres creating the GMT composite (Figure 2.13). Similar to the mat impregnation process, the composite is partially consolidated between two rollers from around 15-20mm to 2-5mm thickness and the sheet cut to the appropriate blank size or pelletized, ready for transport. The full consolidation, where the glass is fully surrounded with no voids or air pockets trapped in the material, will come from the final processing stage when it is stamped into the final shape of the part, giving a density ranging from 1.1 kg/m<sup>3</sup> to 1.4 kg/m<sup>3</sup>, depending on the glass weight fraction. The whole process is depicted by a schematic created by Berglund and Ericson (Figure 2.14)

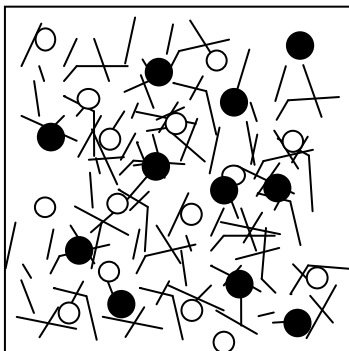


**Figure 2.13 - Fibre and additive dispersion in slurry deposition composite**

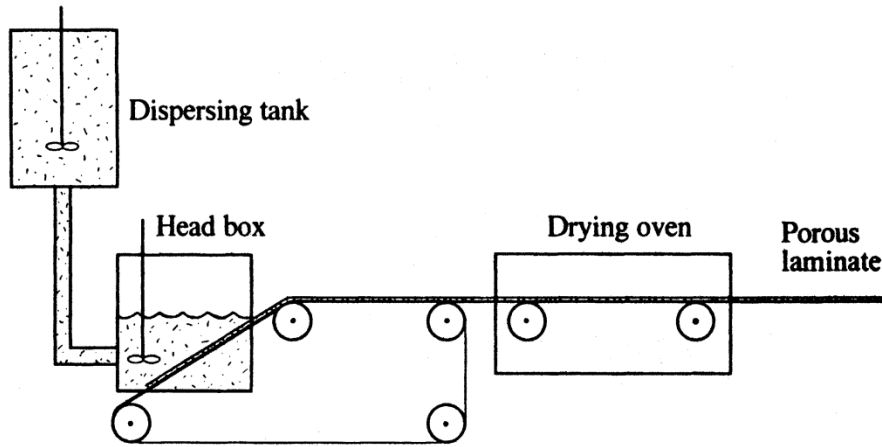


Figure 2.14 - Slurry deposition GMT manufacturing [29]

## 2.4.2. Typical Moulding Process

Due to the glass mat construction of GMT, it is compression moulded. This involves heating the individual material blanks until molten, typically in a hot air oven although contact and infrared heaters can be used. Time and temperature will be dependent on blank size and the type of material but will typically be between 200 and 230°C for 5-10 minutes. The molten blanks are placed in the mould tool in a predetermined pattern to ensure a full consolidation of the part and the two halves of the press are closed rapidly. The part is moulded under a pressure of 10-20MPa and once sufficiently cooled, it is removed. This whole process is displayed in the cycle diagram Figure 2.15 and depicted by a schematic Figure 2.16 created by Davis *et al* [9].

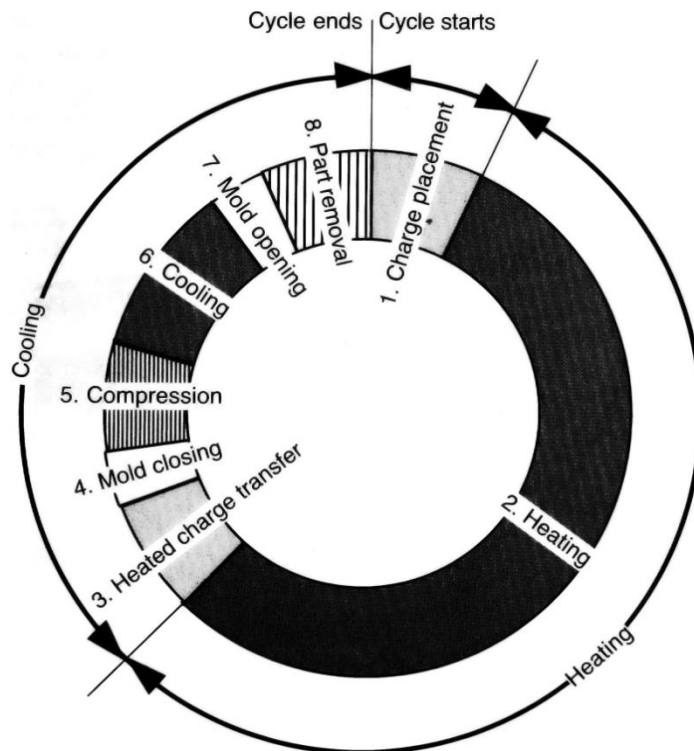


Figure 2.15 - GMT compression moulding cycle [9]

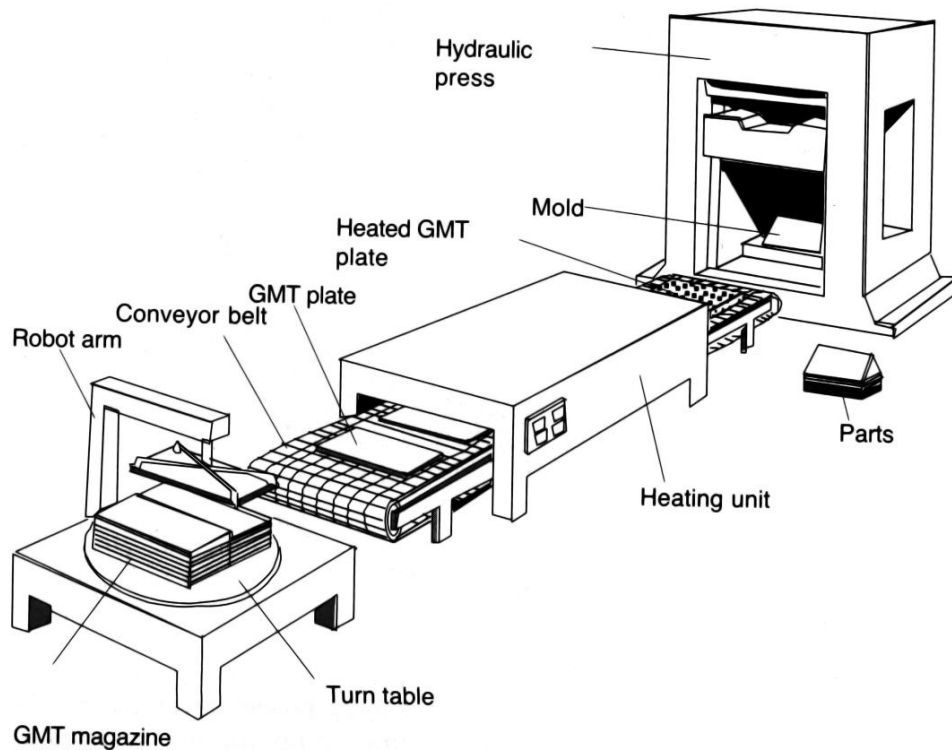
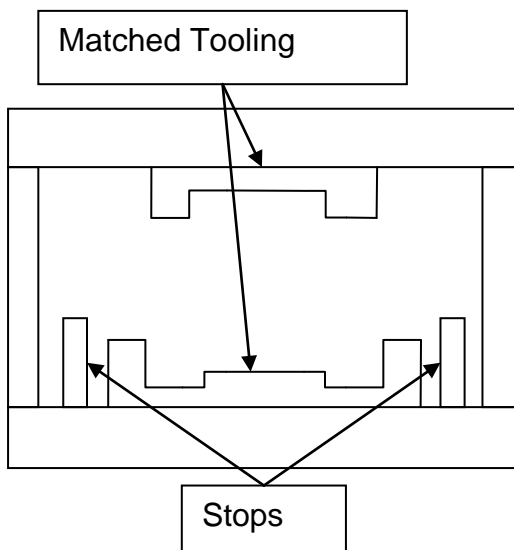


Figure 2.16 - Schematic of an automated compression moulding cycle [9]

### 2.4.3. Physical Properties

GMT's physical and rheological properties change dramatically as the glass content and additives change. Typical glass weight fractions range from 20 percent to 60 percent and when fully consolidated in a moulding press the densities range from 1 kg/m<sup>3</sup> up to 1.3 kg/m<sup>3</sup>. The quoted densities are achieved by fully consolidating the material during final processing, which is crucial in removing all the voids and weaknesses inside the composite, thus giving the quoted physical properties by the manufacturer. Quadrant's SymaLITE can however, have a density as low as 0.3 kg/m<sup>3</sup> after processing by taking advantage of the lofting, which increases the thickness of the blank up to 15mm. The blank is then processed at very low moulding pressure, or with the closing distance physically limited by stops (Figure 2.17), creating a partially consolidated part. With an increased blank thickness, it is possible to create changes in thickness through changes in geometry of matched tooling.



**Figure 2.17 - Processing GMT with moulding press stops**

Data was taken from datasheets provided by Quadrant Plastic Composites AG about three of their materials and is displayed in Table 2.3. It shows that glass-filled polypropylene has higher physical properties, such as strength and stiffness than pure polypropylene. This increase in strength and stiffness comes solely from the increase in fibre fraction.

Material Manufactured by Quadrant EPP	Weight Fraction (%)	Tensile Strength (MPa)	Flexural Modulus (MPa)	Moulded Density (kg/m <sup>3</sup> )
Homopolymer Polypropylene	0	33.1	1240	0.91
C100 F23	23	60	3000	1.06
B100 F40 F1	40	100	5200	1.2

**Table 2.3 - Physical properties of unfilled, 23 percent glass and 40 percent glass filled polypropylene**

The main failure modes of glass-reinforced composites are matrix deformation, fibre pull out and ultimately fibre breakage. J. L. Thomason *et al* [28], extensively experimented with differing glass weight fractions and fibre lengths in GMT manufactured by wet slurry deposition. Two series' of mats were made with fibre lengths varying from 0.1 to 13mm and weight fractions varying from 3-60 percent. This study showed that the glass direction to load, weight fraction, matrix/glass surface interface and to a lesser extent the glass length all have a major effect on the tensile strength of GMT. This would indicate that the glass, rather than the polymer is best at carrying the load and anything that affects the ability to transfer the load from the polymer to the glass, affects the whole composite.

## 2.4.4. Industrial Applications

GMT is used in a wide range of industries such as marine, construction, sports and leisure, wind energy, and utilities. However, the aerospace and automotive industries are the largest users; they use GMT, as they require high, specific strength materials to increase the efficiency of the vehicles. The raw material cost of GMT at around £2,500 per tonne [30] is higher than steels which in September 08, stood at around £600 per tonne for hot rolled plate [31] and in March 09 aluminium was £940 per tonne [32]. This generally means, like for like, a GMT part is more expensive than a metallic one. However, the processing, capital investment and handling costs are far lower due to the ease of mouldability and relatively low density. Additional cost savings come from part integration, where several features and fixture points that would have to be added at a subsequent joining processes, can be eliminated by being moulded at the primary step, usually without the need for secondary operations.

BMW made use of Quadrant Plastics Composites newly updated and customised versions of SymaLITE® GMT, in their 2008, M3 Series car in various areas including the underbody structure and engine shield [33]. SymaLITE® is a high weight fraction GMT, with densities as low as  $0.3 \text{ kg/m}^3$  when correctly processed. This gives it excellent specific strength and wear resistance, which is needed to protect the chassis from flying debris that is kicked up off the road, whilst adding additional stiffness to the structure. AZDEL Inc. is producing polycarbonate (PC) and polyetherimide (PEI) resin versions of its Superlite® composite rather than the traditional polypropylene. These alternatives are designed for the aviation and mass

transit sectors due to the inherent flame retardant properties and increased stiffness [34].

GMT is best suited to flat 2 dimensional panels or forms with minimal profile change as the glass mat can prevent large deformations, and is best utilised where its high specific strength can be used effectively. For forms with large section changes or complex shapes, materials such as LFT, short fibre reinforced thermoplastics or uni directional (UD) tape, which have fewer fibre interactions, but still provides strength would be better suited than GMT. LFT and UD tape can be placed precisely into the mould with predictable fibre directions, once the material has been formed.

## **2.5. Long Fibre Thermoplastic**

Long Fibre Thermoplastic, or LFT as it is better known, has fibre lengths ranging from 5-25mm and are typically processed by injection or compression moulding. Typical fibre lengths used in injection moulding range from 0.01mm to 10mm, so a long fibre would be classed between 5-10mm. The tool geometry and the process itself limit the fibre length. Since compression moulding can process longer fibre lengths, the classifications for a long fibre would be 15-25mm.

LFT was developed to rival GMT but has recently been described as an accompaniment as both materials are best suited to particular areas with little overlap [35]. The biggest advantages of LFT are its ability to carry significant loads whilst being able to create complex shapes due to its high flow and mouldability. The balance between increased strength and stiffness over short fibre composites, together with improved flow over continuous fibre composites, gives LFT a good

market to be exploited. This versatility allows it be used in a high number of applications and industrial sectors by changing the polymer and the glass percentage. LFT has successfully replaced structural steel parts so reducing weight whilst giving either comparable or increased strength and impact resistance.

### 2.5.1. Manufacture

Long fibre thermoplastics can be manufactured with a variety of methods including the same techniques as GMT with little alteration. These methods include fibre coating, co-mingling and co-weaving, film stacking, melt impregnation and slurry deposition [9, 36]. Melt impregnation (Figure 2.12) and slurry deposition (Figure 2.14) are identical to the manufacture of GMT but with long or continuous fibres instead of a partially knitted matt. Conventional production involves extruding continuous or chopped glass fibres in polymer melt through a small diameter die.

Co-mingled and co-woven LFT sheets provide a good impregnation of the fibres with a low void content and high fibre placement. Co-mingled sheets contain bundles comprises of strands of both reinforcement and polymer. The bundles are then woven into a kind of fabric that are then compression moulded into shape. The intimate contact between the polymer fibres and reinforcement fibres ensure a good wet out and highly predictable fibre concentration. Co-woven fabrics are similar to co-mingled fabrics, but the bundles are made entirely of either the reinforcement or polymer. The bundles are generally woven alternately so that a good wet out is achieved.

Film stacking is again very similar to co-weaving and co-mingling, but the whole fabric is made entirely of either the polymer or reinforcement. A stack, alternating between the reinforcement and polymer fabric, is processed by being placed in a compression-moulding tool and heated and compressed at a low pressure to ensure the fabrics impregnate each other without being parted themselves. Film stacking is a slow and labour intensive method and so is generally restricted to very low part volumes or laboratory testing.

Pultrusion production pulls a bundle of continuous glass fibres through a polymer melt or around a polymer infused roller ensuring a full wetting out of the glass by the polymer. The resulting rod would be pelletized and shipped ready for processing. The glass fibres are continuous and so run the length of the pellet, giving an advantage over extrusion, which will have a mixture of fibre lengths.

Fibre coating involves passing a bundle of reinforcement fibre through an extruder that coats the fibre with the polymer. The resulting fibre is either cut to size at the die or cooled and pelletized. When the pellet is processed, the polymer will melt and impregnate the reinforcing fibres.

A manufacturing technique developed by Bayer AG, Leverkusen [37, 38] uses a reciprocating screw design that feeds the reinforcing fibres directly into an un-pressurized zone of the extruder before extruding the composite material.

## 2.5.2. Industrial Applications

LFT is extremely versatile and, by careful design of the mould, allows the production, in a single operation, of complex shapes which would require several parts if manufactured in metals. F. Truckenmuller and H.G. Fritz report that a large number of components including: “*window handles, stone shields, trunk lids, motor/saw housings, sucker rod guides, nails, clamps, stadium seating, seat slides, foot/bike pedals, ski binding base plates, and golf putter heads*” [39], have replaced the metallic original with a glass reinforced polymer version. The natural inertness of the composite makes it ideal for automotive and marine applications where salt and other corrosive contaminants could corrode unprotected metallic structure causing problems in later stages of the life cycle.

LFT gives many processing benefits over short fibre thermoplastics, such as;

- Decreased wear on tooling and processing equipment – this is due to the decreased number of glass fibre ends, which are the primary cause of wear.
- Increased stiffness and strength
- Increased creep endurance performance
- Decreased part shrinkage

## 2.6. Short Fibre Thermoplastics

Short fibre thermoplastics (SFTs) provide increased flow and mouldability over LFT, whilst the fibres are still providing increased strength and stiffness over un-reinforced polypropylene. Short fibre thermoplastics are typically manufactured by slurry

deposition or extrusion. They generally have low fibre weight percentages to ensure the polymer retains a good flow characteristic. The good flow characteristics make short fibre thermoplastics popular in industry for low strength applications, where a complex three dimensionally complex part is required which also has added stiffness.

## **2.7. Recycling Reinforced Polymers**

In the current political and industrial climate, all industrial, commercial and residential sectors are being asked to reduce, reuse and recycle materials that would otherwise be sent to landfill. Most EU companies now have an obligation to take back their products to be recycled, so they are financially encouraged to make their products as recyclable as possible. Steel and aluminium are two of the easiest materials to recycle as they can simply be re-melted and sorted through varying densities. Pure polymers can be recycled in a similar way, as domestic waste plastic is cleaned and separated by flotation. The difficulties arise when polymers are compounded with other polymers or reinforced with fibres, as they ideally need to be separated before re-processing. Unfortunately, due to the similarities in densities for compounded materials they cannot be sorted automatically and have to be sorted by hand. For industry, the typical alternatives to landfill for thermosets and thermoplastics are post-process recovery, pyrolysis or incineration [40-43].

The polymer processing industry reduces the amount of landfill waste and the cost of raw materials by recovering post-production scrap. The level of contamination is kept to a minimum and so both the reprocessed and virgin materials are largely identical

without the need for any cleaning. It is estimated that 95 percent of post production scrap is reprocessed amounting to an estimated 250,000 tonnes of recycled polymer [44]. The percentage of re-grind (ground, recovered material) to virgin material has to be carefully controlled, as the re-ground material affects the processing and so parameters will need to be altered, according to the percentage of re-grind contained in the material [45].

Pyrolysis involves vaporising the polymer at very high temperatures in an oxygen free (typically pure nitrogen) atmosphere. The vapours are then condensed back to its constituent oils and gasses for use in other applications. The fibres can then be recovered and reused from the remaining residue [46].

Combustion or incineration is very similar to pyrolysis, except the material is heated in the presence of air and so the polymer would be converted to soot or ash. The main aim of this process is to use the material as combustion fuel to use the heat energy in another useful form, such as producing electricity or heating water.

Research recently carried out by Raúl Piñero-Hernanz *et al.* at the University of Nottingham, UK [47], showed that the epoxy resin in carbon/epoxy thermoset composites, could be dissolved using supercritical solvents such as methanol and acetone. This enabled the recovery of the carbon fibres with little damage to the fibres themselves, allowing them to be reused in subsequent composites.

The End of Life Vehicle (ELV) UK directive [48], which came into force in 2003, is aimed to reduce the amount of material committed to landfill once a vehicle has come to the end of its life and increase the percentage of the vehicle that can be

recycled. It also aims to reduce the amount of environmentally harmful materials contained in the vehicle that could cause problems in the future. This directive prompted research into the materials that components were made of and whether more recyclable materials could be used instead. One way of making a polymer more recyclable is to reduce the compounds and additives contained in the polymer so that little or no separation is needed to break the material down into its raw form.

## **2.8. Recycled GMT**

Recycled GMT (Re-GMT) is manufactured by extruding a mix of ground or granulated recovered GMT, virgin polymer, additives and if required, additional glass fibres. The mix can be extruded as either a rod, to be pelletized, or a sheet ready to be shipped. The mixture of long and short fibres contained in the thermoplastic will generally give it similar rheological properties to a pure polymer, meaning it can be used for both injection and compression moulding. To give the recycled polymer structural properties, the glass length and content should be retained as much as possible. This can be achieved by ensuring the granule size is kept high by reducing the level of granulation. The glass content is raised by the addition of glass fibres to the mix.

## **2.9. Alternative Reinforced Polymers**

Traditional reinforcing fibres such as glass, carbon and boron can cause problems with recycling as they affect the sorting process by changing the density of the base polymer. The hardness of the fibres increases the wear on the machinery used in the recovery process, increasing the maintenance and running costs. Carbon and boron

fibres are ideally recovered due to their high demand and raw material manufacturing costs. Therefore, the ideal recyclable fibre reinforced polymer would not contain any of these traditional fibres and only a limited amount of filler compounds. This is where self-reinforced polymers have proved to be successful, as the materials physical properties are increased by reinforcing the polymer with fibres of highly aligned molecules of the same base polymer.

Research by P.J. Hine and I.M Ward [49] in the hot compaction of polymer fibres showed that fibre reinforced composites could be made of a single polymer. This research showed that by weaving pre-tensioned polymer fibres into a mat, and partially melting some of the fibres to form the matrix, whilst leaving the majority of the fibres intact, it was possible to manufacture, a single polymer, self-reinforced sheet. This would make the recycling of the sheet far easier than conventional fibre reinforced polymers. Development of this research in 2005, produced self-reinforced polypropylene called Curv™, which is a polypropylene sheet that has up to six times the strength of conventional polypropylene [50]. Curv™ is constructed of highly aligned and drawn polypropylene strands, which are then woven into a fabric, stacked and impregnated with polypropylene to create a sheet. Curv™ does however have limitations due to the nature of the material. For instance, it cannot be used in high temperature applications near the polymers melting point, as the fibres would naturally relax and contract, causing the material to shrivel and shrink. Additionally, problems arose when heating the sheet ready for moulding, as the heat would relax the molecules and allow them to shrink and revert back to they're relaxed natural state [51]. Curv™ does not have sufficient strength to be used in structural applications but is ideal for panelling and protection. It has high impact strength,

meaning it is perfect for personal safety equipment, which is why the material was used on the Lotus Elise for the bonnet access panel once these problems were overcome. The panel's ability to absorb high amounts of energy, allowed any object hitting the panel, such as a person's head, to decelerate slowly and so save it from considerable damage. The panel would naturally deflect back to its original shape without any defects reducing or eliminating panel repair costs. Curv™ keeps its high impact resistance even at very low temperatures (as low as -180°C) making it an ideal material to make luggage out of due to the low temperatures and rugged environment of an aeroplanes cargo hold. Additional benefits that Curv™ give over traditionally reinforced materials is the dramatically reduced density and increased ease in recyclability as there are no differing materials to be separated.

AZDEL, Inc. have produced a basalt fibre-reinforced thermoplastic composite to remove the problems created by glass fibres during recycling. Basalt fibre is produced in a similar manner to glass fibre, where the igneous rock is melted and drawn into a fibre, but the high abrasive nature of the fibre causes high levels of wear on the rollers. Basalt fibres have higher strength, higher temperature stability and modulus than glass fibres, but higher production costs currently prohibit its wide commercial use. The high temperature stability makes it more suitable to composite incineration recovery, as the fibres are less likely than glass fibres to clog up the incinerator [52].

### 3. Thermoplastic Processing

Thermoplastics can be processed in a wide variety of ways depending on the application and the material that is required for that application. Only processes suitable for polypropylene and glass-reinforced polypropylene will be investigated, as all other materials are outside the scope of this research. The main processes for glass-reinforced polypropylene include extrusion, injection moulding, compression moulding, blow moulding and extrusion compression moulding. Most thermoplastic processes use some form of extrusion to melt the polymer, prior to their use in the primary moulding process [53]. This includes compression moulding, which can be adapted to use LFT directly extruded into the mould tool.

During the part design process both the manufacturing process and material selection are decided in tandem as they directly influence each other. Whilst certain materials can only be processed by specific manufacturing processes, some materials are suitable for use in a wide range of processes. For example, very long fibre (15-25mm) or continuous fibre reinforced polymers, are not suitable for processes with small area openings that could clog with the fibres, or processes with large flow distances, as the glass could cause significant flow problems.

The main thermoplastic processes are extrusion, injection moulding, compression moulding, transfer moulding, rotational moulding, structural foam moulding and blow moulding [53]. This report will concentrate on injection moulding, gas assisted injection moulding and compression moulding. Due to the aforementioned processes not able to provide the level of glass reinforcement required, they are not relevant to this research.

## 3.1. Injection Moulding

Injection moulding is, in theory, a simple concept but, in practice, can be complicated, involving several systems and process parameters which require a highly skilled operator to produce a successful moulding. Injection moulding has developed into the largest producer of polymer parts, producing millions of parts annually around the world [1, 53]. Because of the short cycle times (around 40 seconds) it is possible to produce up to tens of millions of parts per year [53, 54]. The high capital and tooling costs mean the process is not economically viable with part productions below ten thousand parts a year. The process involves the injection of molten polymer at high pressure into mould tools, with high accuracy, repeatability and low cycle times. The high pressure forces the polymer to flow into complex shapes with thin walls and ribs, which would not be possible with other processes. An injection moulding machine consists of an injection unit, which is a heated barrel and an internally rotating screw, similar to an extrusion unit. However, unlike extrusion the screw is able to reciprocate (Figure 3.1), allowing the screw to retract, building a head of molten polymer to inject into the mould tool. The polymer is injected into a mould tool and the moulded part ejected once cooled. To withstand the clamping forces required to counteract the high injection pressures, the mould tools are typically very large and made from heavy tool steel, resulting in the need for heavy lifting equipment to be used for tool changes. The whole machine is typically mounted horizontally to reduce energy consumption, as the heavy tools would not have to be moved against the force of gravity. Tie bars support the entire weight of the clamping equipment and mould tool, and ensure the two halves of the mould tools are perfectly aligned. These bars need

regular inspection and maintenance to ensure the smooth running of the machine. The mould tool can be large enough for the operator to stand between the two mould halves.

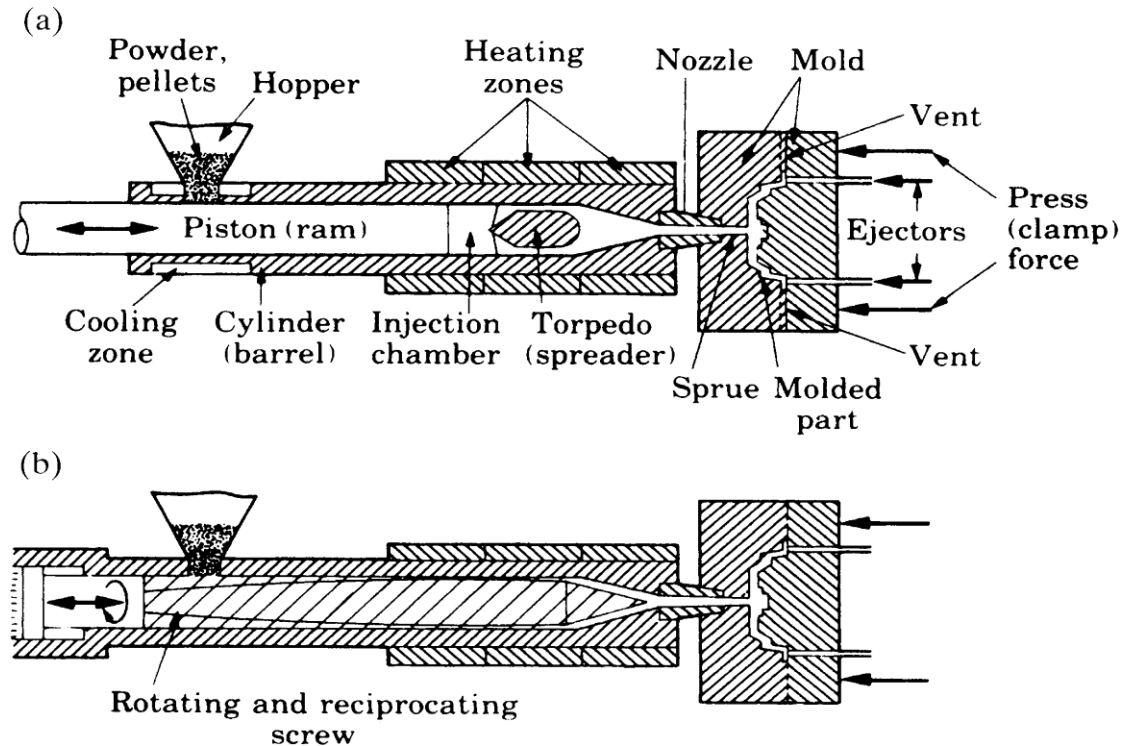


Figure 3.1 - Schematic of injection moulding machine (a) shows ram version (b) shows internal reciprocating and rotating screw version [53]

### 3.1.1. Processing Cycle

The raw polymer is supplied in either pellet or granule form and held in a hopper above a heated barrel with a rotating screw, much like extrusion. The internal screw slowly plasticises the polymer, compacting and mixing as it moves through the zones. As the screw rotates, it slowly retracts to a preset distance inside the barrel, creating a shot weight of molten material behind it. The screw then rapidly moves forward, injecting the material through a runner and gate system into a closed mould, where the polymer immediately starts to cool and solidify. The injection unit maintains

pressure on the part, counteracting the internal pressures that could otherwise cause the material to flow back through the gate. Additional material is injected into the mould tool before the gate has fully frozen to compensate for shrinkage, which is illustrated by section five in Figure 3.2. Section five, is known as the packing stage and helps to prevent surface defects such as sink marks. However, conventional injection moulding cannot eradicate these marks [55]. Shrinkage is caused by the polymer molecules returning to their relaxed and compact state.

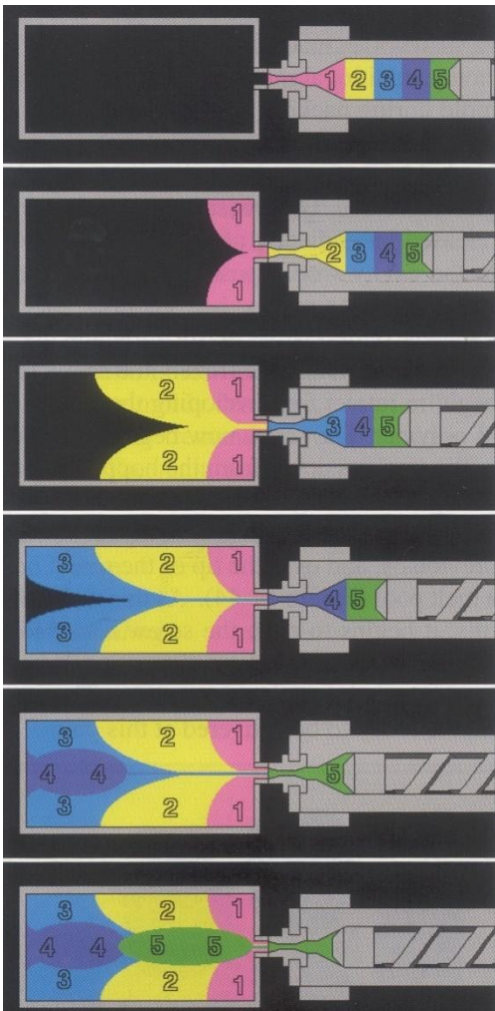


Figure 3.2 - Polymer flow in injection moulding [56]

Liang and Ness [57] used experimental data to derive a formula which could be used to calculate the time taken for the gate to freeze off, after which no more material can flow into the part.

To reduce cycle times, the next shot is prepared whilst the part is left to cool in the mould. Once the part is solid enough to be handled, it is ejected and left at another station, possibly in a restraining jig, to crystallize for up to 24 hours.

A typical injection moulding cycle is:

- Injection Stage
  - Molten material injected through a sprue into closed mould tool
  - Material flows and fills the mould
- Packing and Cooling
  - Cooling system cools the part in mould tool
  - Injection unit maintains pressure to create packing pressure
  - New shot prepared
- Shot Preparation
  - Hopper feeds material into a heated barrel
  - Internal screw mixes , compresses and heats material
  - Screw draws back to create shot weight
- Part Removal
  - Mould tool opens
  - Part Removed
  - Mould tool closed ready for next cycle

### 3.1.2. Processing Parameters

There are a large number of processing parameters involved with injection moulding as it essentially combines two processes. The parameters for the polymer melt stage are similar to an extrusion process, with the addition of injection rate, which is the rate at which the polymer is forced into the mould tool. The most relevant processing parameters for an injection-moulding operator are:

- Barrel temperature
- Residence time
- Melt temperature
- Mould temperature
- Injection rate
- Injection pressure
- Shot size
- Pressure ramp rate
- Packing pressure
- Cooling time

The polymer is typically injected at the upper processing limits of the material to minimise the cycle time. If the injection rate is too low, then the polymer can freeze before the mould cycle has completed which will result in an incomplete or distorted part. If the part has a large volume and the polymer has to be injected at a slow rate due to shear rate restrictions then the mould tool may need to be heated to ensure the polymer is kept molten long enough to fill the mould.

The initial melt temperature and residence times are important as they greatly affect the viscosity of thermoplastics, especially polypropylene. The melt temperature is the set temperature of the heated barrel. The residence time is the length of time the polymer is contained in the heated barrel, before being injected into the mould tool.

Závadský *et al.* [58] investigated “*The time, temperature and shear dependence of the viscosity of polypropylene and its influence upon the extrusion process*”. A master

curve was established to show that the higher the temperature, residence time and shear rate, the lower the viscosity.

As the cooling section of the moulding cycle is longest, the greatest reductions in cycle time can be made in cooling the polymer as quickly as possible. The cooling time can be lengthened by the mould tool being continually heated by the hot polymer. This continual heating can cause problems if it is not controlled, as the polymer would gradually take longer to freeze. To prevent any risk of the polymer being ejected whilst still soft, mould tools can be cooled using chilled water to remove any excess heat. Gas Injection Worldwide [59] developed an advanced tool technology called Rapid Temperature Cycling (RTC) tooling. RTC tooling contains both heating and cooling channels, using each in turn intensively during the moulding cycle. Whilst the shot of polymer is being prepared, the mould is rapidly heated to a preset temperature. Once the part has been moulded, the cooling channels rapidly cool the polymer to below its glass transition temperature and once the part has cooled sufficiently, it is ejected. The mould is then clamped shut and reheated, ready for the next cycle. If the mould tool were left at the chilled temperature, the polymer would freeze immediately after being injected, causing complications such as an incomplete moulding.

The moulded component design should eliminate areas of relatively large mass in which hot molten polymer would cool at a slower rate than the surrounding cooler polymer and possibly distort the part [53]. This distortion arises from non-isothermal cooling caused by non-uniform wall thickness. The polymer begins to cool rapidly, immediately after coming into contact with the relatively cool mould tool surface. Rib

junctions or any changes in section should try to keep as uniform a wall thickness as possible with smooth curved transitions, rather than a sharp 90° angle. The uniform wall thickness helps to prevent formation of large pockets of polymer that would have a higher thermal capacity than the surrounding thin walled sections and so take longer to cool. These pockets will then be isolated from the main flow and pressure of the injection unit, preventing the molten polymer from experiencing the packing pressure. This will prevent the polymer from being packed out as it cools and shrinks, which could cause voids where the wall has frozen and the polymer contracts internally or surface defects such as sink marks, where the material surface contracts away from the mould surface and into the body of the part.

Cox and Mentzer [60] studied the effect of fill time on the properties of an injection moulded part in polypropylene, ABS and in both reinforced and unreinforced nylon. It was found that an optimum fill time can be achieved when the injection pressure is at its lowest, whilst still achieving a complete moulding. At low fill times (high injection rate) the fill pressure was high due to the viscosity of the polymer, this gradually dropped with higher fill times (lower injection rate) until the fill pressure gradually increased again. This fill pressure increase is due to an increase in viscosity as the polymer begins to freeze off in the mould tool, physically restricting the flow. The parts were tested for tensile properties (modulus, peak stress, peak strain), flexural properties (strength and stiffness), surface finish and shrinkage after using various fill times/pressures. It was found that there was no significant change in properties for unreinforced polymers. The tensile modulus and peak stress did increase slightly with fill time, due to the increased molecular orientation effect. The surface finish of the reinforced nylon was significantly affected by the fill time, indicating that the

shorter the fill time, the greater the packing pressure that can be applied. If the injection rate is too high, then the polymer can be subjected to high shear rates, which can adversely affect shear rate sensitive polymers such as PVC.

Shear heating caused by high shear rates can degrade and change the viscosity of the polymer. Crowson *et al.* [61] noted that high shear heating and compression heating, caused by high extrusion pressures ( $140\text{MN/m}^2$ ), raised the temperature of the polymer a maximum of  $70^\circ\text{C}$  above the barrel temperature.

### 3.1.3. Polymer Flow

Understanding the polymers rheology and flow is essential in correctly designing the mould tool and choosing the processing parameters. The polymer flow is predominantly affected by the temperature, although can be affected by other factors.

When the polymer contacts the mould surface, it immediately starts to freeze, creating a frozen polymer skin with a molten core of polymer. The polymer then starts to flow in what is known as a fountain flow. H. Mavridis, *et al.* [62] report that *“Fountain flow describes how liquid particles decelerate as they approach a slower moving interface and spill over towards the region vacated by the advancing interface”*. This essentially describes a layer of polymer which flows from the centre outwards and becomes stationary, whilst another layer of polymer flows over the top and stops. A diagram based on an illustration by A.G Gibson [15] shows the polymer flow through a simple channel along with the polymer velocity and shear rate at a low injection rate. The fountain flow has a high orientation effect on the polymer creating different regions of alignment to the flow direction. This is because the flow stretches

the polymer before solidifying against the mould surface. This can be especially noticed when fibre filled polymers are used.

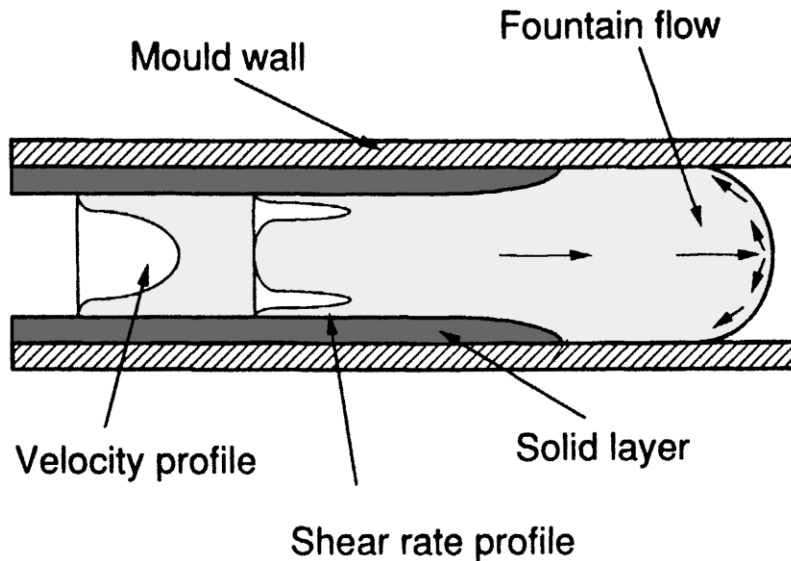


Figure 3.3 - Polymer flow of filling stage by injection moulding [15]

Figure 3.3 shows the velocity and shear rate profile of the polymer melt as it flows along the mould surface, leaving a solid layer behind. The velocity of the polymer is at its greatest in the centre of the melt. The greatest shear rate is towards the edges adjacent to the solid polymer layer. The non-isothermal conditions cause the highest shear rates to be a small distance from the solid layer [15].

Figure 3.2 illustrates a typical filling pattern for an injection moulding in a basic deep cavity mould tool and to what position in the mould each section will flow. The drawing shows how the initial section flows outwards, towards the exterior of the mould in what is known as die swell. Die swell is where the polymer expands after being compacted as it entered the small opening of the die. Sections two and three follow the same pattern as the first. The fourth section flows directly to the end of the mould tool. These sections are not discrete and the mould is filled continuously. The

fifth and final section is the packing stage, compensating for any shrinkage of the polymer and ensuring a full moulding.

Polymer flow is not however always laminar and predictable. Like any fluid material, it can be subject to turbulent flow, which can cause processing problems.

In 1883, O. Reynolds conducted an experiment where water was drawn through a thin tube and observed a streak of dye in the water at different velocities. At low velocities, the dye remained smooth and stable (Figure 3.4 (a)). However when the velocity reached a critical value, the flow became unstable and eddy currents formed (Figure 3.4 (b)). The turbulent state moved towards the tube opening as the velocity increased, but would not go past the opening (Figure 3.4 (c)). Reynolds derived a dimensionless number called Reynolds number, and this equation was used to derive a non-slip condition formula (Equation 3.1). Where  $U$  is the average velocity,  $\nu$  is the kinematic viscosity and  $L$  is the length, over which the characteristic happens, which in the case of injection moulding, would be the height of the channel.

$$Re = \frac{UL}{\nu}$$

**Equation 3.1 - Reynolds number through a channel [63]**

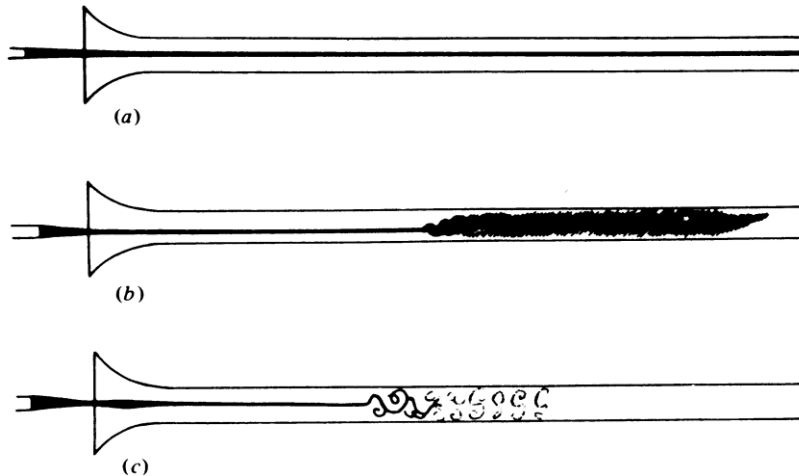


**Figure 3.4 - Drawings of Reynolds die experiments showing stable flow (a) and unstable flow (b,c) due to higher flow rates [63]**

A polymer's flow is directly influenced by the shear rate, which is the rate at which a layer of polymer flows over an adjacent layer. At shear rates within the limits of the polymer, it has an even, laminar flow similar to the flow demonstrated by O. Reynolds in (Figure 3.4 (a)). Outside of these limits, the material can become unstable and show turbulent flow [64]. Turbulent flow is where the linear flow starts to break up creating small eddies. Turbulent flow should be avoided as it can result in poor surface finish and weakened structure due to the random organisation of the polymer. Turbulent flow also causes a rapid cooling effect on the polymer, because the rotating eddy currents in turbulent flow transfer polymer from the hot centre of the flow to the cooler regions next to the wall surface, whilst at the same time, transferring cool polymer at the surface into the centre of the hot polymer melt [64].

Hesitation marks occur when the polymer flow front temporarily stops and the surface freezes, before a second flow front breaks through the central portion of the melt and flows to the mould surface [65]. If the polymer remains stagnant for long enough, then a thick layer can form so preventing the backpressure from breaking through

and resulting in a short moulding. Correct mould design is important in preventing secondary flow fronts starting in areas that would have frozen off, such as small section areas near the injection point. The narrow section would prevent the polymer from flowing into the gate until sufficient pressure had built up from the rest of the part being filled. Since the narrow section would be near the start of the flow, the polymer in this area would have cooled off already and the increase in pressure would result in polymer breaking through, causing a hesitation mark.

### 3.1.4. Injection Moulding of Short Glass Fibre Reinforced Thermoplastics

Short Glass Fibre Reinforced Thermoplastics (SGFRT) are widely used in injection moulding due to the high flow and increased mechanical properties. An additional benefit is that the same machinery for unreinforced polymers can be used for SGFRT. The rheology of SGFRT can be described as viscoelastic melt with a particle suspension [66]. Understanding the rheology is important in predicting and understanding the moulding characteristics and mechanical properties of the moulded part. This is because fibre reinforced polymers are anisotropic and are significantly affected by the fibre orientation. The orientation effect of the process, fibre length, fibre weight percentage and the matrix are extremely complex and numerous studies, of both the mechanical and rheological properties short fibre composites have been carried out [20, 66-72].

A series of papers by Crawson *et al.* [61, 73, 74] investigated the rheology of SGFRT and its application to injection moulding. An initial study of the filling characteristics of

SGFRT with a polypropylene matrix, both unfilled and filled with short 500µm fibre lengths, was carried out. Both materials filled the mould uniformly and cleanly with various injection speeds and gate positions. The viscosity of unfilled and filled polypropylene with fibre lengths and concentrations of 500µm, 20 percent and 350µm, 30 percent at differing shear rates was tested in a capillary die rheometer. It was found that at low shear rates the viscosity increased with fibre concentration, however, as the shear rate increased the viscosity of the three materials started to converge, until reaching the same viscosity [73].

A. Vaxman and M. Narkis [66] described how the short fibres in a polymer melt tumble and rotate as the polymer flows. The rotation increases when the fibre is perpendicular to the polymer flow and slows as it becomes aligned. Increased fibre volumes increase inter fibre interactions, slowing down the rotation of the fibres and even stopping it at high concentrations [75].

### 3.1.5. Injection Moulding of Long Glass Fibre Reinforced Thermoplastics

Glass reinforced polymers, as described previously, are stronger and stiffer than virgin polymers. The glass fibre lengths have been proven to be critical in the impact resistance, strength, tensile modulus and elongation properties. When the enhanced polymer is combined with the mouldability of injection moulding, complex but structurally strong parts can be produced in high volumes. The glass fibres do however produce problems in production.

Glass reinforced polymers for injection moulding are supplied in pellet form, and so are plasticised in the heated barrel with an internal screw. Due to the rotating screw, any long fibres contained in the polymer will get broken up, reducing the overall fibre length to an extent determined by the screw and tool geometry [76, 77]. However, using optimised designs of co-rotating twin screws can reduce fibre breakage, whilst maintaining the thoroughness of mixing [78].

The rheology of glass filled materials change dramatically as the glass fibre interactions increase because both the glass content and length affect the flow. The flow eventually becomes dominated by the inextensibility and orientation of the fibre [72, 79]. The random distribution of the fibres can create an anisotropic flow, which if not taken into account, can produce an unsuccessful moulding. As the glass weight fraction and fibre length increase, the interactions between the fibres become more significant to the rheology of the polymer by increasing the viscosity and shear stresses [72].

Changes in the rheological characteristics of the material such as increased viscosity and shear stresses can cause processing difficulties. This is especially true when injection-moulding long (1-25mm) glass fibre filled polymers. In this case, the small dimensions of the gates and tool geometry can become clogged with glass fibres. This is known as fibre damming and is shown in Figure 3.5.

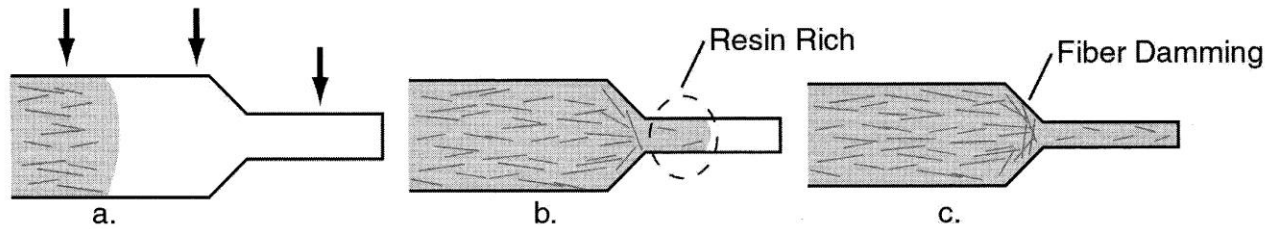


**Figure 3.5 - Diagram showing fibre damming at a reduced cross section [9]**

The process is best suited to thin walled components that will fill and cool quickly keeping the cycle time down and producing an A-Class finished part. For thick sections, it may be desirable to core out (create a cavity inside) the part, reducing not only the wall thickness but also the amount of material used and cycle times. This will increase the efficiency and cost effectiveness of the process.

### **3.2. Gas Assisted Injection Moulding**

Gas Assisted Injection Moulding (GAIM) has evolved ever since the first patent application was filed in 1975 by Friedrich Ernst Dipling [80] over 30 years ago. The premise is to inject gas into the centre of a polymer melt and core out a moulded part. The process typically uses nitrogen gas due to its natural inertness and ease with which it can be produced. If conventional air were used, then the oxygen could react with the polymer potentially causing combustion with severe safety implications.

Using the gas to core out and pack the polymer creates numerous benefits. The nitrogen gas has a far lower density at  $1.165 \times 10^{-3} \text{ kg/m}^3$  than polypropylene at  $0.9 \text{ kg/m}^3$ , with the gas having a viscosity roughly  $10^8$  times lower than the polymer [81]. The lower viscosity allows the gas to be injected at a lower pressure than the polymer. This reduces running costs, as a lower clamping pressure is required to

counter act the injection pressure. A short shot technique is typically used in GAIM, which involves only partially filling the mould tool, using the gas to core out the part and flow the polymer to fill the mould. This technique reduces material costs as less polymer is needed to fill the mould tool, and reduces the cooling cycle time, as a thinner residual wall thickness is produced. Conventional injection moulding could have trapped pockets of molten polymer, which are blocked from experiencing any packing pressure from the injection unit. GAIM produces a clear passage from the gas injection pin to the vast majority of the part, allowing the gas to pack the polymer more efficiently. The increased packing performance creates higher dimensional stability in the finished part.

The initial process is identical to conventional injection moulding, involving injecting polymer into a mould. The next stage however, injects gas through a gas pin into the centre of the polymer melt, keeping the gas pressure applied to pack the material whilst the part cools and then the part is ejected (Figure 3.6). The packing stage uses the gas to create an internal pressure to force the polymer against the mould tool surface, compensating for any polymer shrinkage.

The whole process is continually being researched into and perfected, but the basic premise of a four-stage process remains the same; polymer filling stage, medium (typically nitrogen gas) injection stage, packing stage and solidification.

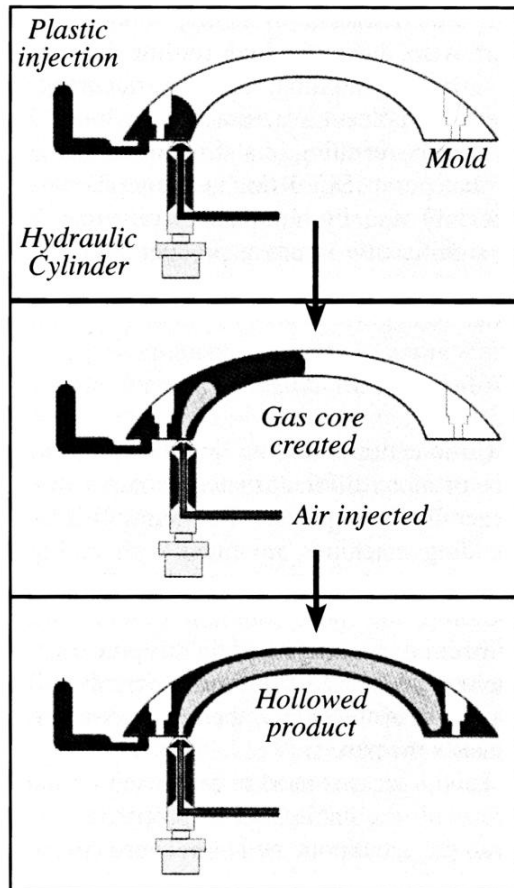


**Figure 3.6 - Diagram showing the polymer injection (top), gas injection (middle) and packing stages (bottom) of GAIM [46]**

Various designs of mould tool have different techniques for filling the mould and creating a cavity, each with its own advantages and drawbacks. The most common, is a short shot technique where the mould tool is only partly filled by the polymer, after which, gas is injected flowing the polymer in a second flow front to fill the mould tool. The mould tool is the shape of the desired part with no run off areas and only the injection sprue needing to be removed in a secondary process. Other mould designs involve designing flash lands and hot runners, into which the molten polymer can flow when displaced by the injected gas. The research reported in this thesis will concentrate on the short shot technique, as it is the most widely used in industry.

### 3.2.1. Gas Injection Stage

The crucial part of the GAIM process is the injection of gas into the polymer. Once the polymer has been injected, a gas, typically nitrogen, is immediately injected into the centre of the polymer melt. The gas cores out polymer by pushing molten material from the centre of the part and further advances the polymer flow front. The gas can be injected into the polymer melt, either through the same nozzle as the polymer injection nozzle or through a separate gas injection nozzle located at another position on the mould tool. The latter technique is preferable for multiple injection points, where the polymer is flowed by the gas to produce multiple cavities.

The internal diameter of the gas injection pin is critical to a successful moulding. If the diameter is too large then polymer can ingress into the pin, freeze and cause a blockage. The diameter does however need to be as large as possible to have the maximum gas flow. If the gas flow is too low, then the part will freeze off before the gas has managed to flow the material to fill the part.

### 3.2.2. Gas and Polymer Interactions

The interaction of nitrogen gas with molten polymer is not always fully understood in industry, but it is not always necessary to fully understand the interactions to ensure a successful moulding. This is mainly due to the operator using trial and error to change process parameters, until the process works. However, for more complex part designs, these interactions become more complex and so need to be understood.

A lower polymer melt viscosity is beneficial to the process as less pressure is required to flow and pack out the polymer. However, a lower viscosity can allow the gas to penetrate areas outside the main gas channel into areas with small cross sections (e.g. ribs), weakening the part as the gas cores out areas designed to be solid. The flow of gas into areas other than the main gas injection channel is known as fingering [82].

Due to flow dynamics, the polymer will always follow the path of least resistance. Therefore, when the gas pressure is applied it will push the polymer along the path of least resistance. This path is significantly affected by the volume of polymer and the thickness of section it has to flow. If a mould tool has identical cavities filled with an identical volume of polymer, with the gas injection point at an equal distance between the two cavities, then any disturbances from machinery or slight differences in cooling would affect the path that the gas would choose. The gas may initially penetrate both cavities but if the gas in one advances further (the longer cavity) than the other, then there will be less polymer to displace and so the resistance would decrease. This would cause gas flow to the shorter cavity to cease and all the flow would go to the longer cavity. Gas flow will only return to the shorter cavity once the resistance in the longer cavity is sufficiently high, for instance, it has reached the end of the cavity. This stagnation in flow, as previously mentioned, would cause hesitation marks but could be prevented by keeping the gas delay time to a minimum, or altering the mould tool design to promote even flow. A short delay between the polymer injection ending and the gas injection beginning, reduces or eliminates the time that the polymer flow front is stagnant. When a low viscosity substance passes over a high viscosity substance at high speed, a phenomenon

known as entrainment can occur [64]. Large differences in speed and viscosity between the two materials causes instabilities between the two surfaces. The unstable flow first causes uneven surface interfaces, then wave like formations, which can lead to complete encapsulation (Figure 3.7). This encapsulation is known as entrainment and can be used to an advantage, by mechanically interlocking two polymers that would otherwise not chemically bond together [83, 84]. Entrainment can occur in GAIM, causing the gas to form small trapped bubbles of nitrogen gas. This is may not necessarily be a disadvantage if the internal surface is not important, it may however produce a less stiff part due to a variance in wall thickness.

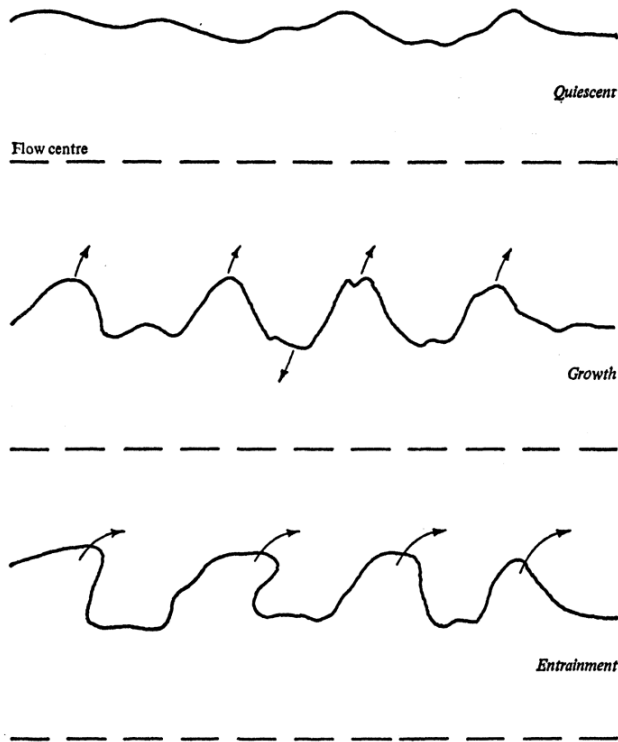


Figure 3.7 - Growth of entrainment eddies in turbulent flow [64]

### 3.2.3. Processing Parameters

Like all processes, the processing parameters have a large effect on the outcome of the moulding. In addition to those parameters GAIM has in common with conventional injection moulding, there are those parameters related to the gas injection stage and they are:

- Short shot weight
- Gas delay time
- Peak gas pressure
- Pressure profile
- Packing pressure
- Gas exhaust time

Numerous studies have been carried out to determine the effects of various processing parameters on a moulded part. Gas bubble penetration (the distance the bubble travels in the polymer melt) and residual wall thickness (RWT) are the most common attributes by which these parameter changes are measured. The reason for bubble penetration and RWT are chosen is that they can be used to define the overall cavity volume. This is of particular interest in industry where controlling and predicting these attributes is important in predicting the parts physical properties.

M.A. Parvez *et al.* [85] investigated shot size, delay time, gas pressure and melt temperature and their effect on bubble penetration, RWT, fingering effects and mechanical properties. It was reported that the shot weight and delay time were the most influential parameters for RWT and gas bubble penetration, whilst adding radius

to sharp corners increased the moulding limits and created a constant wall thickness through the transition. A smaller shot size and lower delay time increased the chance of fingering due to the polymer melt being molten for longer and the lower shot size allowed greater flow. An increased delay time was usually sufficient to reduce fingering. An increased shot size increased the bending load, whilst an increase in delay time decreased the bending load. When experimental data was compared to simulation data produced by Moldflow™, the experimental data showed a lower gas penetration than the simulation.

Shin and Isayev [81] conducted a series of Taguchi array experiments involving; melt temperature, mould temperature, boost pressure, injection speed, shot size, gas injection time, gas delay time and gas injection pressure. Each of the parameters was varied between three or four values and the interactions were investigated to define a set of optimum processing parameters. The length of gas bubble penetration was used as the primary measuring factor. It was concluded that the mould temperature, injection pressure, injection speed and gas holding time did not have a significant effect on the gas penetration length. The conclusions state that the melt temperature was the parameter that had the most significant effect but once it had reached a certain temperature, the shot weight became the most significant contributing factor, which is in agreement with other studies [85-88]. Once the shot weight reached 75 percent of the cavity volume, with a high melt temperature, good bubble penetration was achieved. However, with a low polymer melt temperature, the gas broke through the polymer melt, possibly due to a thicker skin being formed so restricting the amount of material that was able to flow with the gas. Breakthrough is caused by the polymer's inability to contain the gas bubble. Breakthrough is typically

caused by the gas reaching the end and bursting through the end of the polymer flow as the gas runs out of material to flow, but can be caused by the gas pressure being too high.

### 3.2.4. Gas Assisted Injection Moulding Of Glass Reinforced Polymers

The combination of using glass filled polymers with the weight saving process of GAIM enables high production levels of light weight load bearing components.

The process used in this project and GAIM of glass-reinforced polymers have some similarities, where the gas is trying to flow through the glass filled polymer in order to fill the moulded part. The preparation of a glass reinforced material is identical to conventional injection moulding, where the polymer and reinforcement are fed into a heated barrel with an internal screw which mixes and shear heats the material whilst drawing back to prepare the desired shot weight. Unfortunately, during the processing the reinforcement is broken up by a) the screw, b) the injection of the material, c) the gate and d) the tool geometry. However, optimising each of these areas can minimise this breakage [89].

Becker, Koelling and Altan, [90] investigated the effect of glass weight fraction and length on the gas channel appearance in a 12mm diameter, 600mm long spiral gas channel. Both polypropylene and polyamide matrix were used with different glass lengths and glass weight percentages. Each material was tested using both conventional and gas assisted injection moulded parts, each with a specific set of processing parameters. Although this would allow any change in result being

accredited to the material change, the processing parameters may not be optimised for each material and so a better result may have been found if the parameters were optimised. The investigation results showed that all of the GAIM parts with glass lengths over four mm, had some degree of fibre agglomeration or “fuzziness” where glass rich areas occurred in the centre of the gas channel, within the first 75mm length. The channel then generally alternated randomly between clear smooth sections and fuzzy glass rich sections. The extent of these glass rich regions, increased with increasing glass length and loading. Low delay times between the polymer injection and gas injection were needed to reduce the chance of the fibre agglomeration and hesitation marks.

### 3.2.5. Alternatives to Gas Injection

Recent commercialisation of developments such as using water [91] or cryogenically cooled nitrogen gas [92] instead of room temperature nitrogen gas have produced thinner wall sections and reduced production cycle times. Water Assisted Injection Moulding (WAIM) [93], uses water’s higher thermal capacity and conductivity to remove heat more quickly from the polymer. Many aspects of the process are fully understood and documented. However, in industry, some aspects that are not so fully scientifically documented are generally left to the operator’s experience to say what will work and what will not.

## 3.3. Compression Moulding

The simple act of squeezing materials between two halves of a mould dates back to ancient times where materials were either pressed like grapes to extract the juice, or

embossed to create decorative items or coins. Compression moulding generally specifies the processing of polymers where forging indicates metal stamping.

A wide variety of polymers can be compression moulded including elastomer, thermoplastic and thermoset polymers [9], although it may not be the most efficient process for all of these polymers. The general requirement is that the polymer can flow and solidify after a short period, before being ejected. The vast majority of polymers that are processed by compression moulding are fibre reinforced and, of these, the vast majority use glass fibres, with a market of 2.28 billion pounds in 2002 [9]. Although injection moulding has a far higher capacity and able to process short and medium length glass fibres more efficiently over compression moulding, the low fibre attrition, low flow distances and ease of processing, make compression moulding best suited to processing longer or continuous fibres. The attraction of compression moulding is the cheapness and simplicity of the process and machinery. It can run at high production volumes and the cycle time is only limited by the material's properties. The tooling costs are high, although not as high as injection moulding, so the production volumes need to be high enough to justify the initial capital costs, typically  $10^3$ - $10^6$  parts per year [9]. Two of the most popular compression moulded, glass reinforced, thermosetting materials are Bulk Moulding Compounds (BMC) and Sheet Moulding Compounds (SMC) [9]. However, thermosetting polymers are outside the scope of the project. The two most popular compression moulded, glass reinforced thermoplastics, are GMT and LFT, therefore, this section will concentrate on GMT and LFT materials.

### 3.3.1. Processing Cycle

Compression moulding involves using a force exerted by a machine press, to shape a mass of pre-measured material, known as the charge. The pre-measured charge of material is heated in an oven and transferred to an open mould tool. With the heated blank material placed inside, the mould tool is closed and the material forced to flow around the mould to create the part. The types of oven typically used to heat the charge are contact, infrared and forced convection ovens, with the charge passing through on a conveyor belt as part automation. A typical compression moulding cycle is shown in Figure 3.8. **Error! Reference source not found. Error! Reference source not found.**

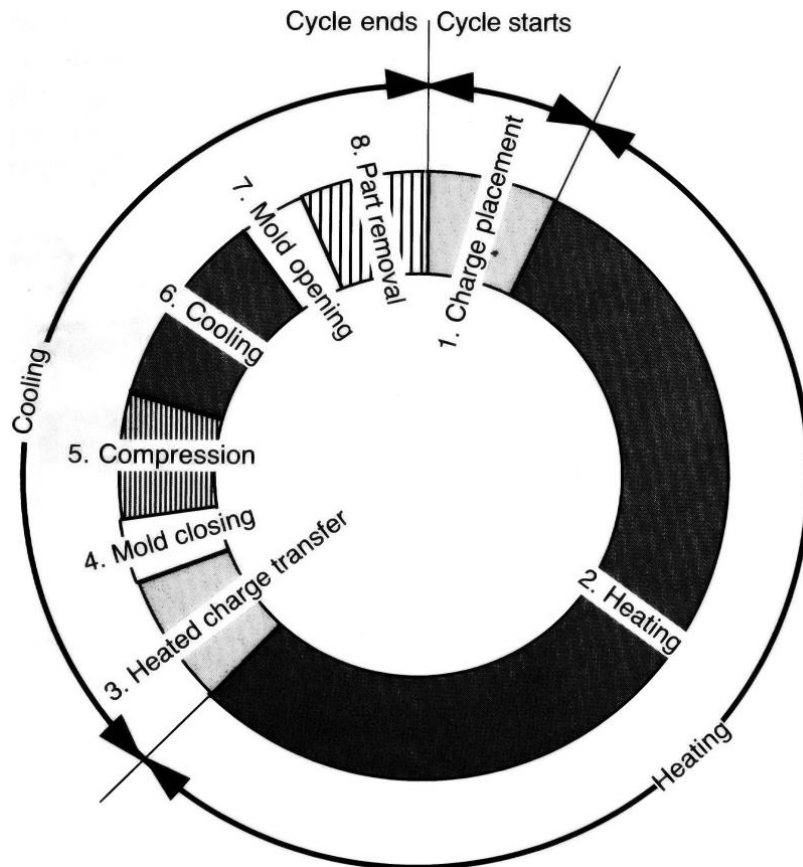


Figure 3.8 - Diagram of typical compression moulding cycle [9]

Once the mould tool has closed, the clamping force is applied until the part has cooled sufficiently to be dimensionally stable whilst it fully cools, as the part will go through two stages of solidification and contraction. In the initial stage, rapid semi-crystallization will take place as it encounters the relatively cold mould tool. Once the part has sufficiently cooled, it is removed and the next blank is placed in the mould, ready for the process cycle to start again. Over the next 24 hours, the part fully crystallizes however, like injection moulding, internal stresses and non-isothermal cooling could cause the part to distort.

The initial cooling time is typically the longest section of the cycle time and many techniques are employed to reduce this time as much as possible. Such techniques as running mould tool heating and cooling channels, where the tool is heated before the material charge is placed in the mould. This prevents the material from cooling below its melt temperature before the part has been filled. Once the component has been fully moulded, the tool is then cooled using chilled water to reduce the cooling time. This requires a lot of energy as the mould tool will go through large temperature changes over short periods. Processing Parameters

Several parameters on the press can affect the moulding process. Firstly, the most desirable cycle is for the press to close as quickly as possible. However in order to protect the mould tool, the press can be set to close at the fastest speed and then slowed when the two halves of the mould tool are in close proximity. If the two halves are not slowed prior to contact, then the mould tool can be easily damaged by the high-energy impact and the material will experience high shear rates, which could affect the flow properties.

The clamping force needs to be high enough to flow the material to fill the mould and provide sufficient consolidation of the composite to remove trapped air and provide dimensional stability as the part cools and contracts. However, even though a higher clamping force than necessary would not cause detrimental effects to the moulded part itself, it would make the process less efficient and increase wear of the tool and the chance of significantly damaging the mould tool surface.

M.D. Wakeman *et al.* [54] carried out a Taguchi array experiment to establish the effects of different processing parameters on the mechanical properties of compression moulded GMT. The parameters investigated were;

- A. Tool temperature
- B. Average GMT temperature
- C. Moulding pressure
- D. Time at pressure
- E. Compression velocity
- F. Transfer time delay
- G. Number of blanks

It was concluded with 95 percent confidence that parameters B, C, D and E had significant effects on the mechanical properties. The time at pressure was concluded to have the largest effect on the void content and therefore mechanical properties of the GMT laminate. It was noted in the paper, that a comparison of current literature for the processing of GMT showed that a range of authors recommended many different parameters.

### 3.3.2. Mould Tool

The shapes produced by compression moulding are generally simple with a single split line, although parts with undercuts and other features can be produced with clever tool design. The three main designs of mould tool are positive, semi positive and flash (Figure 3.9). The main difference between the three moulds is the space in which the material can flow and the amount of force exerted onto the material.

Positive moulds (Figure 3.9 (a)), also known as vertical shear edge tools, exert the full amount of force on the material, creating a high-density part. They are typically used with GMT to ensure the material is fully consolidated, removing any trapped air or voids. The shear edges are the two vertical surfaces on the top and bottom halves of the mould that pass each other, preventing the material from escaping from the mould, whilst allowing any air or volatiles to escape. The typical clearance of shear edges is 0.05mm to 0.08mm [94]. Careful control of the charge weight is needed, as the dimensions of the finished moulded part are very sensitive to the volume of material placed into the mould. External mould stops prevent the moulding surfaces from touching each other if too little or no material is placed in the mould.

Semi positive moulds (Figure 3.9 (b)) are generally volume limiting as external parts of the mould make contact before the internal plug can encounter the bottom of the tool. A small tolerance gap allows trapped air and small volume of material to escape into the flash lands around the edge of the tool. Semi positive moulds give good dimensional tolerances and are not significantly affected by small changes in charge weight, although this should be avoided. The mould should be used for designs with section thickness changes in the part.

The flash mould tool (Figure 3.9 (c)) is the simplest of the three to design and has many properties which are common to positive and semi-positive moulds. It is generally used to mould sheets or simple parts. A charge volume larger than the cavity volume of the tool is compressed causing excess material to escape before the two halves of the mould close on the flash. Flash and semi positive mould tools may need to be processed post moulding to remove any flash, adding cost and time to the part production.

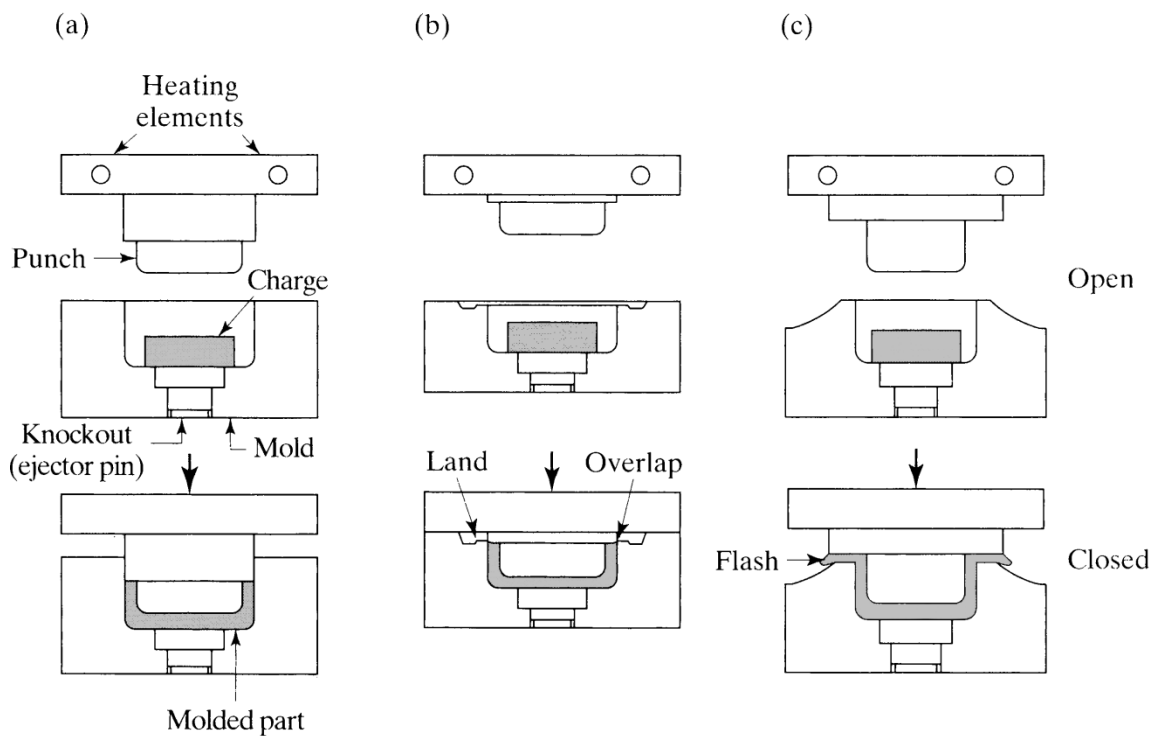


**Figure 3.9 - Compression moulding tools, positive (a) semi positive (b) flash (c) [53]**

Moulding features such as overhangs and undercuts are not possible unless the mould tool shape is orientated so that the part can be released or the mould has sliding sections. In order to help release the part, the tool has a draft angle of 1-3° machined into the vertical sidewalls, allowing the part to be easily removed using ejector pins or by hand.

The material can be isothermally moulded, where cold material is placed into a cold mould and the mould tool closed. The mould tool is then heated until the material is molten, after which full moulding pressure is applied. Both the mould tool and material are then cooled to allow the removal of the part. This method is however very slow as the large mass of the mould tool and material has to be heated as well as cooled in a single moulding cycle. The conventional moulding process is a non-isothermal process, where the material is pre-heated before moulded in an unheated mould.

### 3.3.3. Glass Mat Thermoplastic Rheology

Glass flow and orientation have been strongly linked with mechanical properties such as strength modulus and impact resistance. Some studies have used this relationship to prove fibre flow and orientation in the part when other inspection methods, such as optical microscopy, proved to be too difficult. The rheology is therefore important in understanding and predicting the mechanical properties of the composite part. This section will only cover the rheology of GMT while short and long glass fibre thermoplastics will be discussed at a later stage. The addition of glass fibres to the polymer, in either mat or dispersed form, changes the rheology of the polymer. Glass reinforced polymers exhibit shear flow when flowing through constant sections and extensional flow when passing through thinning section changes such as a die or nozzle entrance. Extensional flow causes the polymer to thin and extend whilst the velocity increases as the polymer passes through smaller cross sections.

M.D. Wakeman *et al.* [54] reported that during the non-isothermal compression moulding flow of GMT, the outer blanks quickly cool and remain in their original position, whilst the blanks in the centre have an initial stage of squeeze flow, before commencing fountain flow. The non-isothermal flow begins as the material next to the cool mould surface creates a frozen skin and the GMT in the centre of the blank flows outwards in a fountain flow. Several studies have characterised [95-97] the rheology during the isothermal stage

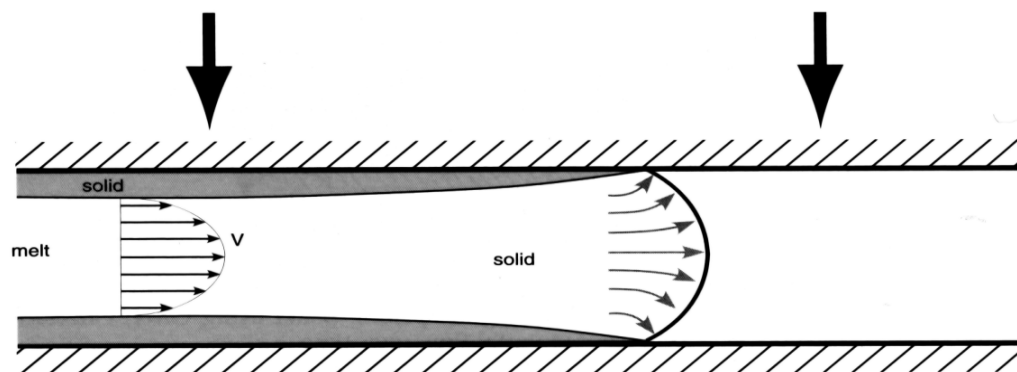


**Figure 3.10- Fountain flow and solidification of GMT during compression moulding [9]**

Polymers are generally shear thinning non-Newtonian materials meaning that their viscosity decreases with increasing shear rate [8]. However, certain factors and additives can alter the rheology, these include:

- Matrix rheology
- Fibre length
- Fibre orientation
- Fibre weight fraction
- Melt temperature
- Shear rate

Davis, *et al.* [9] wrote that the lower the viscosity of the material the higher the fibre-matrix separation. It was also noted that low mould tool closing velocities would cause the polymer to push through a glass mat, separating it from the mat, where as a high closing velocity would be able to force apart any interactions the glass and polymer had with each other, flowing the glass along with the polymer. Polymer flow and fibre distribution in compression moulding are of great interest and importance to the operator, as they will define the physical characteristics of the part. The flow length is directly influenced by the size of the blank. The dimensions, number of blanks and blank position can significantly affect the flow and fibre distribution of the composite.

The act of flow naturally aligns the fibres, so fibres close to or at the initial position of the charge will have the same orientation as the charge. G. Nilsson *et al.* [98] investigated the effects of flow on the fibre orientation and the resultant mechanical properties of compression moulded GMT. Both swirl random mat, manufactured by melt impregnation, and short fibre, manufactured by slurry deposition, with glass fibre weights of 20, 30, and 40 percent, were investigated. It was noted that the extent of fibre orientation was the same in both the swirl mat and short fibre composites.

Stokes and Bushko [99] investigated modulus and strength in random glass fibre thermoplastic composites. They showed that the modulus and strength vary significantly over the surface in the composites. Ericson and Berglund (12) related the modulus and strength to the microstructure in commercial GMT.

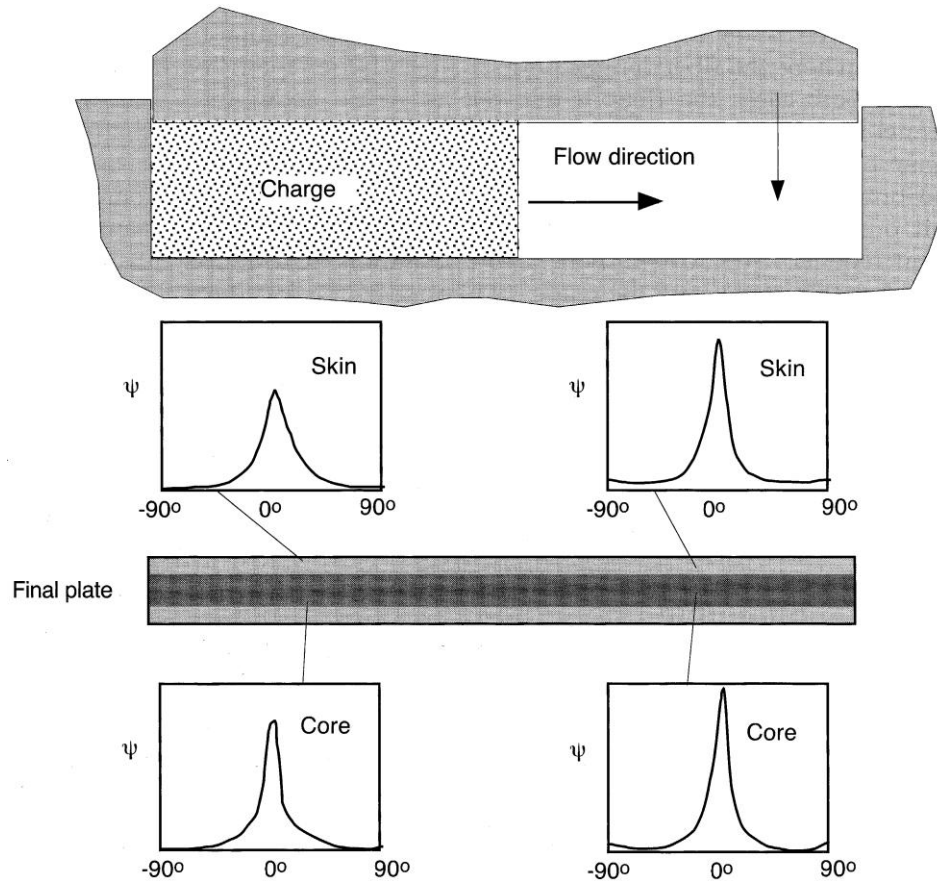


**Figure 3.11 - Fibre orientation distribution in compression moulding flow, where  $\Psi$  is the fibre count [9]**

As with injection moulding, knit lines can appear where the polymer flow has to split around objects in the path of the flow and rejoin. These knit lines are largely resin rich and have no fibre reinforcement across them, causing a weakness in the part [94].

## 4. Literature Review Summary

Key factors established in the literature review were used to create a knowledge base for the experimental work carried out during this project. Key factors about the material, material flow in GAIM and compression moulding were taken forward.

There are various glass fibre architectures contained in glass reinforced polypropylene, with a needled mat being the most common in GMT. A dispersed glass fibre architecture and a unidirectional glass fibre architecture are also possible.

The material flow in compression moulding and GAIM is a fountain flow. The thickness of this frozen skin is affected by the flow rate, where a high flow rate will produce a thin frozen skin.

Hesitation marks occur in thermoplastic processing where a flow front temporarily stops and starts to form a skin of frozen material. This is common in GAIM where the transition from polymer injection to gas injection occurs.

The gas injection of glass reinforced polymers can create alternating sections containing a smooth cavity and polymer/glass fibre separation. The fibre agglomeration could not be eliminated in materials with a glass fibre content greater than 30 percent or glass fibre length greater than 6mm.

The most influential processing parameters in the production of a gas cavity in GAIM were found to be the shot size, the gas injection delay time and the polymer melt temperature.

## 5. Methodology

Figure 5.1 shows a mind map visualisation of the methodology, materials and tool designs used in this project. It shows the different materials and the characterisation methods used for both the material and moulded parts. The rheology and material composition were examined to establish the differences between the materials. The pin and tool designs were changed to investigate the effects they had on the process

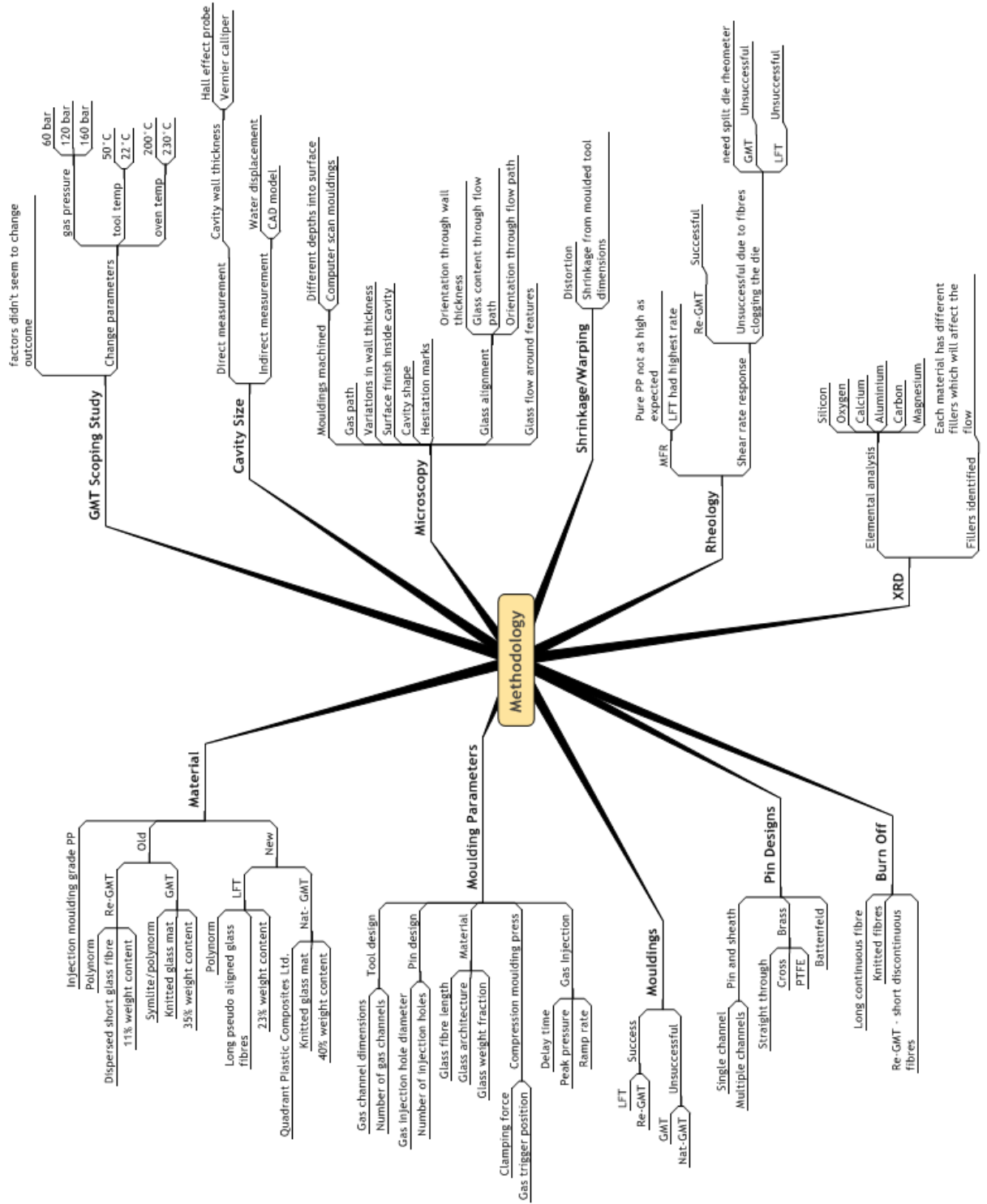
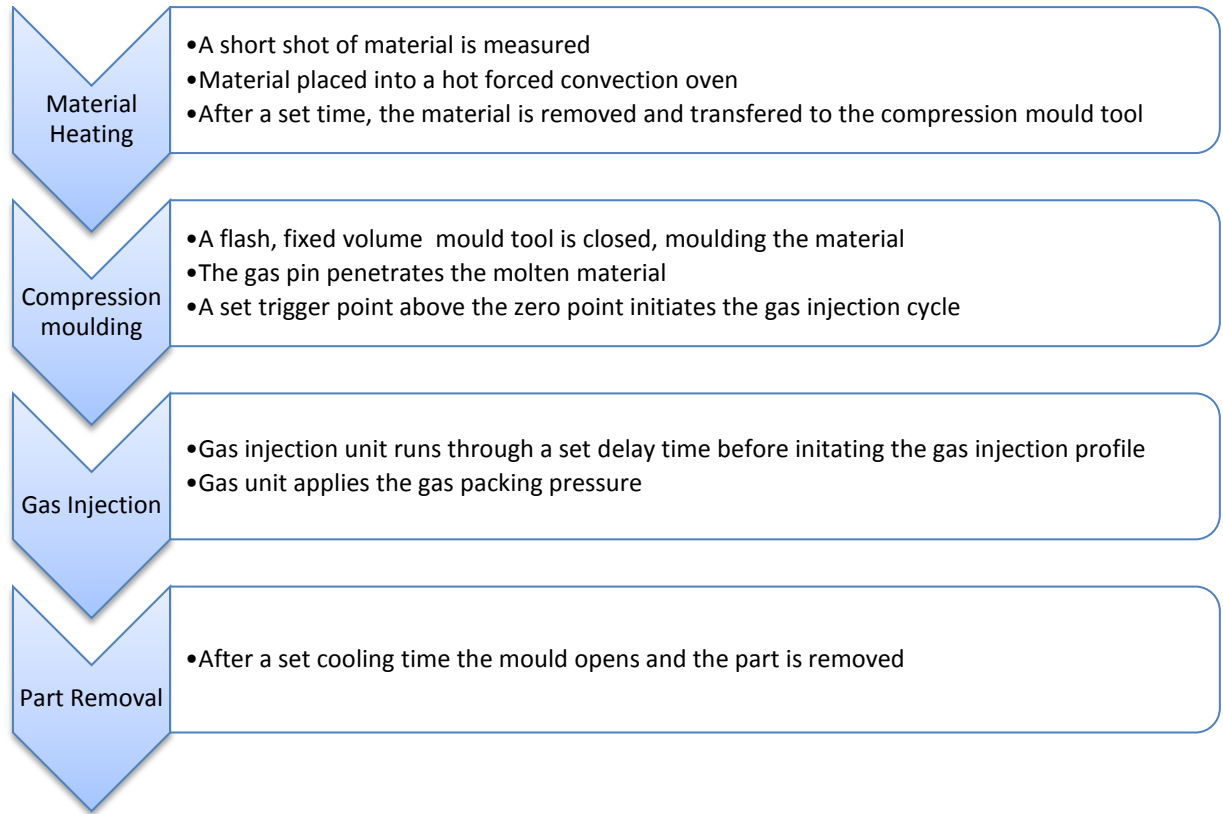


Figure 5.1 - Mind map of project progression and methodology

## 5.1. Processing Cycle

Figure 5.2 shows the sequence of events for a typical GasComp moulding cycle. A short shot of molten material is moulded in a flash, fixed volume compression mould tool. The short shot fills around 80 percent of the cavity volume during the compression moulding stage. A short shot volume of 80 percent was chosen from pre-screening trials and literature from GAIM that showed that this provided a large cavity potential, whilst have a low chance of gas breakthrough. A gas pin integral to the mould tool then injects gas into the centre of the molten material, which cores out the part, causing the material to flow and fill the remaining 20 percent of the mould. The trigger point is a set distance above the point where the mould tool is fully closed. This point begins the countdown of a gas injection delay time after which gas injection profile is followed. Once the gas profile has been completed, any excess gas pressure is released after a set vent time has expired. After the cooling time, the mould tool is opened and the part is removed. These sequence of events is listed in Figure 5.2 and illustrated by Figure 5.3, Figure 5.4 and Figure 5.5



**Figure 5.2 - GasComp process cycle**

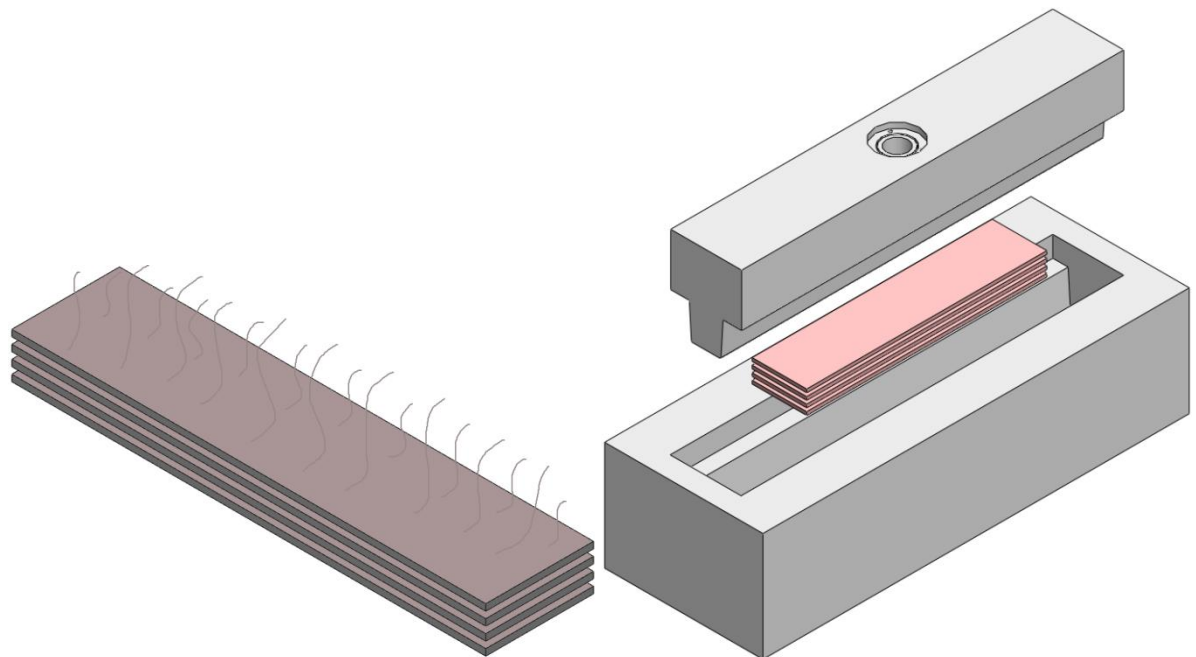


**Figure 5.3 – Illustration showing the heating of material and placing into open mould tool**

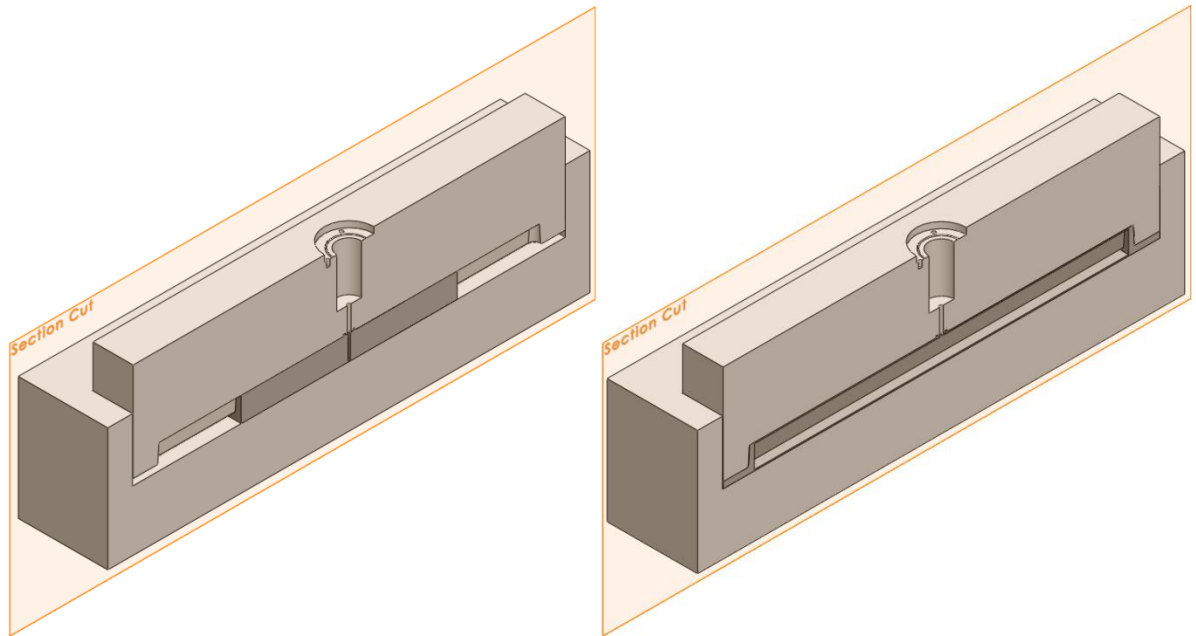


**Figure 5.4 - Illustration showing the compression moulding and gas injection stage of moulding process**

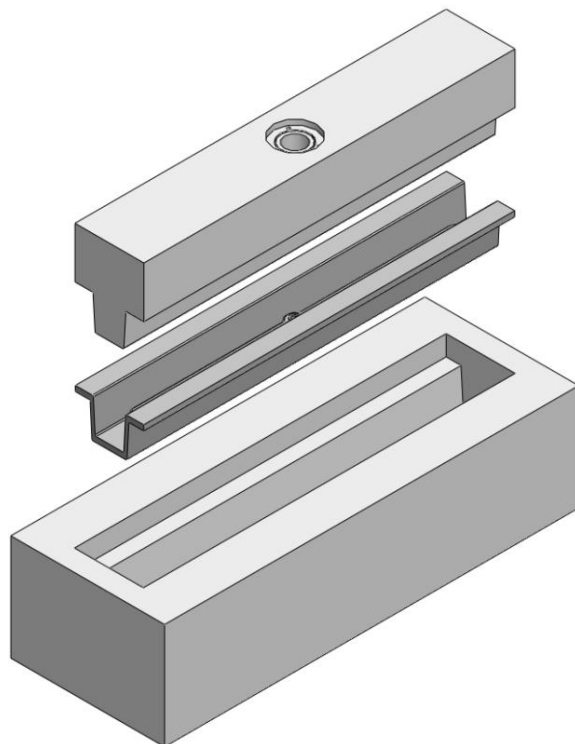


**Figure 5.5 - Illustration showing the removal of fully moulded part**

Pre-screening trials showed that a peak gas pressure between 60 and 180 provided positive results, outside of these values did not give consistently useful results. A ramp time of 1 second, was again indentified during the literature review and pre-screening trails as a suitable value. Figure 5.6 shows a typical gas injection profile. The gas reaches a peak gas pressure of 80 bar over 1 second, which is then held for 20 seconds to pack out the part.

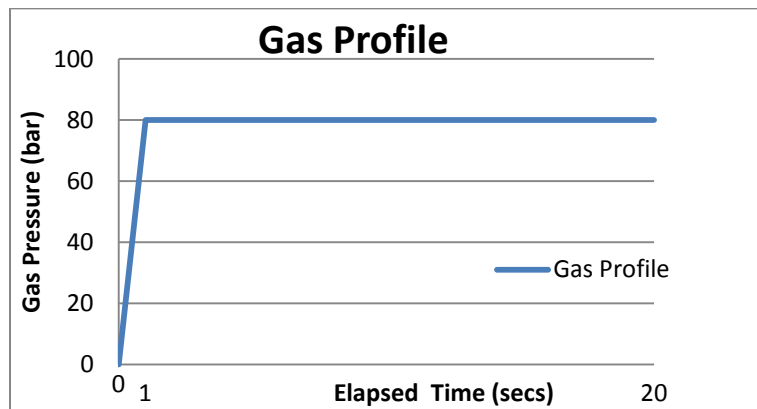


Figure 5.6 - Example gas profile

## 5.2. Processing Parameters

There were several controllable parameters involved with the moulding process. There were however some that proved difficult to control and tended to be human or environmental factors, such as ambient temperature, which will differ in winter to summer. Random factors such as blank placement were kept to a minimum, through the same operator handling the material and the use of visual aids. The blanks of molten material were stacked on top of each other prior to being loaded into the tool. Pre-moulding trials conducted experiments into the significance of the tool temperature. The tool temperatures, reached with the heating equipment available during the pre-moulding trials, did not show to have a significant impact on the

outcome of the trials. For this reason the rest of the moulding trails were conducted at room temperature.

The complexity of the process gave rise to a large number of controllable processing parameters. This is because of the amalgamation of two processes that already contained a number of processing parameters that would otherwise be set by the manufacturer. However due to the innovative nature of the process, the correct manufacturing process parameters had not yet been established. The processing parameters, with a brief explanation, are as follows:

### 5.2.1. Material

- Heating Cycle – The temperature and time at which the material was heated.
- Blank size – The dimensions of the initial material blanks, these were usually tailored to the tool geometry for better material flow. A number of blanks would be stacked on top of each other, in order to create the desired shot weight.
- Shot Weight – The shot weight dictates the volume of the material. Since the mould had a set volume, the shot weight would determine the maximum cavity potential.

### 5.2.2. Press/Mould Tool

- Tool Temperature – Typically at room temperature, but could be heated to around 50°C with an external oil heater.
- Stack – The way that the material was stacked together.

- Trigger Position – The point in the press’s travel, which signaled the Air Mould Control unit to start its processing cycle. The trigger point was between 5mm and 0 mm above the zero point, where the mould was fully closed.
- Clamp Force – The force (N) applied to the mould by the compression moulding press.
- Cooling Time – The time in seconds that the clamping force was applied for after the gas injection cycle had finished.

### 5.2.3. Air Mould Gas Control

- Delay time – The time delay between the trigger position and the commencing of the gas profile.
- Gas profile – A pre-selected profile of how the gas was injected. This was determined by a set gas pressure being reached by a set time.
  - Peak gas pressure – The gas pressure could be applied between 1 and 300 bar, which was limited by the maximum system pressure.
  - Gas ramp – The time, at which the set gas pressure was required to have been reached, was adjustable to within 0.1 seconds. The set time was absolute and not discreet, meaning it was set from the start of the gas injection cycle and not from the last set point.
- Vent time – Time delay between the end of the gas injection cycle and the release of any trapped gas. The gas was released to atmosphere through the gas injection unit.

#### 5.2.4. Additional

- Tool heat soak – The hot material could gradually increase the tool temperature by up to 10°C in extended moulding runs. This however, was not considered a significant increase when compared to the difference between the material temperature of around 200°C and the tool temperature at around 22°C
- Gas injection pin design – The different gas injection pin designs varied the gas flow rate and direction that the gas would flow with respect to the flow experienced by the compressive forces.

#### 5.2.5. Uncontrollable Factors

- Blank positioning - The position in the tool that the material is placed.
- Ambient temperature – The air temperature of the laboratory.

# 6. Investigated Materials

## 6.1. Introduction

During the project, different grades of glass reinforced polypropylene were used.

These different materials were chosen to establish the effects of differing glass lengths, weight fractions and the glass fibre architectures on the moulding process.

Table 6.1 shows, the glass weight percentage, glass length, supplied form and manufacturing method of each of the materials used in the project. The different manufacturing methods provided different glass fibre architectures.

Material	Glass Weight percentage	Glass Fibre Length	Supplied Form	Manufacturing Method
Polypropylene	0 percent	N/A	Granules	Polymerisation
Re-GMT	11.8 percent	Short	Sheet	Slurry Deposition
LFT	23.6 percent	Long	Sheet	Extrusion
GMT	34.4 percent	Long	Sheet	Melt Impregnation
Natural GMT	40.1 percent	Long	Sheet	Melt Impregnation

**Table 6.1 - Materials glass weight percentage, fibre length, supplied form and manufacturing method**

## 6.2. GMT

The GMT used in this project was constructed of two entangled glass fibre mats that had been impregnated with polypropylene, between two press belts. Two glass weight fractions of a quoted 30 percent and 40 percent glass weight fraction were investigated. However, after material characterisation tests, the 30 percent glass fibre

GMT was found to have a 34 percent glass fibre weight content. The glass lengths were found to be up to 25mm and so considered a long fibre length.

### **6.3. LFT**

The LFT was produced using continuous glass fibre filaments that were fed into polypropylene melt through an extruder. The LFT provided a glass content that was between the GMT and Re-GMT. The pseudo unidirectional glass architecture differed from the entangled glass mat of the GMT and the dispersed glass fibres of the Re-GMT. This allowed an investigation into how the architecture affected the process. The glass length was found to be up to and over 25 mm and so was considered continuous.

### **6.4. Recycled – GMT**

The Recycled GMT (Re-GMT) used in this project was supplied by Voestalpine Polynorm Plastics. It was manufactured using slurry deposition, giving a dispersed glass fibre architecture and supplied by in sheet form with a glass content of 20 percent by weight. The fibre lengths were found to be around 10mm and so were considered to be short. XRD and burn off analysis showed that the Re-GMT contained a higher percentage of fillers than the other materials. This would be due to the addition of bulking agents to the additives already present in the ground GMT. A study by Null and Denn [100] has proved that the viscosity of the material increases as the content of bulking agents increases.

## **7. Material Characterisation**

### **7.1. Material Burn Off**

The process of burning off materials in an elevated temperature, is a technique used for removing organic materials, by decomposing the material at high temperatures (300-500°C) and removing them as smoke. In industry, this process is typically used in the removing paint and varnishes from components. However, in research laboratories it is used to allow the examination of internal structures that the organic material would normally be covering. The technique was used in this project, to remove the polypropylene matrix, leaving any remaining glass fibres and filler. The glass fibre length, weight percentage and architecture could be examined as well as the composition of any fillers.

A specimen of unprocessed Re-GMT, LFT, GMT and natural GMT material, in addition to a rib tool moulding of Re-GMT and GMT were heated to 200°C and held for an hour. This initial hour ensured that the material had reached a uniform temperature and any components with a low oxidation temperature were removed. The temperature was then increased in 50°C steps to a maximum temperature of 500°C. Once the maximum temperature is reached, the material was held for a further two hours to ensure all combustibles had been removed. The oven was then left to cool and the specimens removed.

### 7.1.1. Results

The resulting fibre structures of each of the materials were distinctly different. The Re-GMT specimen (Figure 7.1) had reduced to a consistency of ash, containing an equal volume of fillers and dispersed, short glass fibres. There was no identifiable glass mat present in the remains. The LFT (Figure 7.2,) contained a higher percentage of long glass filaments with a small volume of filler. The fibres were pseudo aligned with no evidence of knitting or entanglement, giving a consistency of candy floss. The mat could not fully support its own weight, beginning to disintegrate when it was handled.



**Figure 7.1 - Photo of Re-GMT burn off**



**Figure 7.2 - Photo of LFT burn off**

The two GMT samples (35 percent glass Figure 7.3, 40 percent glass Figure 7.4) consisted of a highly needled glass mat, with strands of long glass fibres. The mats are 3mm thick and could support their own weight when handled. Both photos show

the swirls of glass strands present in the architecture. These swirls of glass fibre strands are produced during the manufacturing of the material.



**Figure 7.3 - Photo of GMT 30 percent glass burn off**



**Figure 7.4 – Photo of GMT 40 percent glass burn off**

## **7.2. XRD**

X-Ray Diffraction (XRD) is an analytical technique that fires X-Rays at a sample of flat, ground material, through a range of angles and records the reflected X-Rays. Each element and compound contained in the sample has a unique crystalline structure. At a certain angle, this structure becomes aligned to the X-Ray frequency, causing excitation of the electrons in the structure. This excitation amplifies the X-Rays reflected back to the collector and displayed as a high-energy peak. This peak is unique and can then be used to identify and quantify the compound or element

using a database. The height of the peak gives the intensity of X-Rays returned to the collector, and so the ratio of that compound contained in that sample.

Each of the materials from the fibre burn off experiment were analysed with a XRD machine. It was found that each of the materials contained similar fillers, and as displayed in

Filler name	Chemical formula	Percentage contained in material (%)
Calcite	$\text{Ca C O}_3$	45.8
Calcite, magnesium	$\text{Mg}_{0.06} \text{Ca}_{0.94}, \text{C O}_3$	16.4
Periclase	$\text{Mg O}$	13.4
Rutile	$\text{Ti O}_2$	6.4

**Table 7.1 - XRD results showing filler percentages**

### 7.3. Melt Mass-Flow Rate

Rheology figures of glass-reinforced thermoplastics are not well documented, even though they have in use for over 40 years. This is because of the extremely large number of variables that affect the flow of the polymer, requiring each material to be characterised specifically. The Melt Mass – Flow Rate (MFR) experiment is one such characterisation test that can help to establish the rheology of the material. Problems arise when glass reinforced thermoplastics are extruded through a small diameter capillary die, required to characterise the material. The glass can clog and dam up behind the die, creating an inconsistent result. A slit die is required for the characterisation of these materials, giving the required space in which the glass fibres can flow. A slit die however was not available for these experiments, so a

conventional circular capillary die was used. The processing parameters were then honed until a consistent result was established.

### 7.3.1. Design of Experiment

The standard used in this experiment was the “*British Standard – ISO: 1133:1997 Plastics - Determination of Melt Mass-Flow Rate (MFR) and the Melt Volume-Flow Rate (MVR) of Thermoplastics*”, using “procedure A” as set out by the standard. The experiment was conducted with the four different materials, Re-GMT, GMT, LFT and Natural GMT. As the Re-GMT and LFT were supplied in a semi-consolidated state, the materials were compression moulded into a flat plate prior to testing. This gave a direct comparison between the materials. Long strips with a cross section of 3mm<sup>2</sup> were cut from the plate.

The strips were packed into the test barrel and heated to the test temperature for four minutes. As the material melted, the weight of the plunger packed down the material, removing any trapped air bubbles, which would give false readings. Once the plunger hit the sampling zone, the test mass was added to the plunger and the timing started. Samples were then cut off every 30 seconds until the plunger had reached the lower sampling limit. The average weights of the samples were used in the Equation 7.1 to calculate the MFR, expressed in grams per 10 mins.

$$MFR(\theta, m_{\text{nom}}) = \frac{t_{\text{ref}} \times m}{t}$$

**Equation 7.1 - MFR calculation equation**

Where;

$\Theta$  = Test temperature in degrees Celsius

$m_{\text{nom}}$  = Test mass in kilograms

$m$  = Average mass of the cut of samples in grams

$t_{\text{ref}}$  = Reference time (10 mins) in seconds (600 s)

$t$  = Cut off time interval, in seconds.

Due to the higher glass content, the test mass used for the two GMT materials was increased to 5 kg, from the 2.16 kg used with the Re-GMT and LFT. The increased mass meant the results between the two GMT materials and the Re-GMT and LFT were not comparable. It does show however that a larger force is required for the GMT to flow.

### 7.3.2. Experimental Results

The MFR experiment results displayed in Table 7.2, show that the LFT with an MFR (200°C, 2.26 kg) of 11.35 g/10mins, had the highest flow rate over the four measured materials. This contradicted predicted results established from the literature review, which suggested that higher glass fibre length and content would increase viscosity and reduce flow rate. The results from a burn off material characterisation test, as described in section 7.1 Material Burn Off, show that the Re-GMT contains a large number of fillers that increase the viscosity of the material. Some of these fillers were flow enhancers and so the combined effect of bulking agents and flow enhancers

created a MFR (200°C, 2.26 g) of 1.39 g/10 mins, which was only just higher than pure polypropylene (0.59 g/10 mins). The burn off results showed that the LFT also contained flow enhancing fillers, which would account for the increased flow rate. The 30 percent GMT had a higher MFR (200°C, 5 kg) of 23.42 g/10 mins than the 40 percent GMT with an MFR (200°C, 5 kg) of 4.89 g/10 mins. This agreed with the literature, which showed that the viscosity increased with increasing glass weight fraction

Plunger Mass (kg)	<b>2.16</b>			<b>5</b>	
Material	LFT	RE-GMT	Pure PP	GMT	Natural GMT
MFR (200°C)	<b>11.35</b>	<b>1.35</b>	<b>0.59</b>	<b>23.42</b>	<b>4.89</b>

**Table 7.2 - MFR Results**

## 7.4. Twin Screw Rheometer

Whilst the MFR experiments gave a good result and comparison between the materials, it was recognised that this was only at one particular shear rate for each material. So that each material could be characterised at several shear rates, a twin screw rheometer was used.

The machine uses two barrels to measure the pressure in a short and a long capillary die as shown in Figure 7.5. The two lengths are needed to give a true indication of the shear stress and shear viscosity for the material by using the two pressures in the Bagley and Rabinowitsch correction calculations. These corrections adjust the viscosity and shear stress calculations by accounting for extensional viscosity which

can occur at the long die entrance and the fact that viscosity decreases as the shear increases.

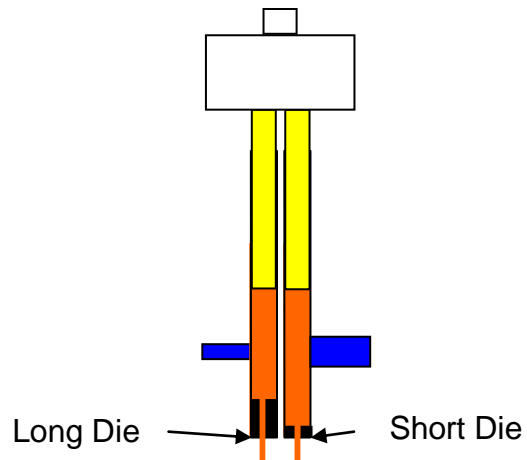


**Figure 7.5 - Diagram showing configuration of the twin screw rheometer test rig**

### 7.4.1. Design of Experiment

Each material was packed into both barrels and heated for four minutes as the plungers were gradually lowered to pack the material and remove any air bubbles. Once the material was fully molten and consolidated, the machine would increase the screw speed to a set speed. Once the material reached a stable state, as measured by the two pressure sensors in the dies, the screw speed would increase to the next test speed and repeated until all of the test speeds were measured.

### 7.4.2. Experimental Results

Unfortunately, due to the glass fibres clogging the capillary, no meaningful results could be gathered or presented.

## 8. Project Mould Tool Design

Four mould tools were used throughout the course of the project, they were;

1. Rib Tool
2. Star Tool
3. Picture Frame Tool
4. Spoke Tool

All of these mould tools were manufactured in-house, with the star tool, picture frame tool and spoke tools being designed by the author during the research, using Solidworks 3D CAD design software [101]. However, only the rib tool and star tools were used for scientific study and so the report will concentrate on these tools. The picture frame and spoke tools were successfully used for proof of concept.

The rib tool contained a gas injection pin in the centre of a single, small cross sectional area rib. The star tool was considerably larger in area, containing four ribs with a significantly larger cross sectional area. The gas injection pin was located above a large hemispherical cut out, creating a large mass of molten material around the pin. This was designed to reduced freezing around the pin and increasing the thermal mass.

### 8.1. Rib Tool

The initial mould tool used in the project was intended for moulding GMT, and so was a positive plug design with a vertical shear edge as the mould tool parts which required a full consolidation. This design created a variable volume part depending

on the shot size. To enable the GasComp process to work, a mould tool with a fixed cavity was required, so the gas could continue to flow the material after the compression moulding stage. To create this fixed volume cavity, moulding stops were used to prevent the tool from fully closing and create a 5mm gap between the moulding faces. The gap allowed the injected gas to push the material into the remaining volume created by the shot short. The mould tool was manufactured from aluminium and bolted to top and bottom steel bolster set. This bolster set would allow quick and easy modular tool changes, reducing the number to clamping systems used on the press and the time taken to change a tool.

Figure 8.1 shows the technical drawings of two views of the rib tool showing the internal cavity, one with the tool together and the other side-by-side. Figure 8.2 shows the mould tool with the side removed to show a moulded part between the upper and lower mould tools. Figure 8.3 shows the dimensions of a moulded part with a mass of 218.01g and a volume of 222.45 cm<sup>3</sup>.

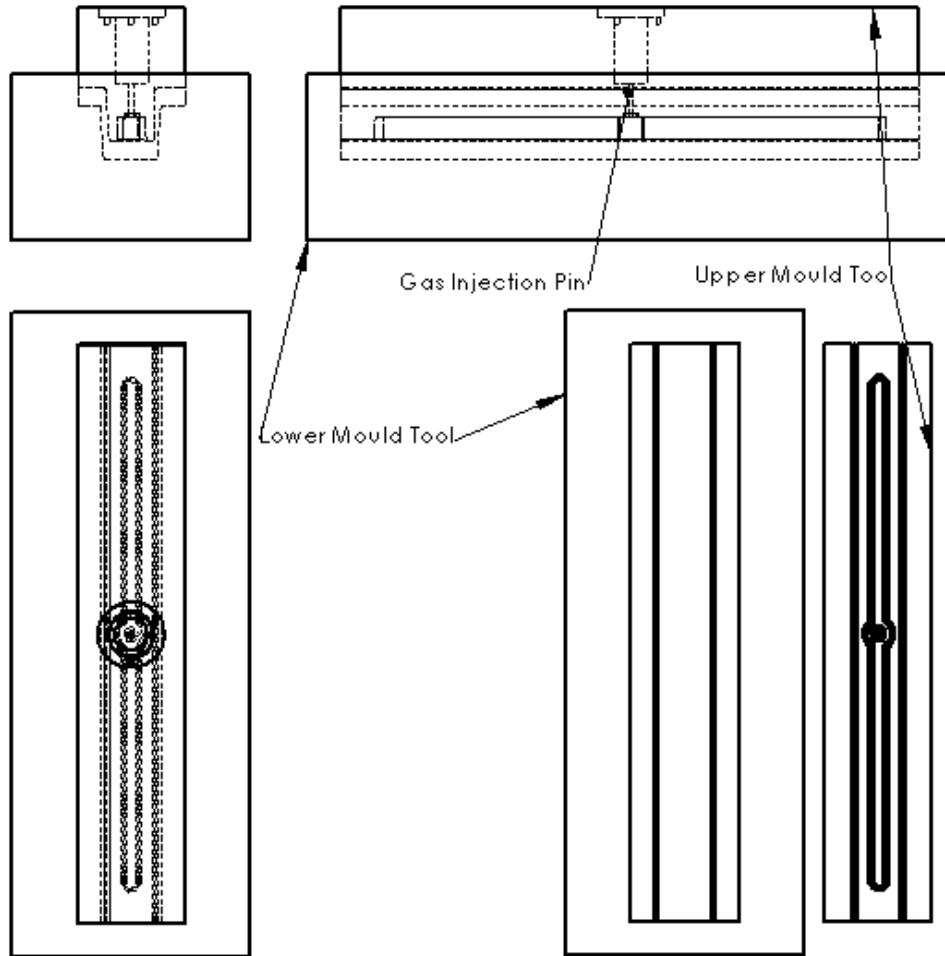


Figure 8.1 - Technical drawing of rib tool

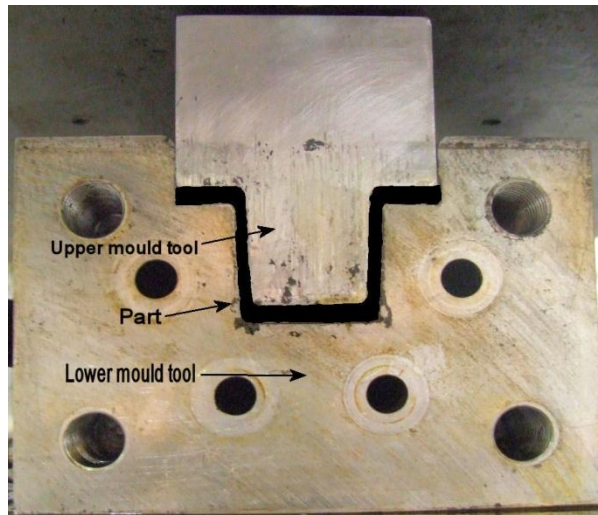


Figure 8.2 - Photo of rib tool with its side removed, showing upper and lower halves of rib tool with moulded part inside

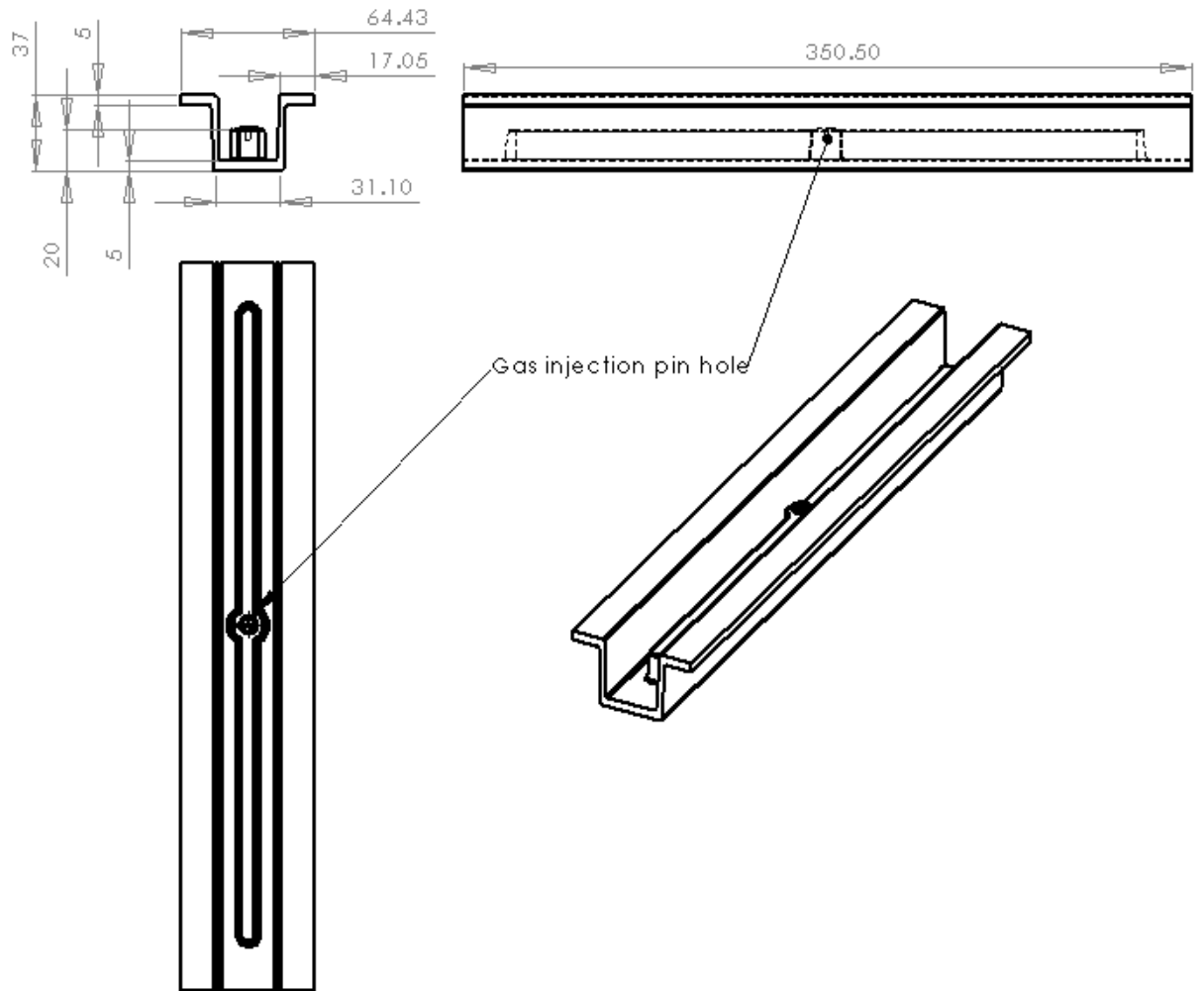


Figure 8.3 – Technical drawing with dimensions of part created by the rib tool

### 8.1.1. Mould Tool Development

During the course of the project, due to the results of the experiments, some dimensions of the rib tool were altered. Both the sidewalls and bottom flange thicknesses of the tool were increased using shims of aluminium plate. This was to investigate how a reduced part wall thickness would affect the gas fingering away from the main rib.

The rib tool contained oil heating channels which could be connected to an external tool heater. The heater was limited however, as temperatures above 100°C required an additional, external water chiller, which was not available during the project.

## **8.2. Star Tool**

The star tool was a new flash plug design with a deep rib section and a horizontal clamping face, rather than a positive plug mould design with a vertical shear edge. This meant that the tool would always clamp onto the flat face of the tool creating a fixed part volume. The large clamping face eliminated the need for a tight tolerance, vertical shear edge that would prevent the material from escaping from the mould tool. This would dramatically reduce the complexity of the mould tool design as well as the high wear rate that a vertical shear edge would experience. As this project has shown, the upper half of the mould tool can become modular, dramatically reducing capital costs.

A large hemisphere cavity was machined around the point where the gas injection pin would lie in the mould tool. This meant that a large volume of material would be formed around the pin, providing a large mass of molten material for which the gas can flow. The large mass would stay molten for a longer period than a small mass, decreasing the chance of the material from freezing around the pin flow the material before it freezes off.

The tool was manufactured from an aluminium block to enable it to be part of a modular system that would allow it to be changed quickly by hand. The prototype level of production meant that the tool would not see excessive wear from the

production of high number of parts that would necessitate a steel tool. All subsequent tools were made in this fashion.

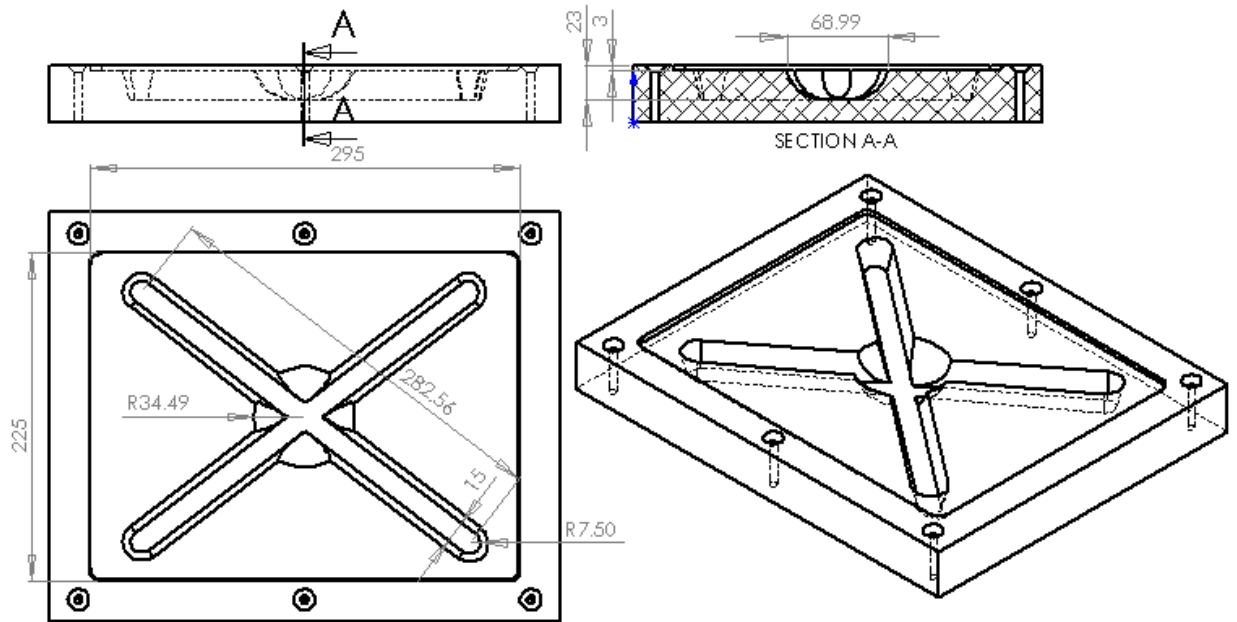


Figure 8.4 - Technical drawing of star tool

### 8.3. Other Tools

The picture frame and spoke tools used in this research were used for the proof of concepts. The picture frame Figure 8.5 was initially designed to establish the maximum length of cavity, produced by a single gas injection pin. However, the large mould tool volume used over 500g of material per part. With the limited material resources, the number of mouldings produced by the picture tool design was limited.

Figure 8.6 shows the technical drawing for the spoke tool, containing eight ribs with a small cross section. The concept was to ascertain if the gas could flow into numerous ribs and the flow pattern of the gas. The concept proved to be successful with pure polypropylene parts containin approximately 25 percent cavity volume.

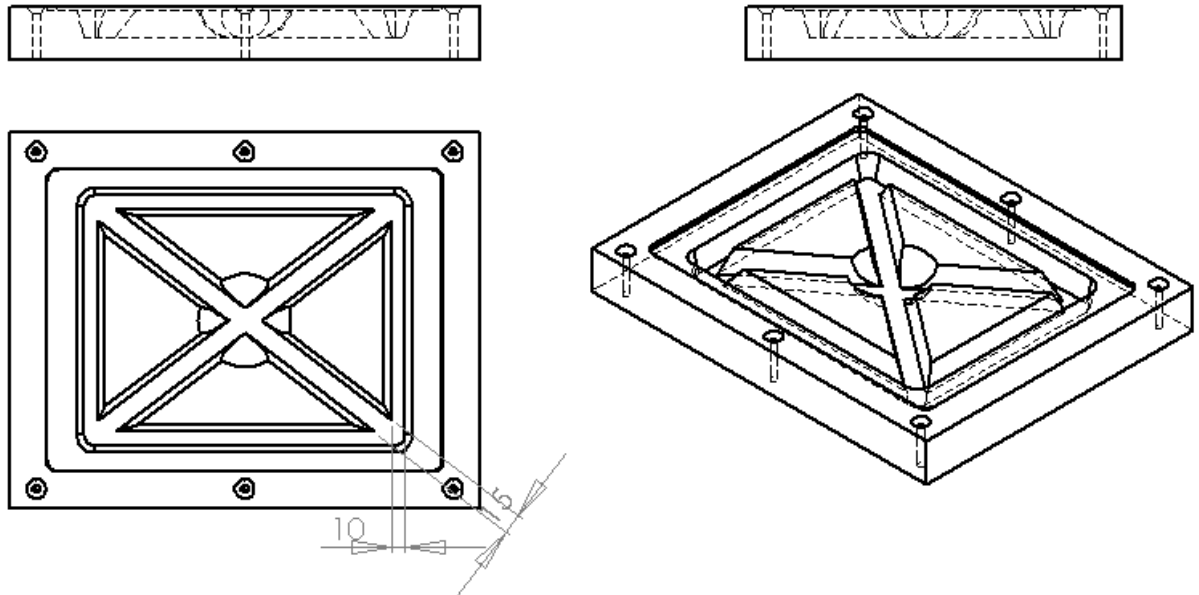


Figure 8.5 - Technical drawing of picture frame tool

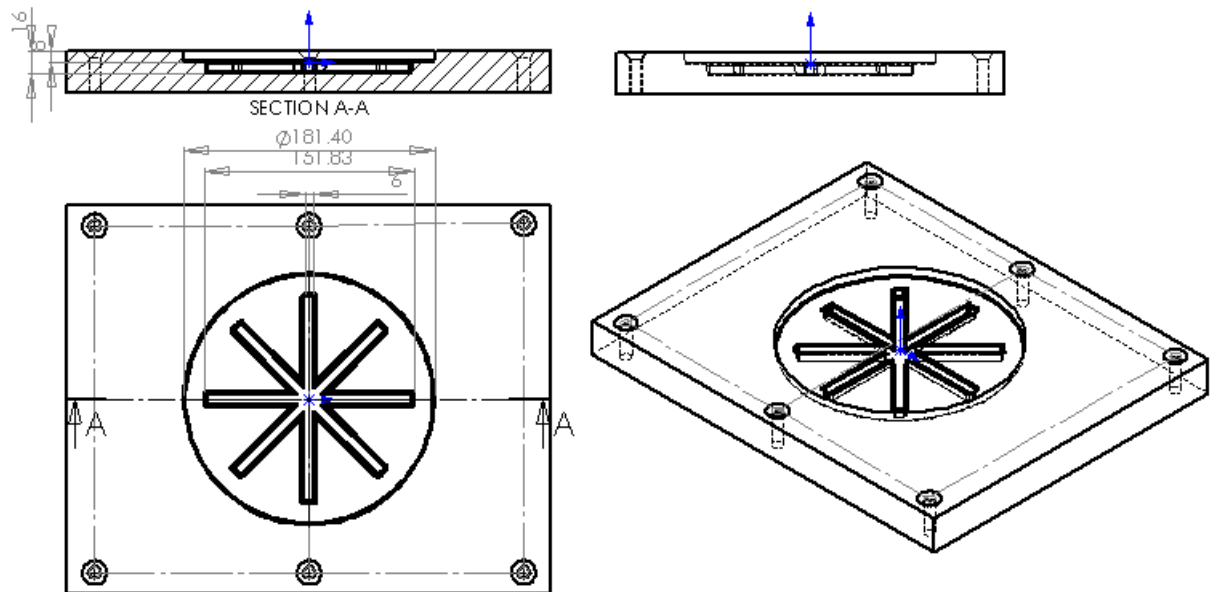


Figure 8.6 - Technical drawing of spoke tool

## 8.4. Gas Injection Pins

Several designs of gas injection pins were manufactured to determine their effect on the outcome of the moulding. The rib tool had an integral, spring-loaded pin designed by Battenfeld IMT. The star and spoke tools were designed to accommodate a

variety of pin designs that could easily be changed (Figure 8.7). The depth of the gas pin injection was always positioned in the centre of the polymer melt to ensure an even gas flow through the material.

A notable problem of the material freezing onto the pin, which blocked the gas from penetrating the material was investigated. An additional pin was manufactured in PTFE with a single through hole. Unfortunately, on first use: the PTFE pin melted, collapsed, and then stuck in the moulded part. This was surprising as the maximum working temperature for PTFE is around 250°C. One possible reason for failure was the high gas pressure stripping the pin of its thread.

Various solutions were tried in order to help prevent the material freezing on to the pin. One was to apply heat directly to the pin using a heat gun held close to the pin and then taken away in the last moments before the material was loaded into the press. This did not prove to be a successful technique as the brass pin, with a high thermal conductivity, conducted the heat straight into the steel plate. This could not be avoided, as a close fit between the pin and the upper tool was required to prevent gas leaks. The largest heating effect came from extended moulding runs, where the hot part was left to cool in the mould tool until the next batch of material was ready.

#### 8.4.1. Rib Tool Pins

The gas injection pin used in the rib tool was designed by Battenfeld Ltd. The pin had a spring loaded shut off valve that kept the valve shut whilst it penetrated the material. The pin was forced open by the applied gas pressure, allowing the gas to flow into the material. This design prevented any ingress of material during the compression

moulding cycle, which could block the pin and prevent any gas from reaching the material. This pin design was the only design used with the rib tool.

### 8.4.2. Star Tool Pins

As the star and spoke tools used the same upper mould tool, the pin designs outlined in this section could be used for both bottom mould tool designs.

There were several initial designs for the gas injection pin for use with the start tool.

All of which had:

- 10° draft angle to aid part removal
- 8mm thread for securing into the tool
- 1mm outlet hole

The initial design (Figure 8.7 (A)) had a simple, machined 1mm diameter gas outlet for maximum airflow. As the gas injection hole was machined in the same direction as the vertical movement of the mould tool, polymer could be pushed up into the pin, blocking the gas. The design was modified to contain four cross-holes (Figure 8.7 (B)), allowing for a greater gas flow and remove the outlet hole from the direction of penetration. A third design (Figure 8.7 (B)) involved covering the pin in a PTFE sheath to reduce the freezing effect of the pin. It was found that these pin designs experienced polymer ingress due to the relatively large diameter of the gas injection hole. The manipulation of the gas profile, where a low gas pressure was applied as the pin encountered the material, reduced the blocking effect. It was also found that the gas pressure was generally sufficient in unblocking the holes.

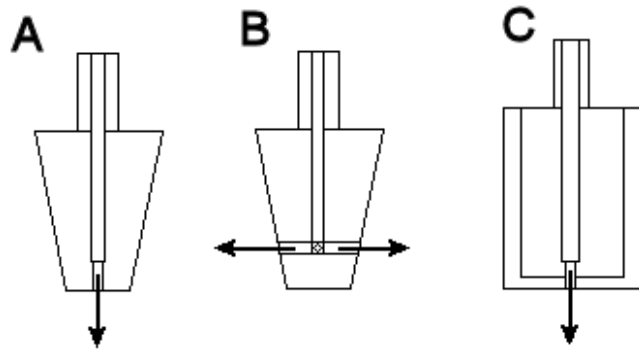


**Figure 8.7 - Design drawings of brass gas injection pins. A: Straight through B: Four way cross hole C: PTFE sheathed. Arrows denote gas direction.**

A new pin, designed by Kylash Makenji of WMG, University of Warwick, UK, provided a smaller section for the gas outlet. The smaller section prevented the ingress of polymer but did also lower the gas flow rate. The pin involved having a barrel with a shallow, 0.025mm deep, cross groove cut into the end face. A screw with an internal gas hole then clamped down on to the top face. The resultant cross section proved to have a too low a gas flow rate, with the pin producing low cavity volumes. Figure 8.8 shows the components of the gas pin design whilst Figure 8.9 shows the assembly of the two components.

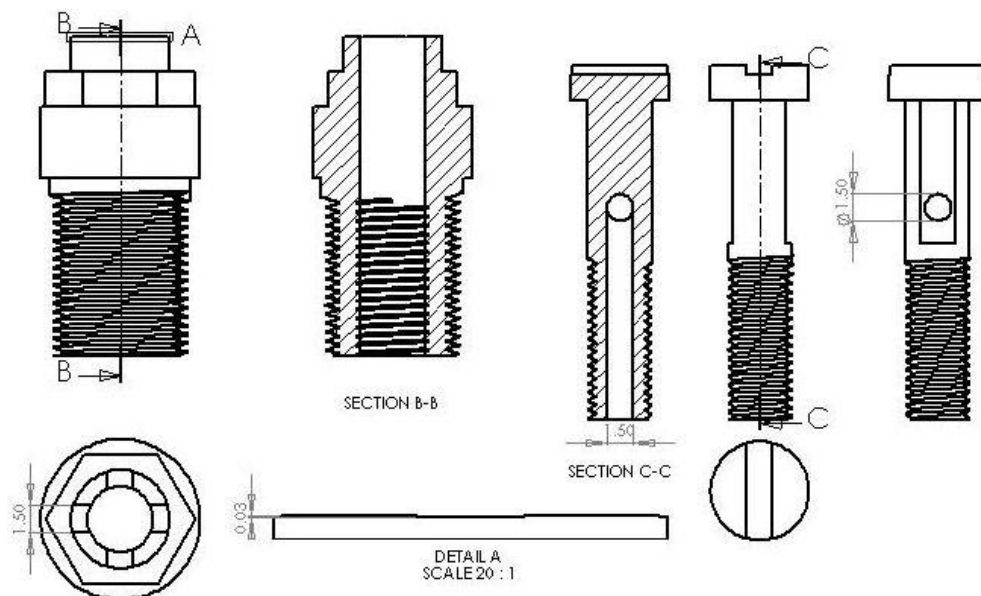


**Figure 8.8 - Cross cut bolt gas injection pin**

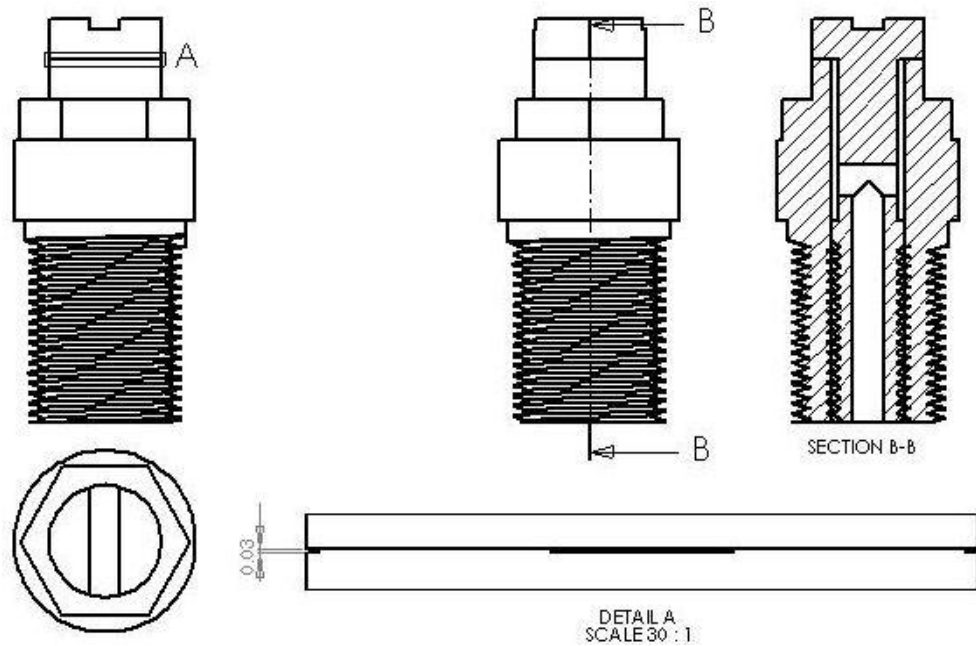


**Figure 8.9 - Screw down pin and collar gas injection pin design**

The design was altered to accommodate different gas outlet shapes, with a deeper cross section of 0.25mm, to increase the gas flow rate. A modular design was adopted where several sheaths had different patterns machined into the end. A bolt of identical design in Figure 8.8 would then seal against the sheath, creating the correct thickness of opening to allow the gas to be injected into the material. Figure 8.10 shows the pin and sheath and the assembled construction. This pin design proved to be successful with a high gas flow and minimal polymer ingress.

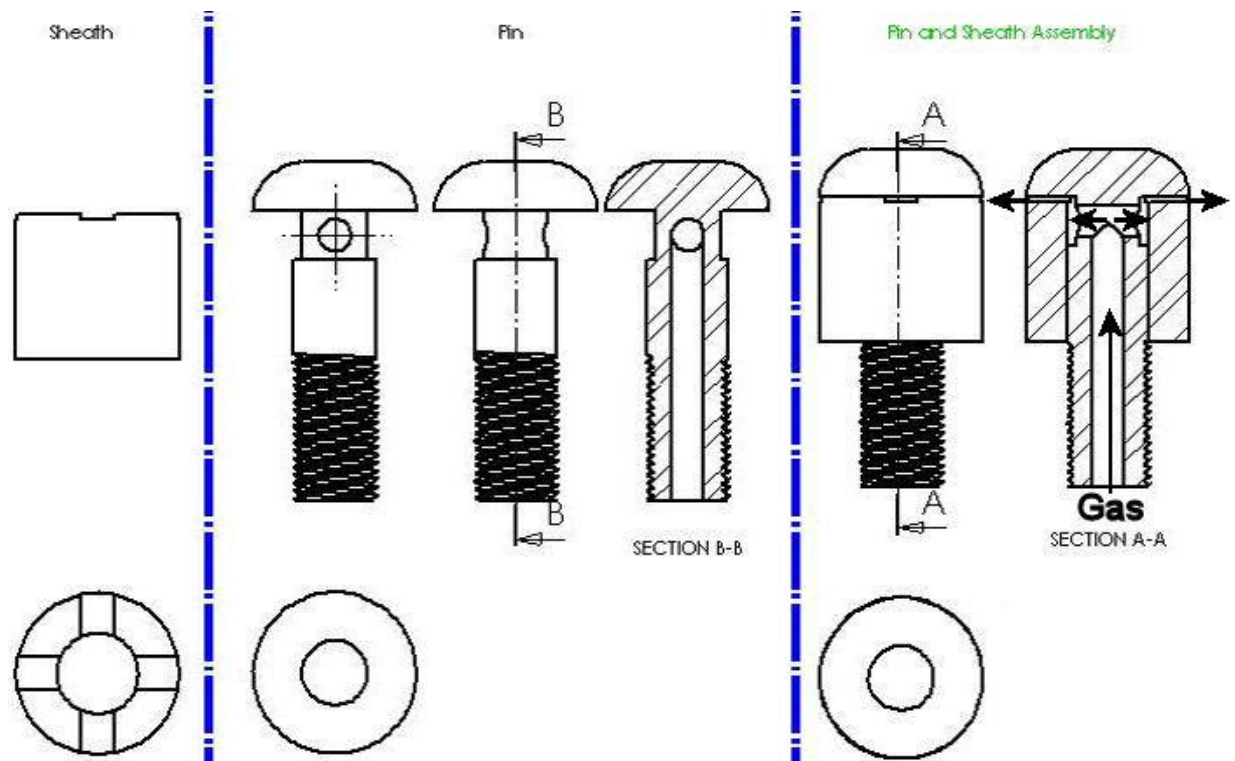


Figure 8.10 - Pin and sheath gas injection pin design and assembly

### 8.4.3. Gas Seal

The gas seal is a machined profile that encircles the gas injection point. Its purpose is to prevent any gas from escaping up and around the pin and straight out into atmosphere without penetrating the material. The gas seal does this by creating a thin ring of material that will quickly freeze, creating a physical barrier around the pin to contain the gas.

The latest pin design contained a very aggressive mould seal, with a deep section encircled by a high ridge before dropping to the level of the top mould surface. The mould seal was contained in a removable section of the top half of the mould tool to allow the mould seal to be changed if necessary in later studies. The mould seal and

modular unit can be seen in Figure 8.11 and Figure 8.12. This design proved to be successful with no gas escaping through the mould seal.

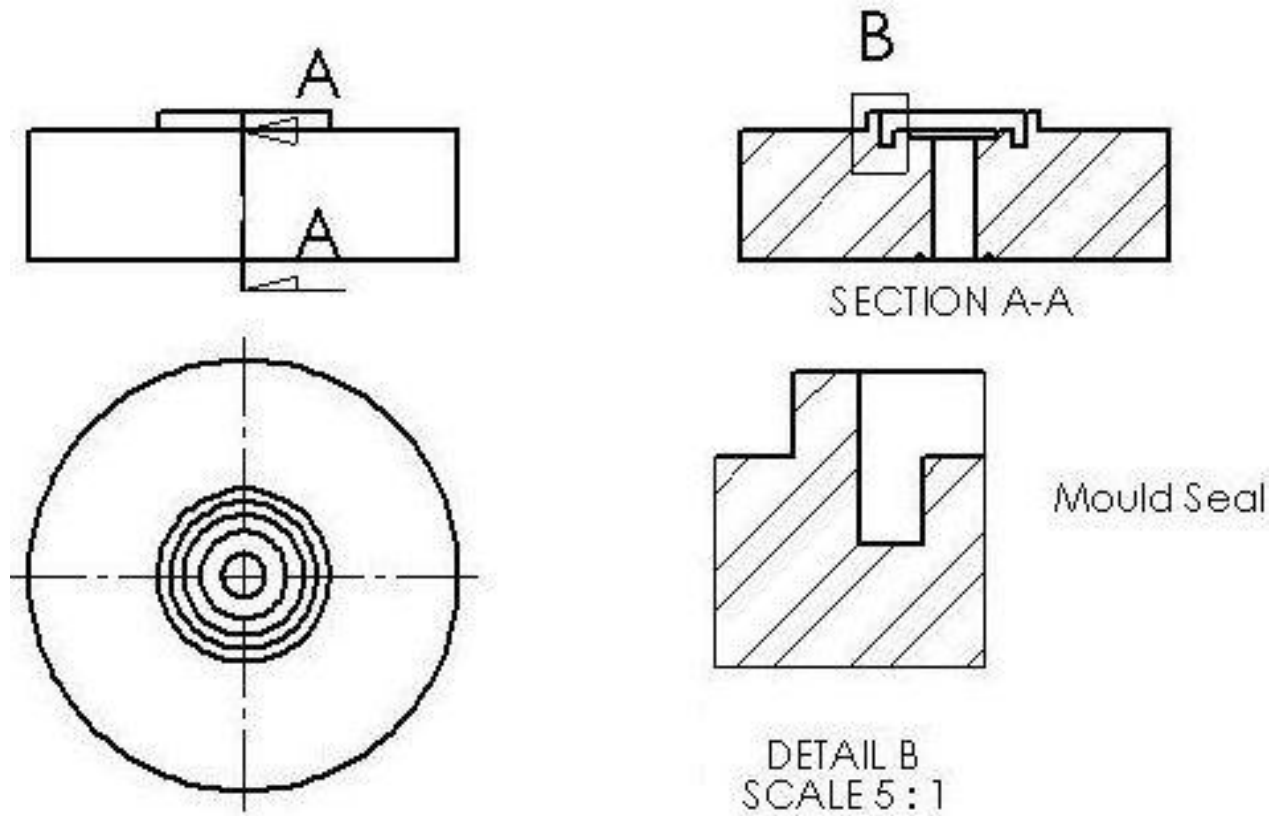


Figure 8.11 - Mould Seal

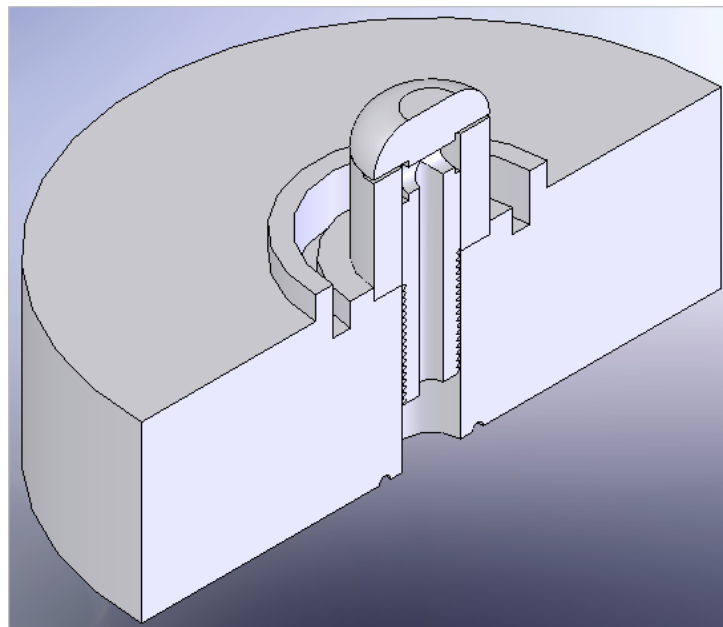


Figure 8.12 – Sectional view of pin assembly with gas seal

## 9. Moulded Part Characterisation

A number of techniques were employed to characterise the moulded parts, which allowed them to be analysed in detail. The characterisation concentrated on the cavity formation, moulded part glass architecture and the dimensional stability of the part. Optical analysis equipment such as a photographic camera, a flatbed optical scanner and optical microscope were used to produce high definition images. These images were processed using photo editing software to produce quantitative as well as qualitative results.

Measurement techniques used to calculate the cavity volumes were developed during the research; involving indirect and direct cavity measurements. Indirect cavity measurements used a combination of the materials density and the mass and volume of the moulded part, to calculate the cavity volume. Direct cavity measurement involved measuring the dimensions and volume directly. To retrieve the required information, the moulded part was sectioned and measured using accurate measuring equipment

Part dimensional stability and cavity measurements enabled an accurate comparison between parts and the effects of varying processing parameters. The measurements were performed using digital linear vernier callipers and a Hall effect probe to measure the wall thickness of the parts. These measurements were then imported into an excel spreadsheet for analysis.

## 9.1. Microscopy

Moulding features to be examined at a microscopic scale were chosen and sectioned to an appropriate size. Samples both parallel and perpendicular to the material flow were taken. The smaller sections were then cast in cold slow setting epoxy resin from MepPrep. The slow setting, cold epoxy resin was chosen due to the reduced shrinkage and exothermic reaction of the thermoset, which could alter the specimen dimensionally. The resin filled any voids in the specimen, preventing any pockets that could accumulate debris which would scratch the specimen at lower polishing grades and contaminate any polishing cloths. The specimens were polished down to a 3 $\mu$ m polishing solution, on a semi automated polishing machine. Several moulding features were chosen to be examined with the results shown in section 11. Moulding Features.

## 9.2. Indirect Cavity Measurement

Indirect cavity measurements relies on the assumption that the density of the gas assisted processed part is identical to a conventionally processed part. The density of the material was determined by measuring both a pre-processed blank, and a post processed full part. The two densities were almost identical and well within acceptable experimental error limits.

The various techniques employ different methods to establish the volume of moulded part. This measured volume is a combination of the material volume and the cavity volume. Using the weight of the part, the volume of material contained in the part could be calculated. The difference between the calculated volume and the

measured volume gave the volume of the cavity. This calculation was based on the density formula (Equation 9.1) and is set out in Equation 9.2.

$$Density = \frac{Mass}{Volume}$$

**Equation 9.1 - Density formula**

$$\begin{aligned} \left( \frac{Actual\ Part\ Mass}{Calculated\ Part\ Volume + Gas\ Cavity\ Volume} \right) &= \left( \frac{Calculated\ Part\ Mass}{Actual\ Part\ Volume} \right) Density \\ &= \left( \frac{Actual\ Part\ Weight}{Calculated\ Volume + Gas\ Cavity\ Volume} \right) \\ &= \left( \frac{Calculated\ Part\ Weight}{Actual\ Part\ Volume} \right) \end{aligned}$$

$$Cavity\ Volume = Actual\ Part\ Volume - Calculated\ Part\ Volume$$

**Equation 9.2 - Cavity calculation through difference of mass and volume**

### 9.2.1. Water Displacement

A technique was devised to measure the volume of a gas injected part using water displacement. The part was submerged into a brim full container with the overspill of water giving the volume of the part. The benefit of this technique over dimensional measurement and direct cavity techniques is that any distortion and shrinkage in the part is taken into account giving an accurate measurement of the volume. As the density of the material was known, using a density calculation (Equation 9.1.), the mass of the processed part was used to calculate the volume of a theoretical, non processed, part that contained no cavity. The internal cavity volume contained in the

processed part, would account for any difference between the calculated volume of the theoretical part and the processed part.

The water container shape was critical in receiving accurate results from the water displacement. If the ratio between the depth and the open area section were too large, then the change in water level would be too low when the part displaced the water. A large change in water level would reduce the effect of water tension had on the test and give a higher resolution on the test. A container shape that closely matched the smallest section profile of the part was chosen to reduce this problem significantly. This ensured that the part was submerged “length” ways, so there was a large change in height in the water as shown in Figure 9.1.

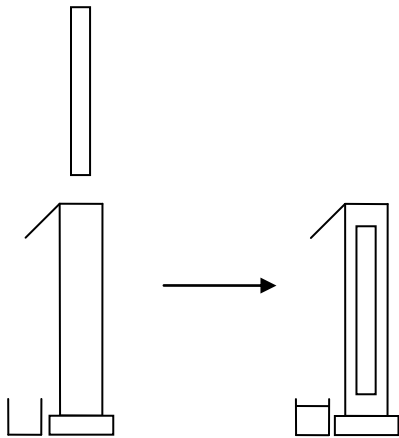


**Figure 9.1 - Part orientation in water displacement measurement**

The container used was a tall, rectangular polypropylene cereal container. For the spout, a short copper pipe was heated and pushed through the wall of the container, at a 45-degree downward angle. This created a smooth transition between the wall and the spout, to create a smooth flow of water. Silicon sealant was then used around the spout to prevent any leaks. A small quantity of light soap was added to

the water to reduce the surface tension, allowing the water to flow more freely and consistently down the spout of the container.

The only drawback to this technique was the length of time it took to take the measurements. To ensure an accurate and consistent result, the water was left until it had stopped dripping, both before and after the part was submerged. This could take up to seven to eight minutes before the water had stabilised. The measurement was repeated three times with each part to ensure an accurate result.

Another drawback was that only the total part volume was given without any dimensional information that would give the extent of shrinkage. This valuable information would show the effect the processing parameters had on the extent of shrinkage of the part. The part would have to be measured to retrieve this information.

### 9.2.2. CAD Model

The same principles as those used with water displacement were used in conjunction with a CAD model to calculate an estimated cavity volume. The calculations involve subtracting the parts' theoretical solid part volume, calculated from the part weight, from the actual part volume. The difference of the two volumes is the theoretical volume of the produced cavity. The way that the actual part volume was measured was however different from water displacement.

Using key measurements taken from the part, a three dimensional computer CAD model was produced. The model gave a part weight and volume that were then used in the cavity calculations. The key measurements were;

- Rib height
- Bottom flange thickness
- Top flange thickness
- Side flange thickness
- Part length

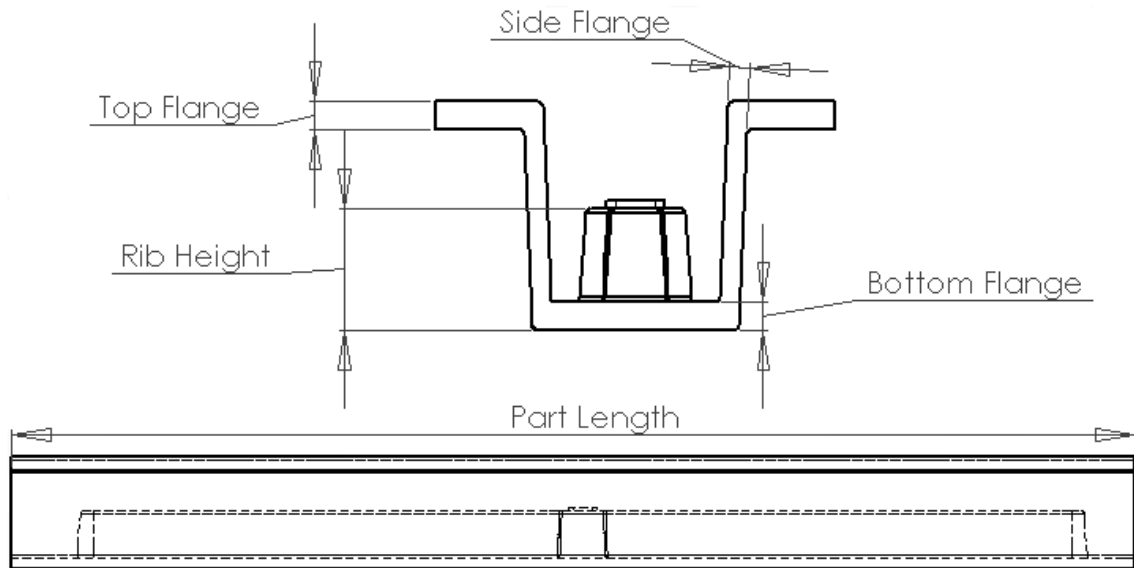


**Figure 9.2 - Drawing showing key part measurements**

Using CCM measurements of the mould tool, a CAD model was produced of a full part with a 5 mm top and bottom flange thickness. The shrinkage of the part was calculated using the length of the mould tool and the length of the measured part. With the assumption that the percentage of shrinkage would be equal around the part, the shrinkage was applied to other measurements such as the height of the part and width of the bottom flange. However, when the part height and bottom flange width were compared to the actual dimensions on the moulded part, it was found to have twice the amount of shrinkage than the part length. With the increased level of shrinkage, the volume CAD model lay within one percent of the water displaced

volume. The model was further validated with parts that were moulded without injected gas. The volume calculated from the shot weight using the materials density, the volume measured through water displacement and the volume given by the CAD model all lay within one percent of each other.

Part Number	Shot Mass	CAD Mass	Shot Volume	Cad Volume	Water Volume
1	218.40	216.92	222.86	221.35	223.00
2	202.4	203.91	206.53	208.07	206.40

**Table 9.1 - Comparison between, shot volume, CAD model volume and water displacement volume measurements for a full moulding**

These validations gave the confidence to use the CAD model as an accurate comparison between moulded parts as well the accurate prediction of internal cavity volume. The model however cannot predict the dimensions, shape and distribution of the cavity. In order to establish these cavity attributes the part would have to be sectioned and examined directly using a variety of techniques.

### 9.2.3. Direct Cavity Volume Water Measurement

A direct measuring technique was used on some moulded parts to establish a cavity volume before the part was sectioned for further analysis. The technique involved filling the internal cavity with water to calculate the volume.

Firstly, the part was weighed in a dry state and small, 2-3mm holes were drilled into rib at several positions along the length. The part was then submerged with the holes allowing the water to fill the cavity. To ensure any trapped air bubbles were removed,

the part was rotated and violently shaken whilst still submerged. Once all of the air had been dispelled, the part was dried of any excess water and weighed. The difference between the dry and wet weight would give the weight of the water. Using the density of water, of  $1\text{mm}^3 = 0.001\text{g}$ , the volume of water and so the volume of the cavity could be calculated. One drawback of this technique was that it was difficult to ensure the entire cavity was measured as some pockets may not be filled with water. As water has a higher density than the nitrogen gas used in the process, it may not be able to penetrate thin sections created by the gas under high pressure. This technique was used as an indicative analytical technique. Other techniques were used that could account for any trapped gas pockets that the water would not be able to reach.

### **9.3. Direct Cavity Measurement**

Direct cavity measurements involved exposing the main internal cavity and measuring the wall thickness to establish the volume of the cavity. This involved sectioning the moulding lengthways along the rib, cutting the cavity in two as depicted by . This would show the cavity length and shape as the gas flowed along the rib. Due to the inaccessibility of the gas fingering, these were not measured. This would not give a true account of the total cavity contained in the part. However, the technique would give an accurate shape and dimensions of the cavity contained in the main rib.

### 9.3.1. Hall Effect Probe

To measure the thickness of the part walls, an ElektroPhysik FH2100 Hall effect probe and small magnetic ball bearings were used. Varying the distance between the ball and the probe varies the magnetic field strength. The probe calculates the distance from the strength of the magnetic field. The probe was connected to the computer so each value could be recorded and used for analysis. As the probe was moved along the rib, the thickness was recorded at regular 10mm intervals. This gave a good resolution to how the rib's wall thickness changed along the length. The probe had a threshold of 8mm; this did not present a problem for the large majority of measurements, but did limit its use in some areas.

### 9.3.2. Digital Linear Vernier Callipers

In conjunction with the Hall effect probe, a "Linear Tools" Electronic Digital Vernier Calliper was used to measure the wall thicknesses where the Hall effect probe would be difficult or impossible to be used. Strips of paper with graduated lines 10mm apart were glued onto the mouldings lengthways along the rib to give an accurate measuring guide that would be used for both the probe and digital callipers. In order to help distinguish between the different parts of the rib have been split up into different definitions. These are "Wall Width" and "Wall Depth", with the positions shown in Figure 9.3

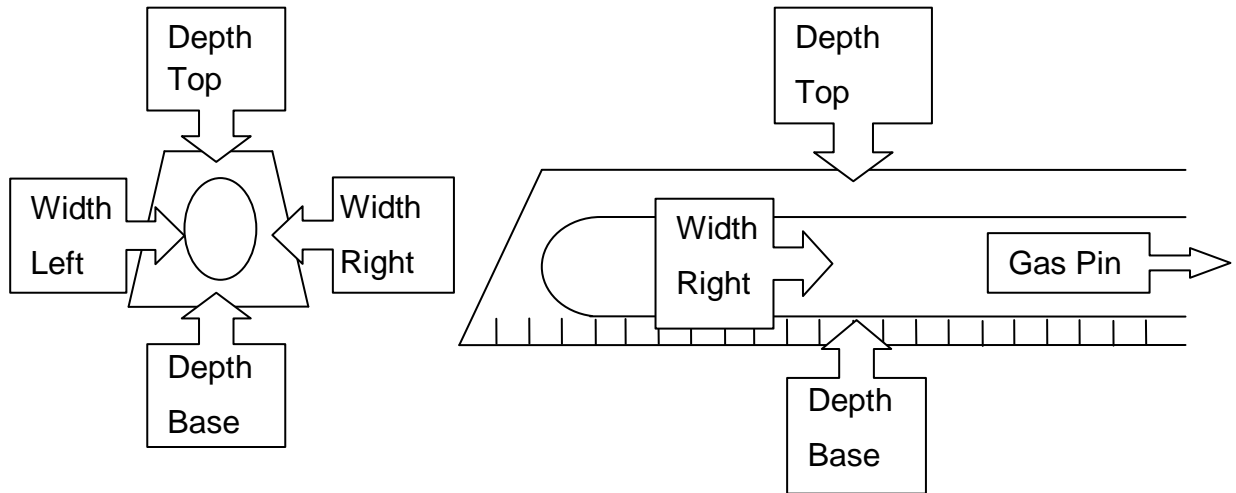


**Figure 9.3- Diagram of cavity measuring points**

Both the top and base wall thicknesses were recorded. If a cavity was not present at a measuring point, a value equal, to half of the rib thickness was recorded. At points, the wall width was above the 8mm threshold of the probe and so depth callipers were used to calculate the thickness by using the rib's average whole thickness and subtracting the individual depth measurements. Where the cavity shape allowed the Hall effect probe measurements were used over the depth measurements as they have a higher degree of accuracy.

## 9.4. Part Sectioning

So that the moulded parts could be fully analysed, each one was sectioned in an identical manner. Each one was sectioned along the central rib in a vertical plane as shown by Figure 9.4 and then shown side by side in the same plane (Figure 9.5).

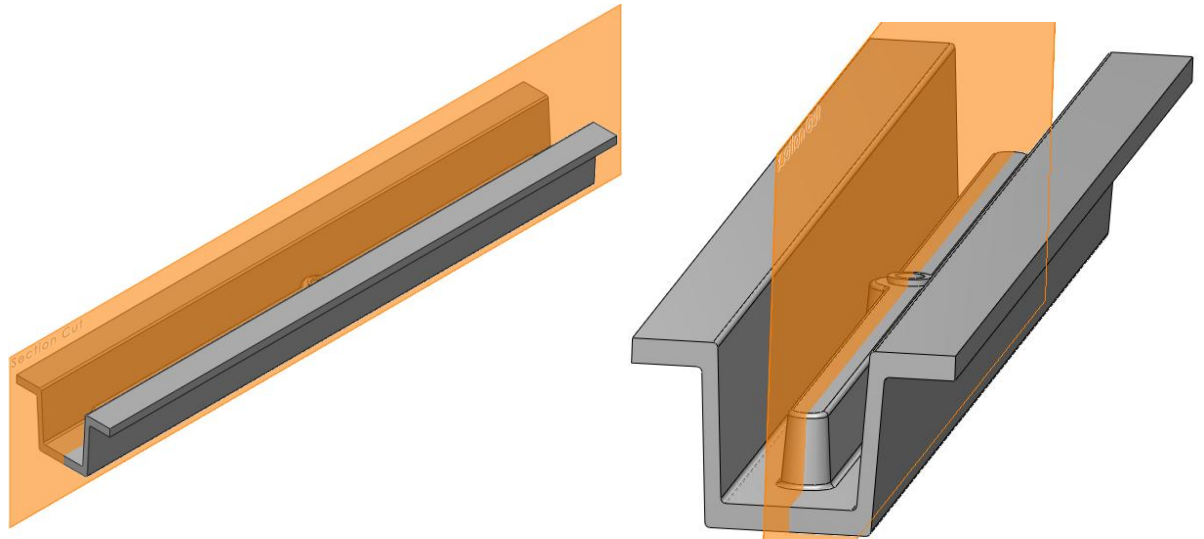


**Figure 9.4 - Illustrations showing the plane and position of the section cut, used in the analysis of the cavity**

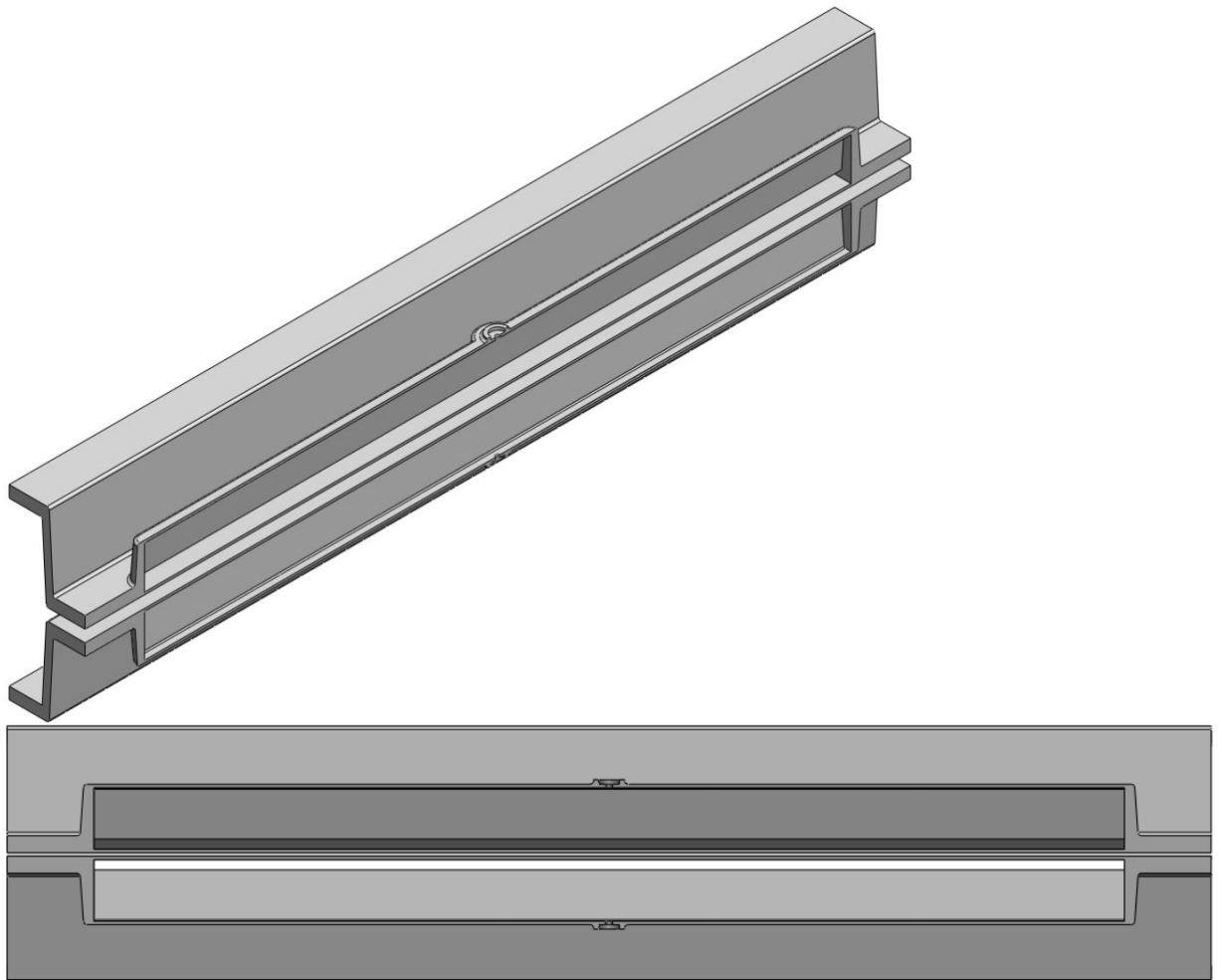


**Figure 9.5 - Two halves of a sectioned part shown side by side**

# 10. Effects of Process Parameters

Numerous experiments were carried out to determine how the material and process parameters affected the internal gas cavity of a successful moulding. An initial parameter scoping study was carried out to establish the effects of processing parameters on GMT. To compare the mouldings and resultant cavity shapes, the mouldings were sectioned as per set out in section 9.3 Direct Cavity Measurement

## 10.1. GMT Parameter Scoping Study

An initial parameter scoping study was carried out to establish the effect of the processing parameters, peak pressure (delay time of 1 second and ramp rate of 1 second), tool temperature and oven temperature on the creation of a gas cavity in GMT. A Taguchi array was used to investigate the key parameters that would significantly alter the outcome. Taguchi arrays are widely used in research, as they provide a quick result, with reduced work loading, over traditional orthogonal arrays.

The different values for each processing parameter are shown Table 10.1 and the resulting Taguchi array and experimental plan is shown in Table 10.2. Studies into the effects of processing parameters in GAIM, showed that the material temperature had a significant effect on the cavity penetration length whilst the peak gas pressure also showed to have an effect. For these reasons, the gas pressure and oven temperature were chosen. The tool temperature was varied to change the rate of cooling. Low, middle and high gas pressures were chosen, giving 60 bar, 120 bar and 180 bar. The tool temperature was heated as high as the external tool heating module would allow, giving an unheated, room temperature (22°C) and heated tool

temperature of 50°C. The oven temperature was set to 10°C higher than the melting temperature of polypropylene (190°C) and the upper processing limit of GMT (230°C) above which, the polypropylene would rapidly degrade. This gave oven temperature settings of 200°C and 230°C.

Code	Parameter	Level 1	Level 2	Level 3
A	Gas Pressure (bar)	60 bar	120 bar	180 bar
B	Tool Temperature °C	Room Temperature	50°C	
C	Oven Temperature °C	200°C	230°C	

**Table 10.1 - Taguchi scoping experiment**

These parameters gave a twelve experiment array with each experiment repeated for consistency, giving a total of 24 moulded parts. This gave a wider sample size for each set of parameters, and so giving a more consistent result reducing the effect of any outlying results. In order to ease power consumption with large tool temperature changes, all of the experiments with low tool temperatures were performed before the high temperatures experiments. This did not provide a randomised experiment order, but a check of experiment order with results did not show any correlation, and so it was concluded that the run order did not have any affect.

		Experiment Number											
		1-2	3-4	5-6	7-8	9-10	11-12	13-14	15-16	17-18	19-20	21-22	23-24
Parameter Level	A	1	1	1	2	1	2	2	2	3	3	3	3
	B	1	2	1	1	2	1	2	2	2	2	1	1
	C	1	1	2	1	2	2	1	2	1	2	2	1

**Table 10.2 - Taguchi array and experimental plan**

The numbers in the centre of the array Table 10.2 denote the level that each parameter was set to for that particular moulding cycle. For example, in experiments seven and eight, the material was heated to 200°C, with the tool temperature unheated and gas pressure set to 120 bar.

### 10.1.1. Results

All of the parts produced in the study contained some form of cavity. However, the majority of cavities produced, were situated at the end of the rib and contained fibre/polymer separation. This is discussed later in the discussion section of the parameter study. Only seven parts contained continuous smooth wall cavities. Only a few parts contained small cavities near the gas injection pin and were not consistent with a particular parameter or combination of parameters. No cavities present in the scoping study were symmetrical about the central axis of the rib. The cavities were situated to one side of the rib, making the wall thickness on either side of the cavity different. This can be seen in Figure 10.2 (relative position on the moulding shown in Figure 10.1) where the top section contains a deep cavity, whereas the same position on the bottom section does not. The same effect was seen in the vertical orientation, where upper wall thickness was significantly thinner than the bottom wall thickness.

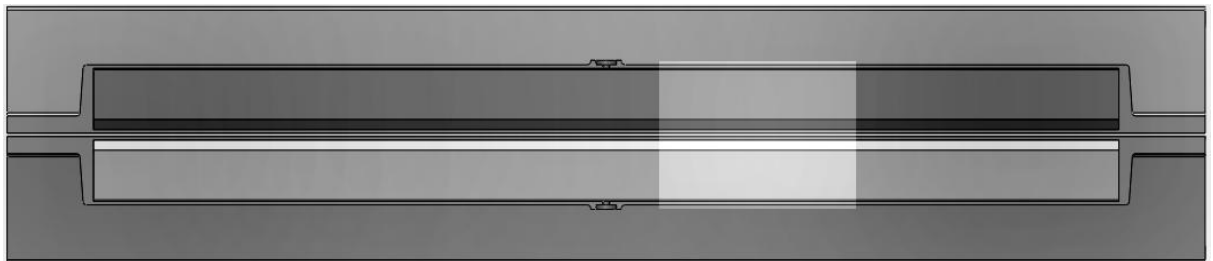


**Figure 10.1 - Illustration showing the position of the unsymmetrical gas cavity in Figure 10.2**

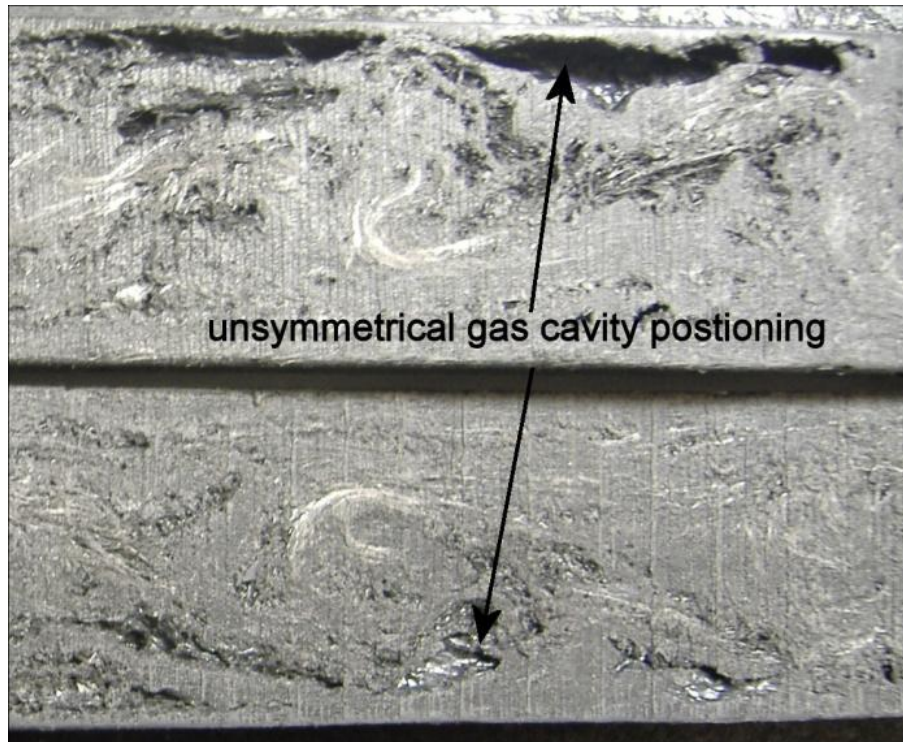


**Figure 10.2 - Picture of unsymmetrical cavity position in GMT**

This inconsistency in results made a quantitative analysis difficult, as it would not be possible to measure multiple regions of fibre agglomeration. For this reason, qualitative data of all of the mouldings was taken in the form of an observational checklist of moulding features. These features included the formation of a large cavity, if the cavity was dry and fibrous or smooth walled and if the part was porous. The checklist formed part of a pseudo quantitative analysis with each criteria combining to give a score out of five. This enabled the parts to be ranked, giving an indication to the effect of processing parameters. The results of the checklist showed that the top ten individual mouldings, contained an even number produced with a gas pressure of 60 bar and 180 bar and with high and low oven temperatures. However, eight of the ten mouldings were moulded with a low oven temperature.

Figure 10.3 shows the moulding that produced the largest smooth walled cavity, which was moulded with the parameters;

- 60 bar
- 50°C tool temperature
- 200°C oven temperature

A small smooth walled cavity was formed near the gas injection pin in the centre of the part. There is also evidence of the gas fingering through the glass creating glass rich, porous areas. As the gas travelled towards the end of the rib, the gas occasionally pushed both the polymer and glass creating a thin, smooth walled cavity. A smooth walled cavity is shown at the end of the rib in Figure 10.3, where there is no separation of the polymer from the glass fibres.



**Figure 10.3 – Photo showing rib tool GMT moulded with parameters 60 bar, 50°C tool temperature and 200°C oven temperature. It contains a smooth cavity and hesitation mark**

Where Figure 10.3 shows a moulding with processing parameter levels, 1,2,1 respectively, Figure 10.4 shows a moulding with the processing parameter levels of

3,1,2 respectively. Although the volume of the cavity is similar, the cavity contains fibre agglomeration with no smooth walled cavity. The gas has burst through the end of the rib causing the gas pressure to drop off. The material has then sagged due to the reduction of internal gas pressure that would otherwise keep the material in contact with the mould tool surface.

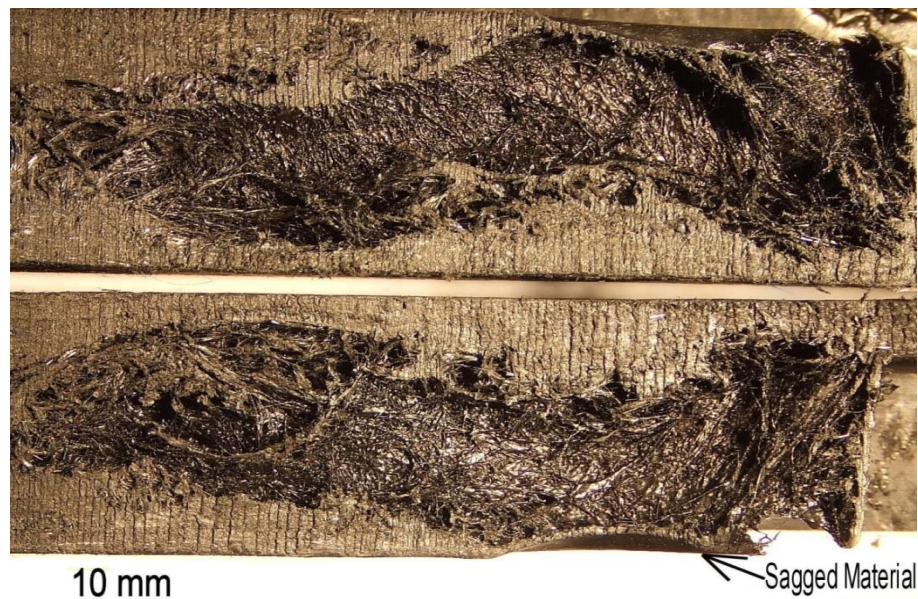


**Figure 10.4 - Photo of the end of a rib tool GMT moulded with 180 bar, 22°C tool temperature, 230°C oven temperature. It shows a burst hole, with sagged material and a fibrous cavity.**

### 10.1.2. Discussions of GMT Parameter Scoping Study

This parameter scoping study suggests that the oven temperature had a significant effect on the formation of a smooth walled cavity, whereas the gas pressure and tool temperature settings investigated in this study did not. The tool temperature and peak gas pressure did not appear to affect the volume of the cavity, as both large and small cavity volumes were formed at each of the levels. It was observed that the very high gas pressure of 180 bar, was the only gas pressure to burst through the end of the rib.

Studies produced in GAIM state that a higher melt temperature gives a better cavity penetration. The finding that a lower oven temperature produced a more successful cavity, suggests that the finding disagrees with those found in GAIM. However, in the study, the aggressive heat of an oven temperature of 230°C would have caused the GMT to loft sooner than the material heated to 200°C. The lofting would have then insulated the core of the material, reducing the conduction of heat. The material at 200°C would have possibly lofted later in the heating cycle and so increasing the time at which the heat could be conducted to the centre of the material effectively. Since the heating time was identical for both temperatures, the change in conduction rates, could result in the material heated to 200°C having a more uniform temperature through the thickness of the blank, than the material heated to 230°C. This agrees with Wakeman *et al.* [54] who concludes in a compression moulding study of GMT that the surface of a lofted blank heats faster than the interior, with conduction being the dominant heat transfer mechanism.

Becker *et al.*[90] produced a study on the gas assisted injection moulding of glass reinforced polypropylene with varying glass fibre lengths and concentrations. It was found that a glass fibre filled polypropylene with a concentration above 30 percent and a fibre length above 6mm, similar to the material used in this parameter scoping study, produced alternating sections of fibre/polymer separation and clear cavity. These findings are consistent with the findings of this parameter scoping study, where sections of both fibre/polymer separation and smooth walled cavities were produced.

The large majority of the cavities produced were situated at the end of the rib where the compression flow would have disrupted and dispersed the tightly needed architecture of the glass mat. This would suggest that the gas was generally not able to push the glass fibres aside whilst they were still in the original needed architecture of the blank. The mouldings show evidence of the gas fingering through the initial blank section of the moulding until it reached the end of the rib. Here the gas encountered an enclosed frozen layer produced by the end of the rib. It then started to produce a backpressure that pushed the material aside, creating a cavity. This action is similar to the inflation of a long thin modelling balloon, where the inflation of the initial section is restricted by the neck, until the air reaches the end of the balloon, where it starts to expand back towards the opening.

The outcome of this parameter scoping study shows that a cavity can be produced in GMT with a wide range of gas pressures and tool and oven temperatures. Only the oven temperature appears to have an effect on the creation of a smooth walled cavity. However, although a cavity was produced, the position, size and appearance was not consistent, showing that a GMT with a 34 percent glass fibre content and a long fibre length of up to 25mm was not suitable for further scientific study. For this reason, two additional materials were investigated with a lower glass content, as per the findings from the study produced by Becker *et al.*[90], which stated that clear cavities were produced with materials with a lower glass fibre concentration. These were Re-GMT with short (10mm), dispersed glass fibres with a concentration of 11 percent, and LFT with a long glass fibre length (up to 25mm) and a “pseudo aligned” glass fibre concentration of 22 percent. The fibre orientation of the LFT is largely in one direction, due to the continuous sheet extrusion process as it was manufactured.

## 10.2. Effects of Different Material

The effect of different material was then investigated. A large number of mouldings were produced to establish the suitability of each of the materials in the use of GasComp. A selection of parts moulded with each of the materials, with the same moulding parameters was taken to show the difference in cavity formation.

Each of the materials produced different moulding characteristics. The gas flow in Re-GMT consistently produced a successful cavity and did not cause fibre/polymer separation. LFT did produce large cavity volumes, comparable to cavities produced in Re-GMT, they were however not consistently reproducible. GMT did not produce any distinct, reproducible cavity.

Sample Name	Figure numbers	Peak Gas Pressure (bar)	Gas Ramp Time (s)	Delay Time (s)	Shot Weight (g)
RE –GMT 1	Figure 10.6 Figure 10.7	120	1	1	147.9
RE–GMT 2	Figure 10.8 Figure 10.9	120	1	1	151
LFT 1	Figure 10.10 Figure 10.11	120	1	1	168
LFT 2	Figure 10.12 Figure 10.13	120	1	1	187
GMT1	Figure 10.14 Figure 10.15	120	1	1	180
GMT2	Figure 10.16 Figure 10.17	120	1	1	184

Figure 10.5 - Table showing the processing parameters of moulding discussed in section 10.2

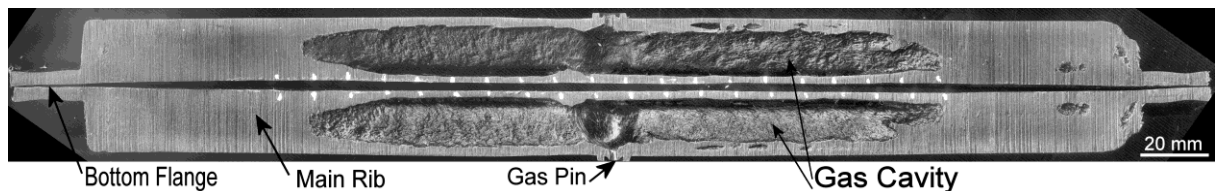
### Effects of Different Material

#### 10.2.1. Cavity Structures Produced

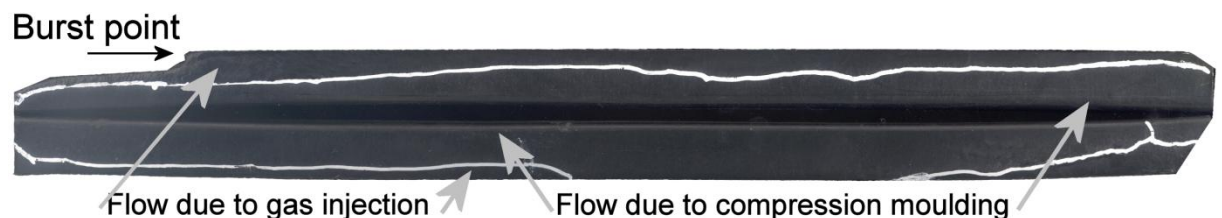
A series of rib tool mouldings produced with each of the materials at 120 bar gas pressure with a 1 second ramp rate were examined. Images of each moulding show

the cavity and the flow of the material on the top flange. The ends of the top flange are the last places to fill with material and so can be short, showing the edge of the flow front. The hesitation mark is highlighted by the white lines, while the white dots denote sampling points at 10mm intervals, used for measuring the cavity dimensions.

Figure 10.6 through to Figure 10.9 show the cavity shape and flow front, present at the top flange of two Re-GMT mouldings. The cavities are a regular elongated oval shape, with a consistent wall thickness until the end of the rib where it begins to taper. The side of the pin, with the longest cavity corresponds to the largest material movement after the hesitation mark (white line). The whole of the right hand side of Re-GMT moulding 1 (Figure 10.7) is full, indicating that the gas filled this section first before filling the left hand side, before finally bursting out of the top flange.



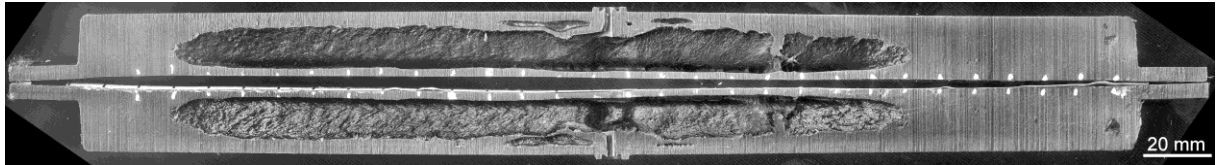
**Figure 10.6 - Image of a Re-GMT moulding 1. Moulded at 120 bar gas pressure with a 1 second ramp rate and delay time of 1 second**



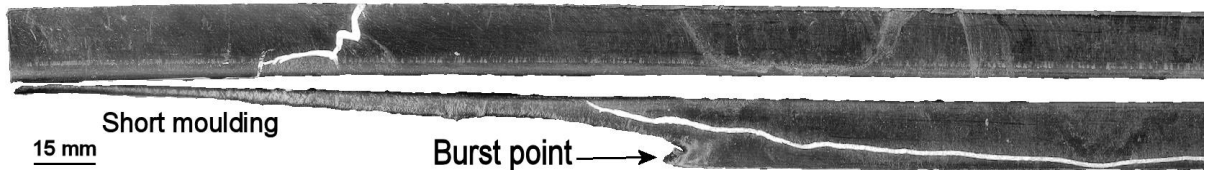
**Figure 10.7 - Image of the top flange of a Re-GMT moulding 1. Moulded at 120 bar gas pressure with a 1 second ramp rate and delay time of 1 second.**

Figure 10.8 and Figure 10.9 show a second Re-GMT moulding. Again, the side with the longest cavity shows the largest material movement on the top flange, after the

hesitation mark. There are several phases of gas flow, which are examined in detail in section 11.4 Gas Flow Mechanics



**Figure 10.8 - Image of a Re-GMT moulding 2. Moulded at 120 bar gas pressure with a 1 second ramp rate and delay time of 1 second.**



**Figure 10.9 - Image of the top flange of a Re-GMT moulding 2. Moulded at 120 bar gas pressure with a 1 second ramp rate and delay time of 1 second.**

Figure 10.10 through to Figure 10.13 show two LFT rib tool mouldings. Figure 10.10 and Figure 10.12 show LFT rib mouldings with a cored out ribs. The residual wall thickness (RWT) varies massively on the bottom flange but is relatively stable on the top half of the rib. This would indicate that the gas was able to core out the top half, pushing the material down as it moved along the rib. Figure 10.10 shows how the gas created a smooth cavity as it flowed to the left of the gas pin, but caused fibre agglomeration to the right of the pin. This shows the instability in how the material reacts to the gas pressure. Figure 10.11 and Figure 10.13 show the corresponding top flanges with Figure 10.13 showing that the top flange has been completely filled. Figure 10.11 shows the top flange with an uneven flow of the LFT due to the gas pressure.

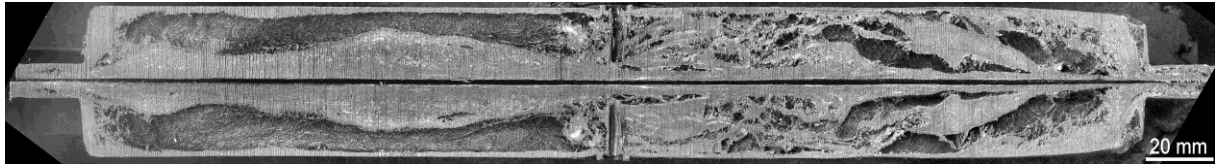


**Figure 10.10 - Image of a LFT moulding 1. Moulded at 120 bar gas pressure with a 1 second ramp rate and delay time of 1 second.**

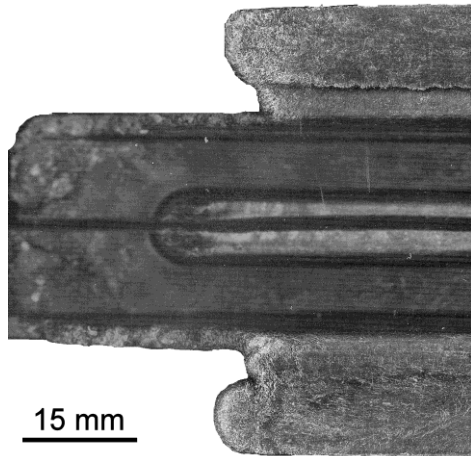


**Figure 10.11 - Image of the top flange of a LFT moulding 1 – material breakthrough flow is shown at the end of the flange at the bottom of the picture. Moulded at 120 bar gas pressure with a 1 second ramp rate and delay time of 1 second.**

0

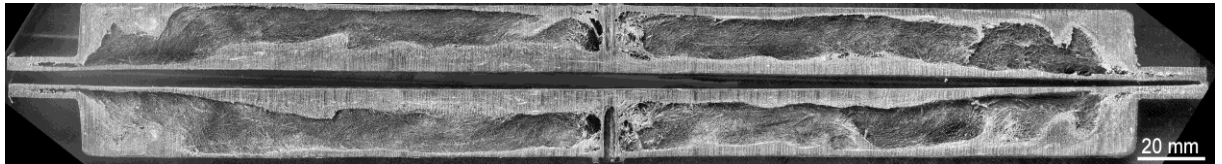


**Figure 10.12 - Image of a LFT moulding 2. Moulded at 120 bar gas pressure with a 1 second ramp rate and delay time of 1 second.**

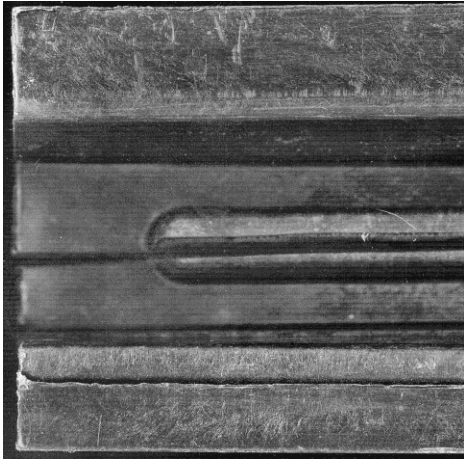


**Figure 10.13 - Image of the top flange of a LFT moulding 2. Moulded at 120 bar gas pressure with a 1 second ramp rate and delay time of 1 second.**

Figure 10.14 and Figure 10.16 shows GMT rib tool mouldings with only small areas where the gas has fingered along the rib. The material reacted differently to the Re-GMT and LFT, causing a great extent of fibre agglomeration. Figure 10.15 and Figure 10.17 show that the parts were not filled, with the edge of the flow front being jagged and uneven. The uneven flow is due to localised areas where the polymer was able to break through the glass mat and occasionally caused the fibres to flow with it.

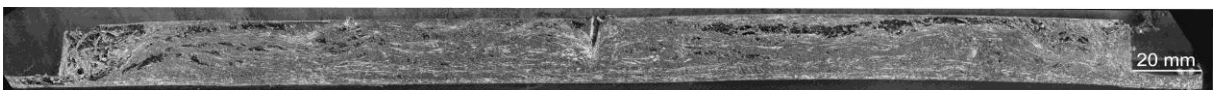


**Figure 10.14 - Image of a GMT moulding 1. Moulded at 120 bar gas pressure with a 1 second ramp rate and delay time of 1 second.**

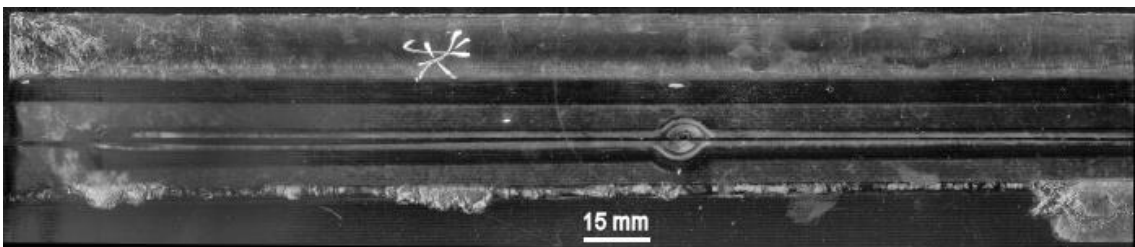


**Figure 10.15 - Image of top flange of a GMT moulding 1. Moulded at 120 bar gas pressure with a 1 second ramp rate and delay time of 1 second.**

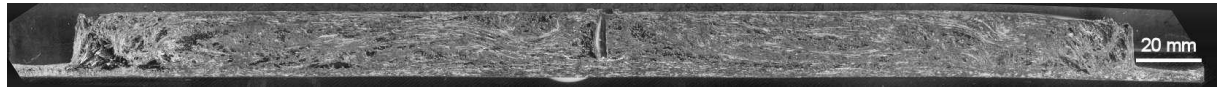


**Figure 10.16 - Image of a GMT moulding 2. Moulded at 120 bar gas pressure with a 1 second ramp rate and delay time of 1 second.**

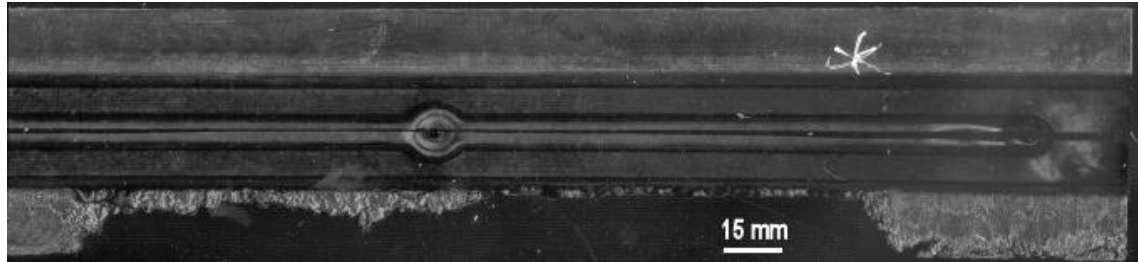


**Figure 10.17 - Image of top flange of a GMT Moulding 2. Moulded at 120 bar gas pressure with a 1 second ramp rate and delay time of 1 second.**

The natural GMT with a glass weight fraction of 40 percent is not shown as no cavity was produced. The gas could only create a porous part and did not push the glass fibres to create a cavity.

### 10.2.2. Discussions of the Effects of Different Material

GMT was identified as an unsuitable material for the GasComp process, due to the tight fibre architecture. The process was able to produce a cavity but cavities were not of a significant size nor readily reproducible. Due to the needed glass architecture in the blank, no cavity was produced around the pin. A cavity was only produced at the end of the rib, where the flow due to the compression moulding had dispersed the needled mat. This dispersion allowed the gas pressure, creating a cavity by pushing the glass fibres aside. The gas was only able to core out small, localised cavities between the gas pin and the end of the material blank.

Re-GMT was identified as the most suitable material for the GasComp process. The materials ability to produce a cavity with no fibre separation, with a consistent wall

thickness enabled the reliable analysis of how varying processing parameters would affect the process. During the analysis, only the gas injection trigger position of the compression moulding parameters were changed, with the concentration on the analysis of gas injection parameters. The compressive force and platen velocity remained consistent throughout the project.

The cavity shapes are distinctive between the three materials.

- Re-GMT produces a consistent wall thickness cavity in the centre of the rib.
- LFT produces a thinner cavity biased towards one side of the cavity. The cavity is fibre rich with some fibre agglomeration occurring. The extent of fibre agglomeration is greatly reduced compared to GMT.
- GMT showed a large extent of agglomeration producing sporadic smooth walled cavities along the length of the rib. The location of a successful cavity was primarily beyond the initial blank position, at end of the rib. This would suggest that the gas would finger along the material, until it reached a frozen wall of material at the end of the rib. The gas would then expand and push the material back towards the pin creating a small cavity in the process. A large sample size of GMT mouldings was photographically analysed and showed that a solid section of material absent of any cavity would appear a short distance from the end of the rib. The section would be between 15mm and 30mm thick. It is not clear what produced this feature.

The top flanges of the mouldings were examined to show the differences in flow fronts between the materials.

- Re-GMT - Flow front similar to pure polypropylene. There were no fibre or polymer rich areas, creating a smooth flow front
- LFT – A rough flow front with some additional localised flow fronts. A series of small breakthrough protrusions would occur from the flow front, rather than advancing as a solid front. This is shown in Figure 10.11.
- GMT - A very uneven and rough flow front was produced. Small polymer rich areas were evident where the polymer had broken through the glass fibres. GMT has a similar flow front to LFT but with a higher frequency of polymer rich breakthroughs (Figure 10.15, Figure 10.17).

### **10.3. Effect of Gas Injection Delay Time in Re-GMT**

The effect of a 0.5 seconds, 1.5 seconds and 2.5 seconds gas injection delay time, when moulding Re-GMT was investigated. The study was carried out using an unheated star tool, containing four ribs, with a straight through gas injection pin. The material was heated to 220°C over 6 minutes. Table 10.3 shows the how each of the mouldings had an identical gas profile of reaching 80 bar over 0.1 seconds and held for 20 seconds. The table shows how the time delay before the gas profile is initiated, changes. These profiles are represented in graphical form in Figure 10.18. The variation in shot size arose from the slight variation in blank dimensions. A large number of mouldings were produced during the trial, however, for clarity three mouldings that displayed typical properties were selected for presentation.

### 10.3.1. Process Parameters Used

Gas Profile			Delay Time (s)	Shot Weight (g)
MouldingNumber	Peak Gas Pressure (bar)	Gas Ramp Time (s)		
0.5	80	0.1	0.5	325
1.5	80	0.1	1.2	330
2.5	80	0.1	2.5	324

Table 10.3 - Table showing process parameters with changing delay time

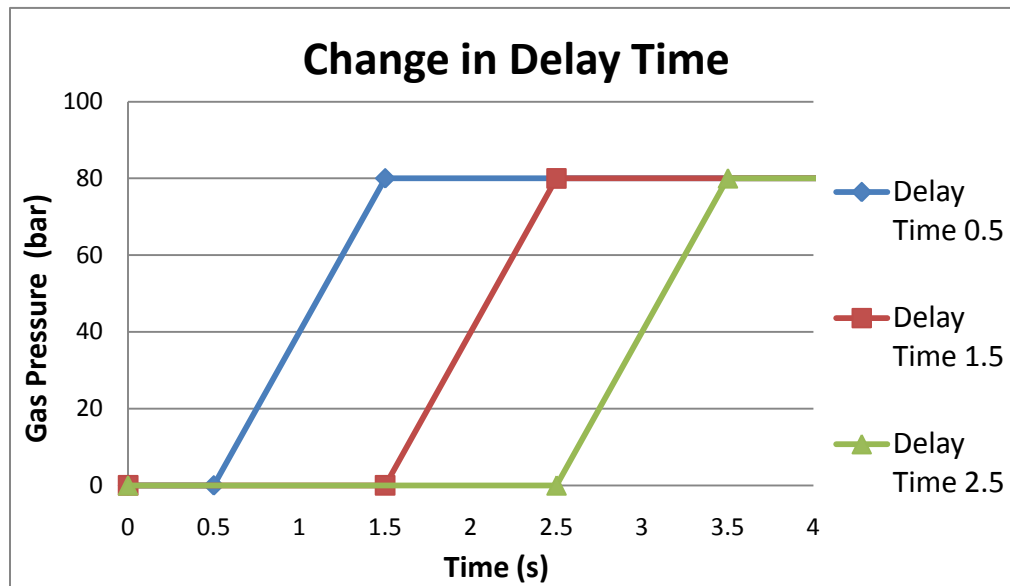


Figure 10.18 - Experimental gas profiles with differing delay times

Each of the mouldings were sectioned and cleaned of any burs. The internal cavity was then characterised using the Hall effect probe and vernier callipers. Each rib was measured at 10mm intervals for the length of the cavity. The length of the cavity was also measured. The three measurements of cavity width, height and length were used in the calculation of a long oval shape, to give a total cavity volume. The volumes of the ribs were then combined to give an overall part volume. These measurements for each of the delay times are shown in Table 10.4, Table 10.5 and Table 10.6

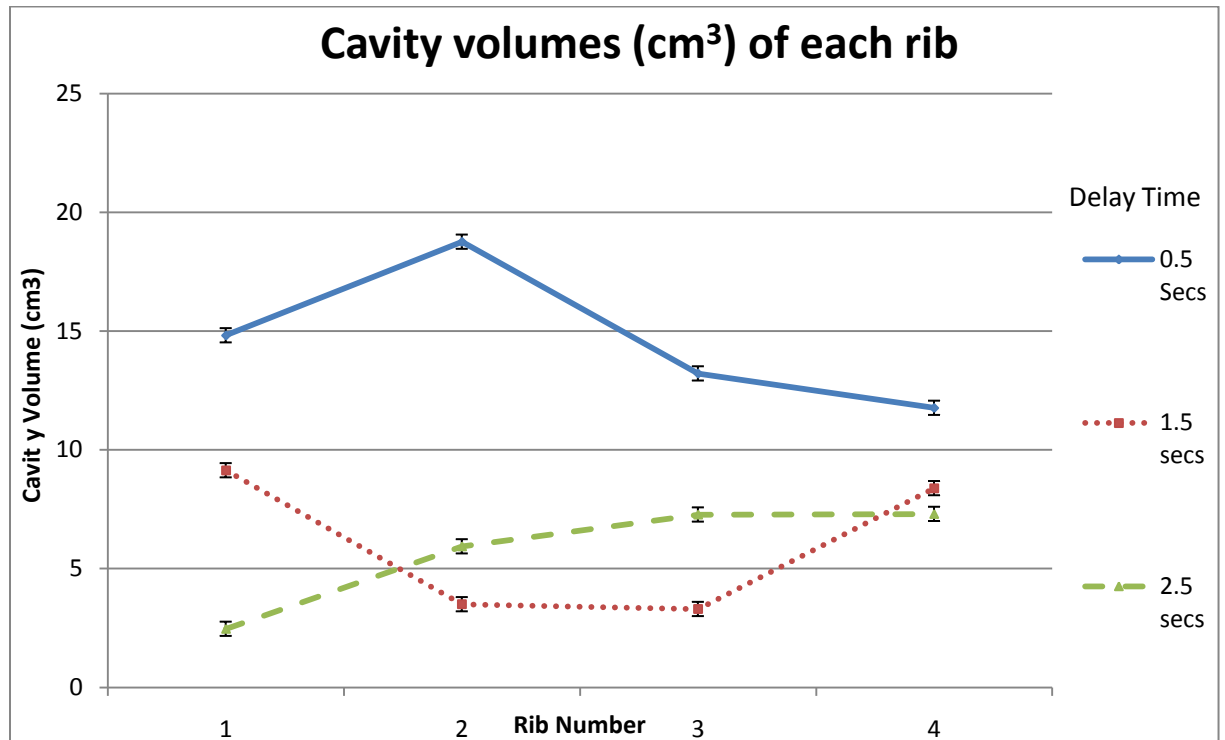


Figure 10.19 - Cavity volumes with respect to gas delay time of each or rib with an error of  $\pm 0.3\text{mm}$

### 10.3.2. Results

Figure 10.20, Figure 10.21 and Figure 10.22 show that the shapes of the cavities between the three delay times are similar, however the lengths are not. The moulding with a 0.5 second delay time (Figure 10.20) contains a fully cored out rib, where as the other two mouldings do not. The moulding with a 2.5 second delay (Figure 10.22) contains more voids and breakthroughs. Breakthroughs are small sections where the material has solidified and the gas has broken through to the molten material behind, at a later stage in the gas injection cycle.

Table 10.4 (0.5 secs), Table 10.5 (1.5 secs) and Table 10.6 (2.5 secs) show the wall thickness, cavity length and cavity volumes data for each of the delay times. They show a decrease in wall thickness, cavity length penetration and total cavity volume

over the first 1.5 seconds. The wall thicknesses between 1.5 seconds and 2.5 seconds do show a small increase, but the cavity

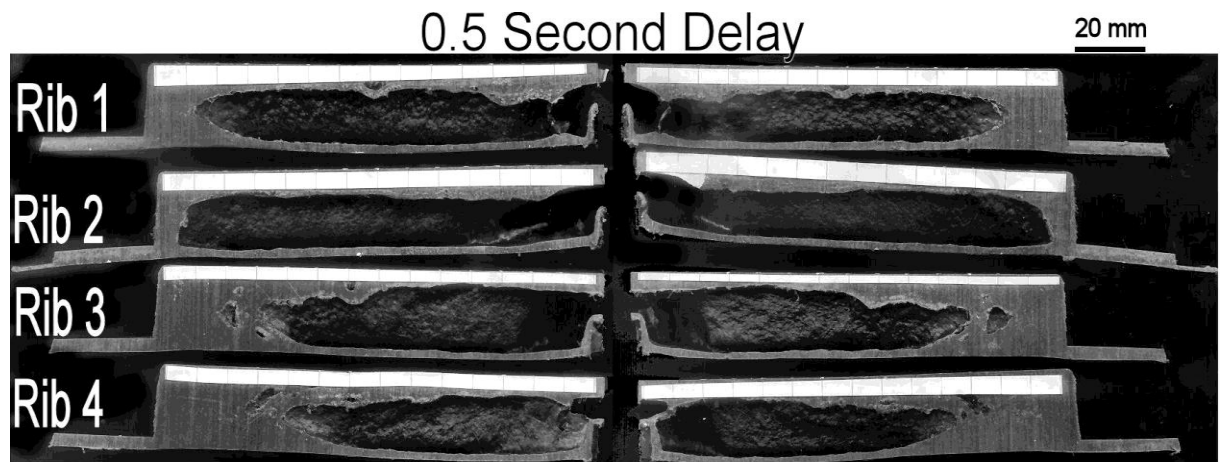


Figure 10.20 – Picture of the cavities produced by a 0.5 second delay time

0.5 Seconds Delay					
Rib number	1	2	3	4	
Mean top wall thickness (mm)	3.32	2.54	3.51	3.52	
Mean bottom wall thickness (mm)	3.17	2.37	3.30	2.87	
Cavity length (mm)	128	135	107	100	
Cavity volumes (cm <sup>3</sup> )	14.82	18.76	13.22	11.77	Total Volume: 59

Table 10.4 - Wall thickness and cavity length dimensions of 0.5 secs delay moulding

# 1.5 Second Delay

20 mm

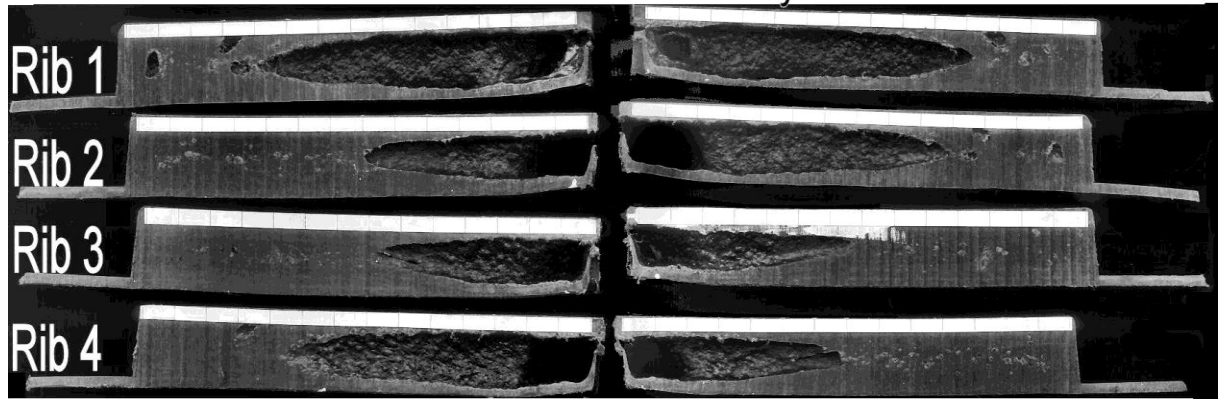


Figure 10.21 - Picture of the cavities produced by a 1.5 second delay time

1.5 seconds delay					
Rib number	1	2	3	4	
Mean top wall thickness (mm)	5.56	6.80	6.86	4.47	
Mean bottom wall thickness (mm)	4.32	5.45	5.20	4.07	
Cavity length (mm)	99	69	68	93	
Cavity volumes (cm <sup>3</sup> )	9.14	3.50	3.30	8.39	Total Volume: 24

Table 10.5 - Wall thickness and cavity length dimensions of 1.5 secs delay moulding

## 2.5 Second Delay

20 mm

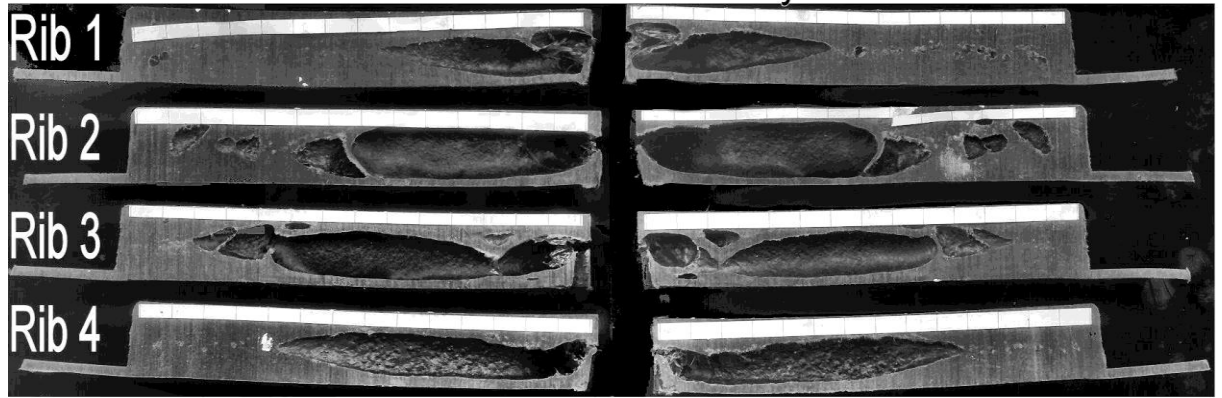


Figure 10.22 - Picture of the cavities produced by a 2.5 second delay time

2.5 seconds delay					
Rib number	1	2	3	4	
Mean top wall thickness (mm)	7.82	6.09	6.80	8.23	
Mean bottom wall thickness (mm)	5.28	4.00	3.73	4.65	
Cavity length (mm)	64	75	93	120	
Cavity volumes (cm <sup>3</sup> )	2.46	5.94	7.28	7.30	Total Volume: 23

Table 10.6 - Wall thickness and cavity length dimensions of 2.5 secs delay moulding

Table 10.7 shows a summary of the mean wall thicknesses and cavity length and the total cavity volume of each of the delay times.

Gas delay time	0.5	1.5	2.5
Mean top wall thickness (mm)	2.93	4.76	4.42
Mean bottom wall thickness (mm)	3	5.92	7.24
Mean cavity length (mm)	61	26	27
Total cavity volume (cm <sup>3</sup> )	59	24	23

Table 10.7 - Summary of moulding data

### 10.3.3. Gas Delay Time Discussion and Conclusions

These findings show that the cavity wall thickness increases and cavity penetration decreases as the delay time increases up to 1.5 seconds. This is consistent with findings produced by Parvez, *et al* [85], that state that the delay time has a significant effect on the RWT. The total cavity volumes between 1.5 seconds and 2.5 seconds are very close at  $24\text{cm}^3$  and  $23\text{cm}^3$  respectively. This would indicate that at some point between 0.5 seconds and 1.5 seconds a significant frozen skin forms, which then insulates the rest of the polymer melt from the cold surface of the mould tool, meaning there is no significant change in wall thickness.

All of the mouldings show a preference of gas flow with the clearest illustration in the moulding with a 0.5 gas delay time (Figure 10.20). The gas fully cores out one rib with another cavity length slightly less, whilst the two others are significantly shorter. This indicates that the gas fully cored out the two larger ribs before flowing to the two shorter ribs until the part filled the mould tool. The gas flow preference is discussed further in section 11.4 Gas Flow Mechanics

As gas delay increases from 0.5 second up to 1.5 seconds, the thickness of the frozen layer significantly increases, reducing the maximum potential cavity. The wall thickness between a moulding with a delay time of 1.5 seconds and 2.5 seconds does not significantly change. The point at which the increase delay time no longer significantly affects the cavity volume lies between 0.5 seconds and 1.5 seconds.

## 10.4. Effect of Gas Ramp Time Variation with Re-GMT

The rate at which the gas pressure was increased, was investigated in a series of experiments. This was done by setting a peak pressure and the time by taken to reach it. The Airmould control unit then continually adjusts the flow of gas to achieve this goal. The gas injection had a delay time of 1 second. Gas pressures below 40 bar and above 120 bar are not presented as no quantitative data was collected. It was found that gas pressures below 40 bar did not consistently produce a cavity and gas pressures above 120 bar consistently burst through the gas seal around the pin. The gas ramp time study used Re-GMT heated to 220°C for 6 minutes, in an unheated rib tool.

### 10.4.1. Process Parameters Used

Table 10.8 and Figure 10.23 show the varying processing parameters carried out in this study.

Moulding Number	Gas Profile		Delay Time (s)
	Peak Gas Pressure (bar)	Gas Ramp Time (s)	
60-1	60	1	1
60-2	60	2	1
60-3	60	3	1
60-5	60	5	1
80-1	80	1	1
80-2	80	2	1
80-3	80	3	1
80-5	80	5	1

**Table 10.8 - Study processing parameters, with varying ramp time and peak pressure**

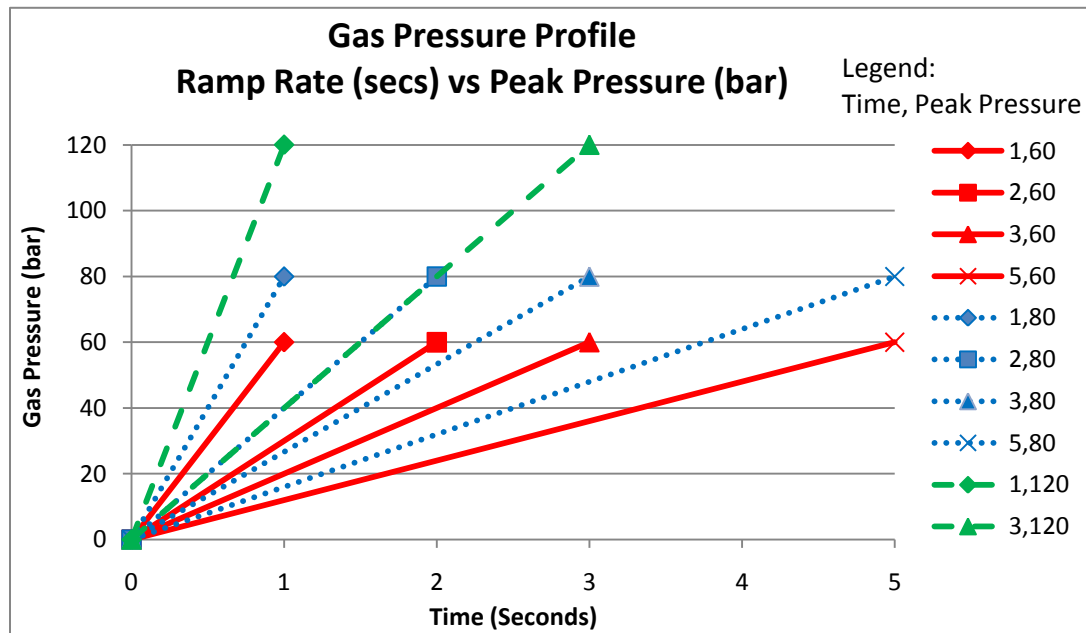


Figure 10.23 - Experimental gas ramp time profiles showing the time taken to reach the peak pressure

### 10.4.2. Results

Figure 10.24 shows the cavity lengths created by each peak pressure and ramp rate. The graph appears to show that as the ramp rate increases, the cavity length increases. The large variability in cavity length arises from the instability of the gas bubble in the main rib. As discussed in detail in section 11.4 Gas Flow Mechanics, the gas will always choose the path of least resistance. Once the gas fingers away from the main rib, it will not return, as it would have already chosen an easier path and would most likely burst through the material on the top flange. The reasons for the gas flow deviating away from the main rib could be due to the rib becoming full, localised freezing or a localised high concentration of glass fibres, which could create a dam, preventing the gas from advancing. If the sidewalls were still molten, the gas would then finger up the sidewalls to the top flange where the gas would either flow the material until the mould was full, flow the material until the gas burst through or

flow the material until the material had sufficiently frozen as to contain the gas. Due to the unpredictable path, the extent of fingering could not be measured.

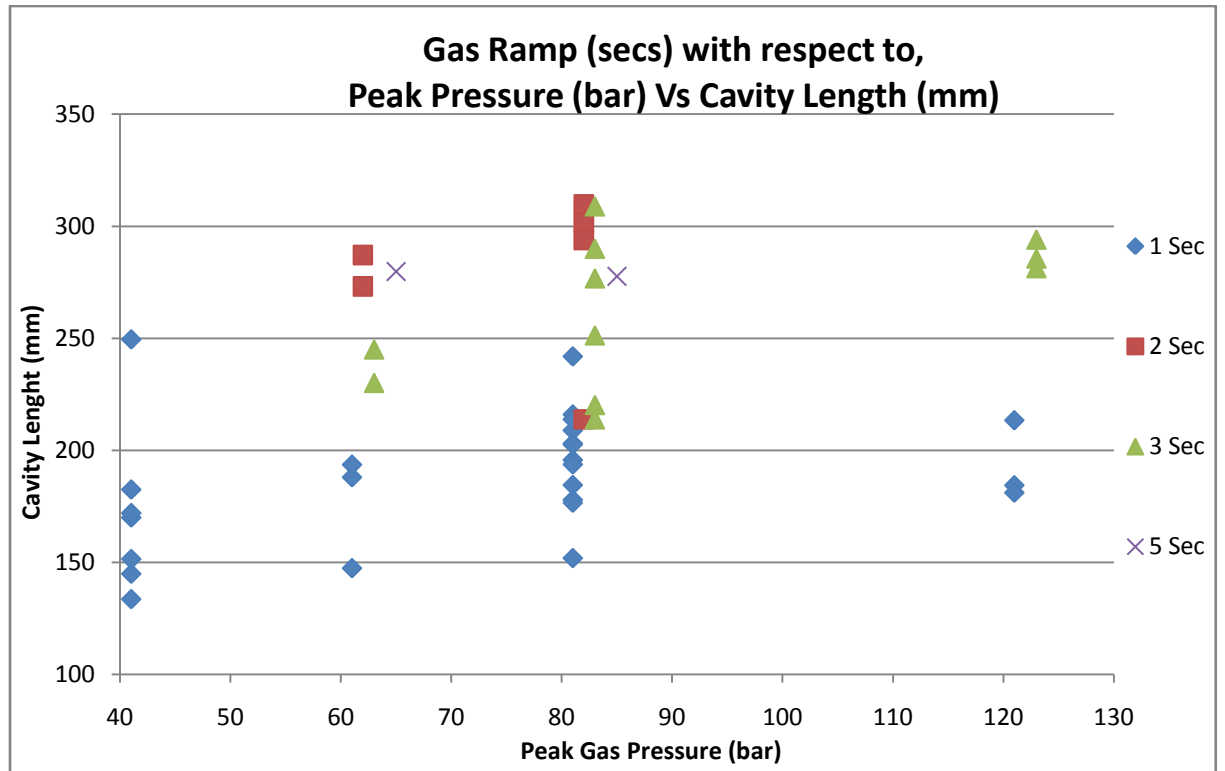


Figure 10.24 - Graph showing the peak gas pressure (bar) vs cavity length (mm), with respect to gas ramp time with an error of  $\pm 0.1$  mm on all of the length measurements.

Photos taken from four samples at the shortest and longest ramp rates show how the cavity sizes changes between the parameters. The photos show that the mouldings with the shorter ramp time (Figure 10.25, Figure 10.26), have a shorter cavity length than the mouldings with a longer ramp rate (Figure 10.27, Figure 10.28).

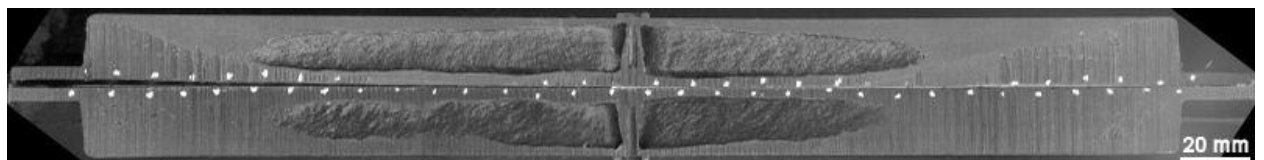
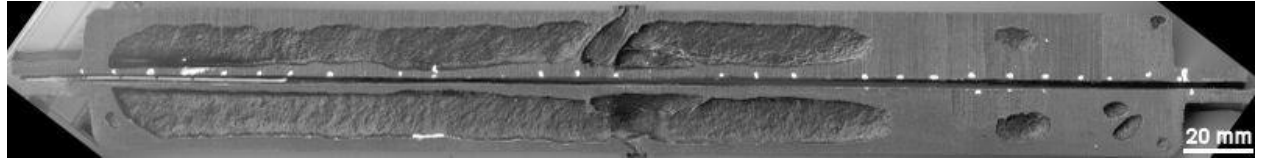
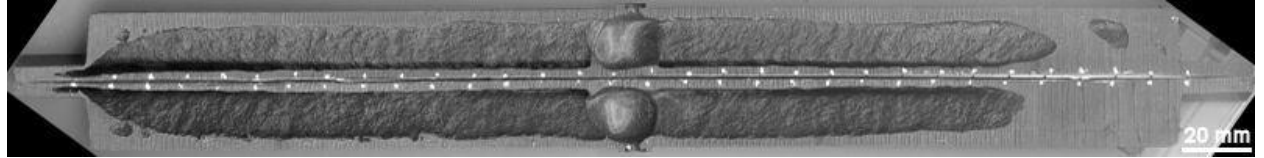


Figure 10.25 - Photo of moulding with gas profile, 60 bar over 1 second



**Figure 10.26 - Photo of moulding with gas profile, 80 bar over 1 second**



**Figure 10.27 - Photo of moulding with gas profile, 60 bar over 5 seconds**

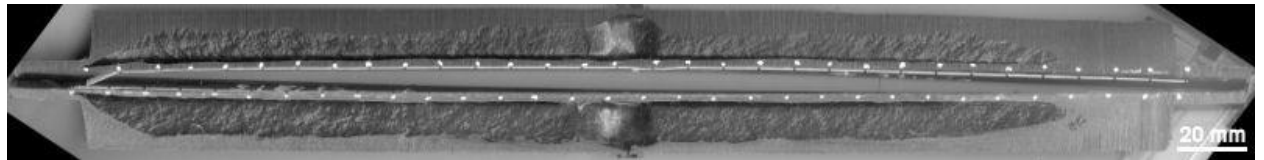


**Figure 10.28 - Photo of moulding with gas profile, 80 bar over 5 seconds**

An observational difference between the short ramp time (Figure 10.25, Figure 10.26) and the long ramp time (Figure 10.27, Figure 10.28), is that the mouldings with the shorter ramp time had material frozen around the pin. This did not occur in the mouldings with the longer ramp.

The cavity volumes of the mouldings, as calculated via CAD, as displayed in Figure 10.24, are displayed in Figure 10.29. Figure 10.29 shows a large variation in cavity volume within the same processing parameter. This is due to the different shot sizes which results in variations in the fullness of the part and the burst through of the gas. The graph does indicate that the gas ramp time and pressure does not significantly affect the volume of the cavity, giving a wide processing window. It also indicates that another parameter not investigated in this study had a larger effect on the cavity volume of the part. The blank positioning could be having a more significant effect, as

this would affect the flow path of the gas. The larger the mass of material in front of the gas flow, the less likely that the gas will break through, ceasing the advancement of the cavity. The gas flow mechanics are discussed further in section 11.4 Gas Flow Mechanics.

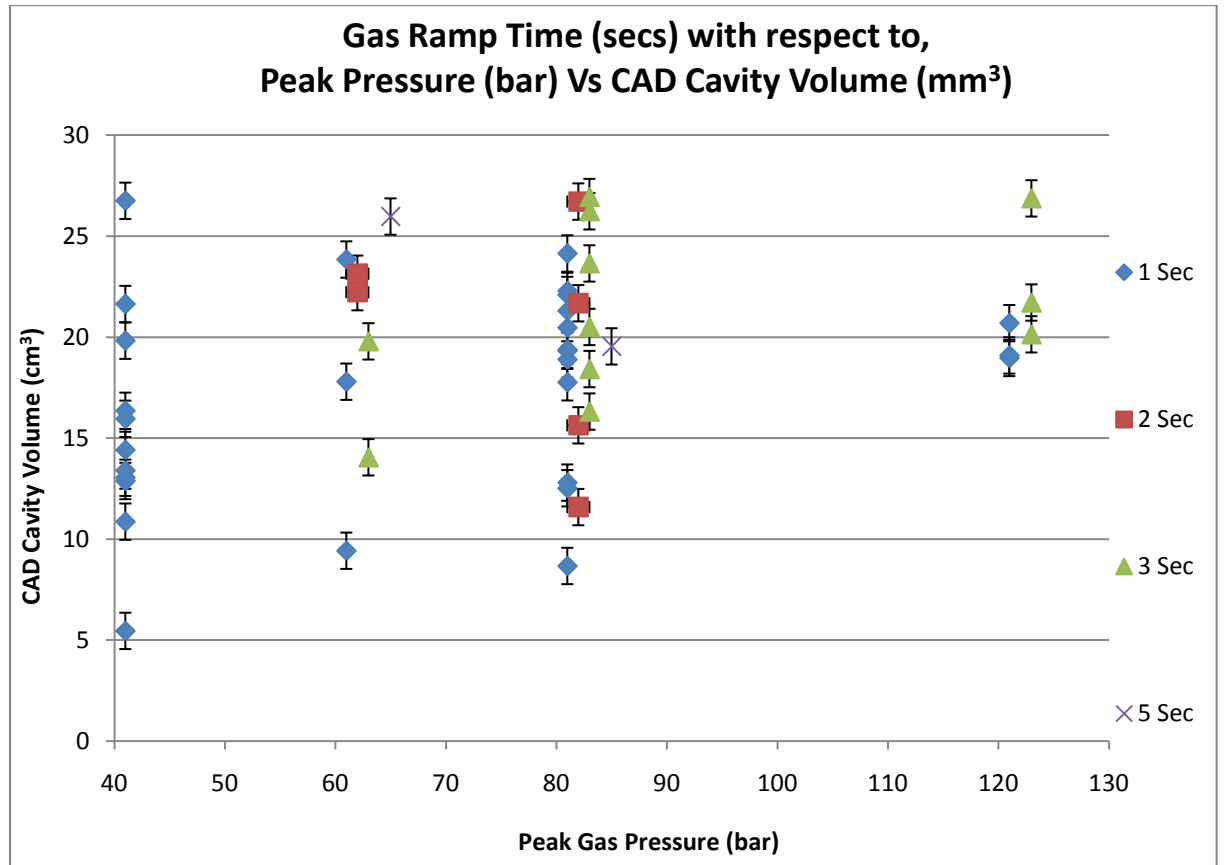


Figure 10.29 - Graph showing the peak gas pressure (bar) vs CAD cavity volume (mm<sup>3</sup>), with respect to gas ramp time. CAD Cavity volume has an error of +/-0.9mm.

The cavities were characterised with a vernier calliper as described in section 9.3.2 Digital Linear Vernier Callipers. Table 10.9 shows the cavity dimensions and the standard deviation of those dimensions taken along length of the rib. The table shows an increase of 2.4mm in cavity height and 1.5mm in cavity width, from a gas profile of 60 bar over 1 second ramp rate up to a gas profile of 60 bar over 5 seconds ramp rate. The increase is not apparent once the gas pressure is increased to 80

bar. This shows that once the gas pressure reached 80 bar, the change in ramp rate did not affect the cavity height or width.

Table 10.9 shows the change in the standard deviation of the cavity wall thickness with respect to gas ramp time and gas pressure. The table shows a decrease in deviation as the gas ramp increases, showing that the cavity dimensions are more consistent and stable at a higher ramp rate.

Ramp time	Peak pressure	Cavity dimensions			Cavity St Dev	
		Height	Width	Length	Height	Width
1	60	9.99	4.06	187.98	3.00	1.20
2	60	11.65	4.97	280.15	2.30	1.23
3	60	11.22	4.94	237.55	2.64	1.32
5	60	12.40	5.37	279.78	2.15	0.84
1	80	10.66	4.63	199.29	3.29	1.48
2	80	9.64	4.27	279.72	2.18	1.11
3	80	9.50	4.45	281.73	2.24	1.07
5	80	10.49	5.54	277.68	2.28	0.93

**Table 10.9 - Table showing the cavity dimensions and the standard deviation of the cavity height, width and overall area at each sampling point**

Figure 10.30 through to Figure 10.37, show the mean gas cavity height and width at 10mm samples points along the gas cavity rib. This shows how the gas cavity changes in height and width for each of the moulding parameters, as it moves away from the gas pin. Sample points to the left of the gas pin are shown as a negative distance, where sample points to the right of the gas pin are shown as a positive distance.

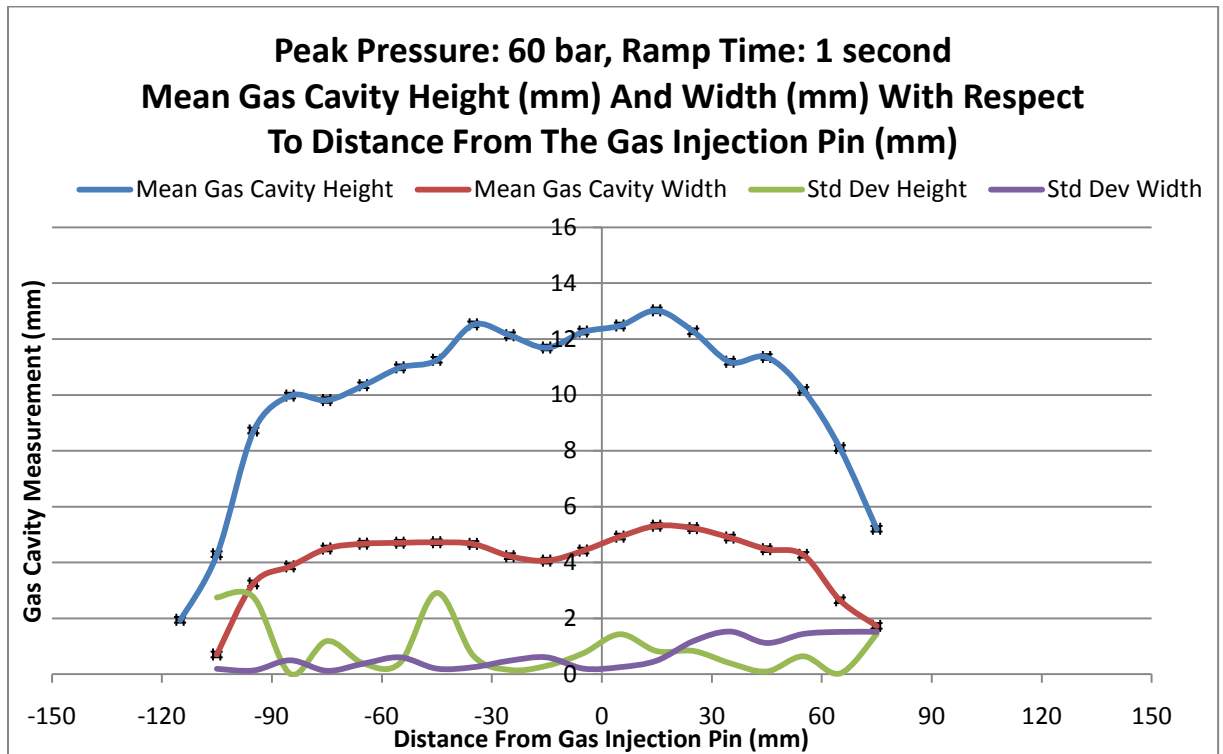


Figure 10.30 - Graph Showing the gas cavity dimensions for mouldings with a peak gas pressure of 60 bar and ramp time of 1 second. The error for measurements is  $\pm 0.1$ mm.

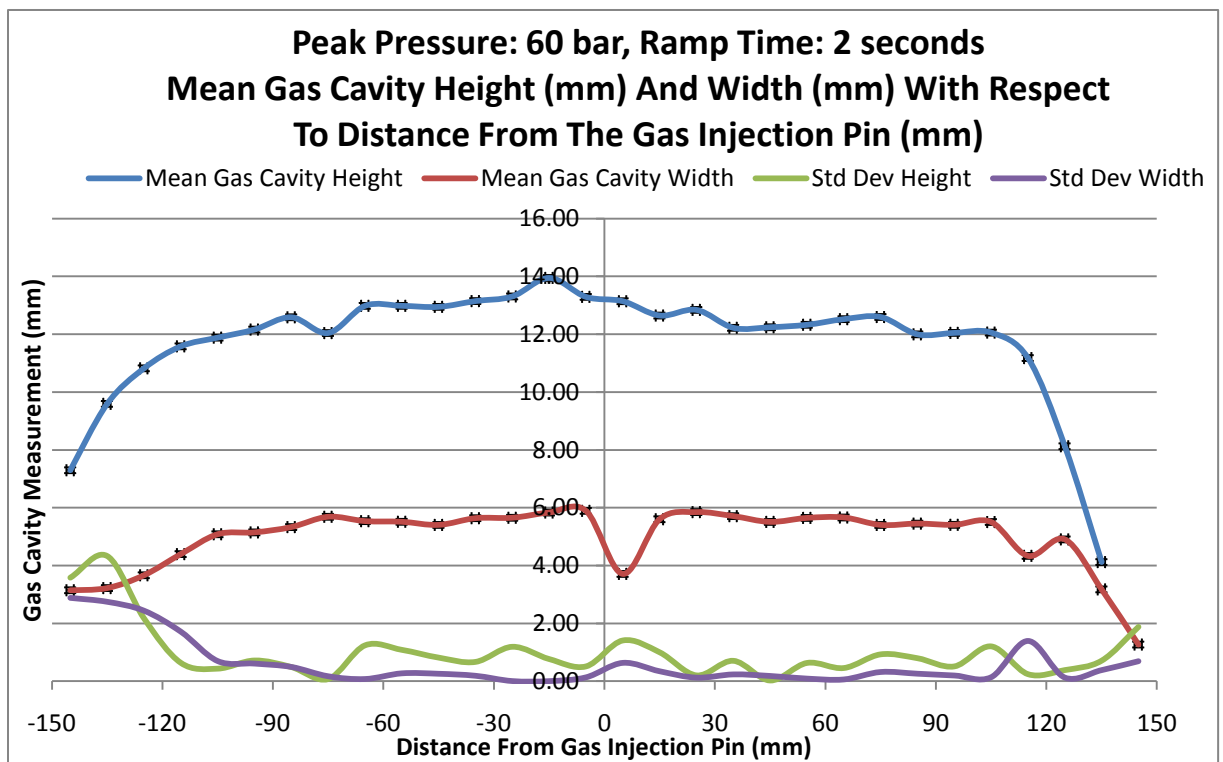


Figure 10.31 - Graph Showing the gas cavity dimensions for mouldings with a peak gas pressure of 60 bar and ramp time of 2 seconds. The error for measurements is  $\pm 0.1$ mm.

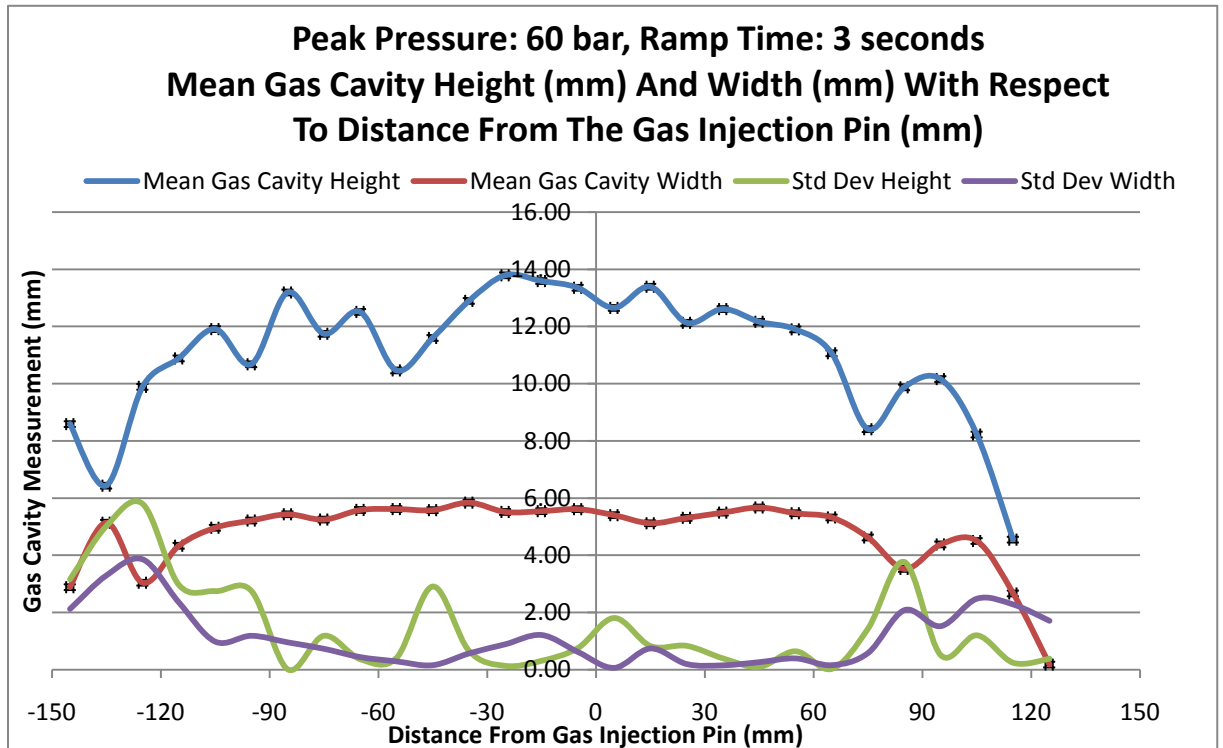


Figure 10.32 - Graph Showing the gas cavity dimensions for mouldings with a peak gas pressure of 60 bar and ramp time of 3 seconds. The error for measurements is  $\pm 0.1$ mm.

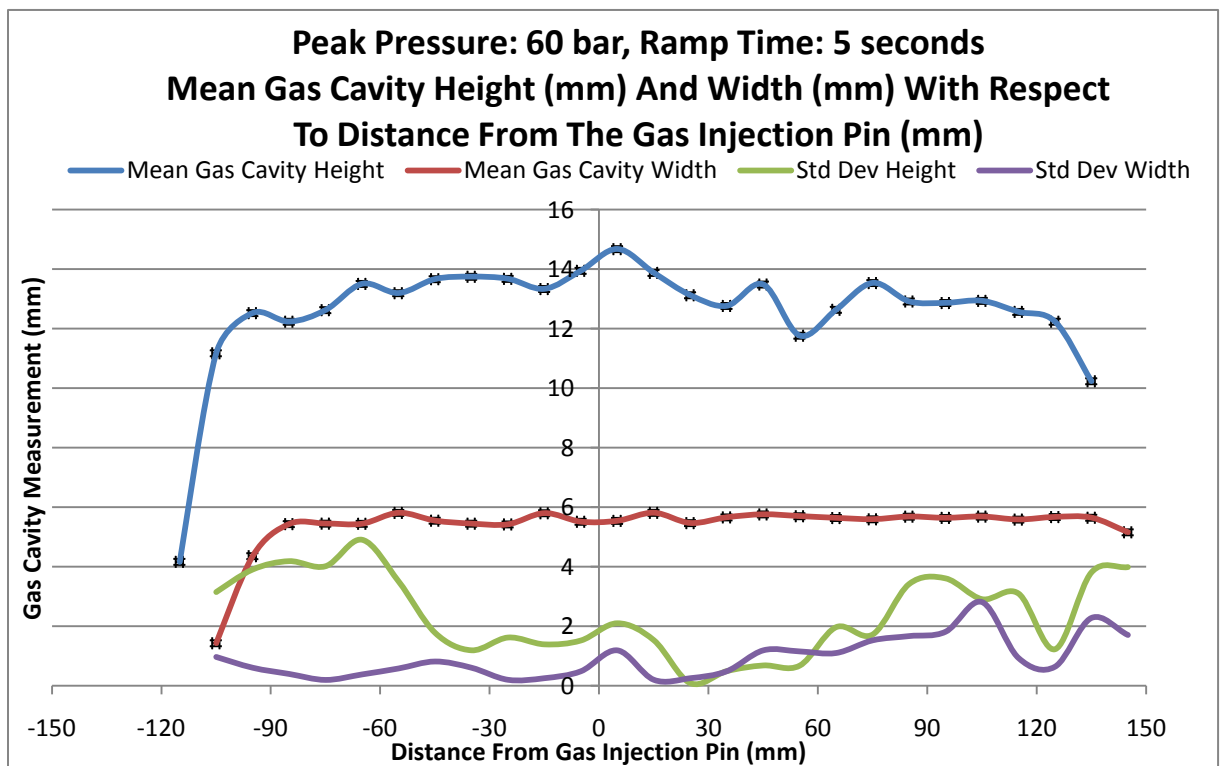


Figure 10.33 - Graph Showing the gas cavity dimensions for mouldings with a peak gas pressure of 60 bar and ramp time of 5 seconds. The error for measurements is  $\pm 0.1$ mm.

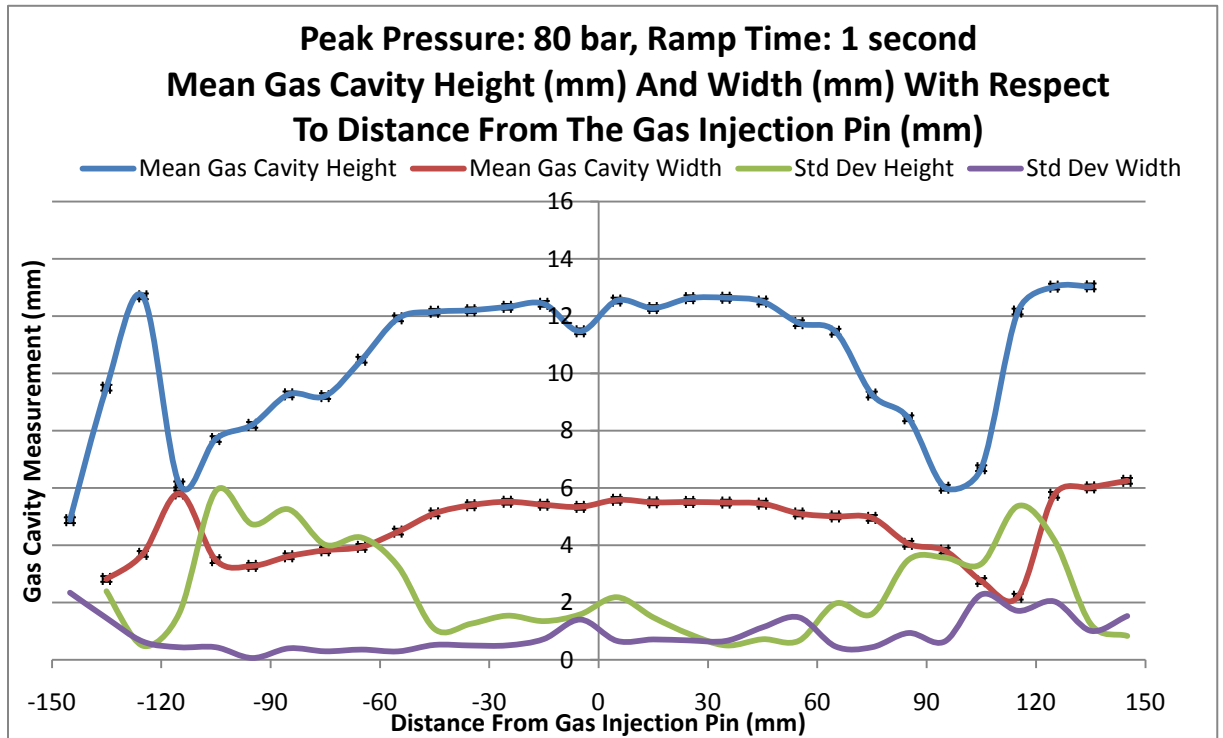


Figure 10.34 - Graph Showing the gas cavity dimensions for mouldings with a peak gas pressure of 80 bar and ramp time of 1 second. The error for measurements is  $\pm 0.1$ mm.

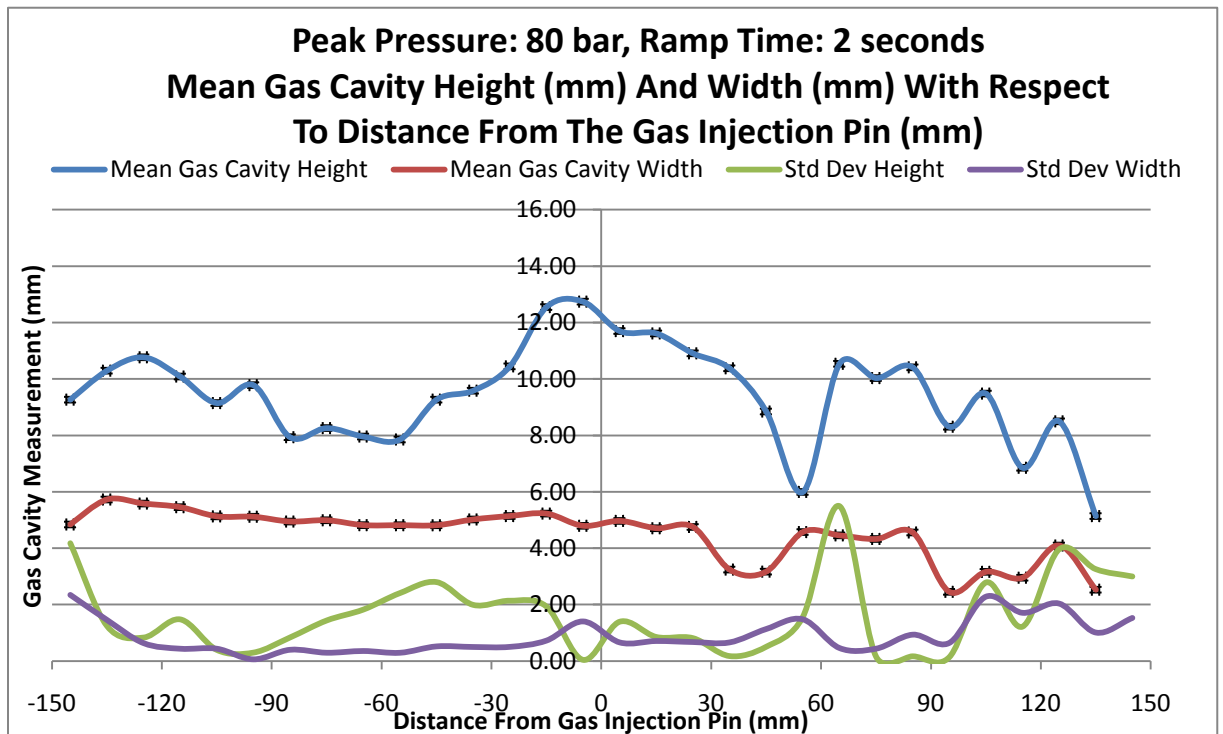


Figure 10.35 - Graph Showing the gas cavity dimensions for mouldings with a peak gas pressure of 80 bar and ramp time of 2 seconds. The error for measurements is  $\pm 0.1$ mm.

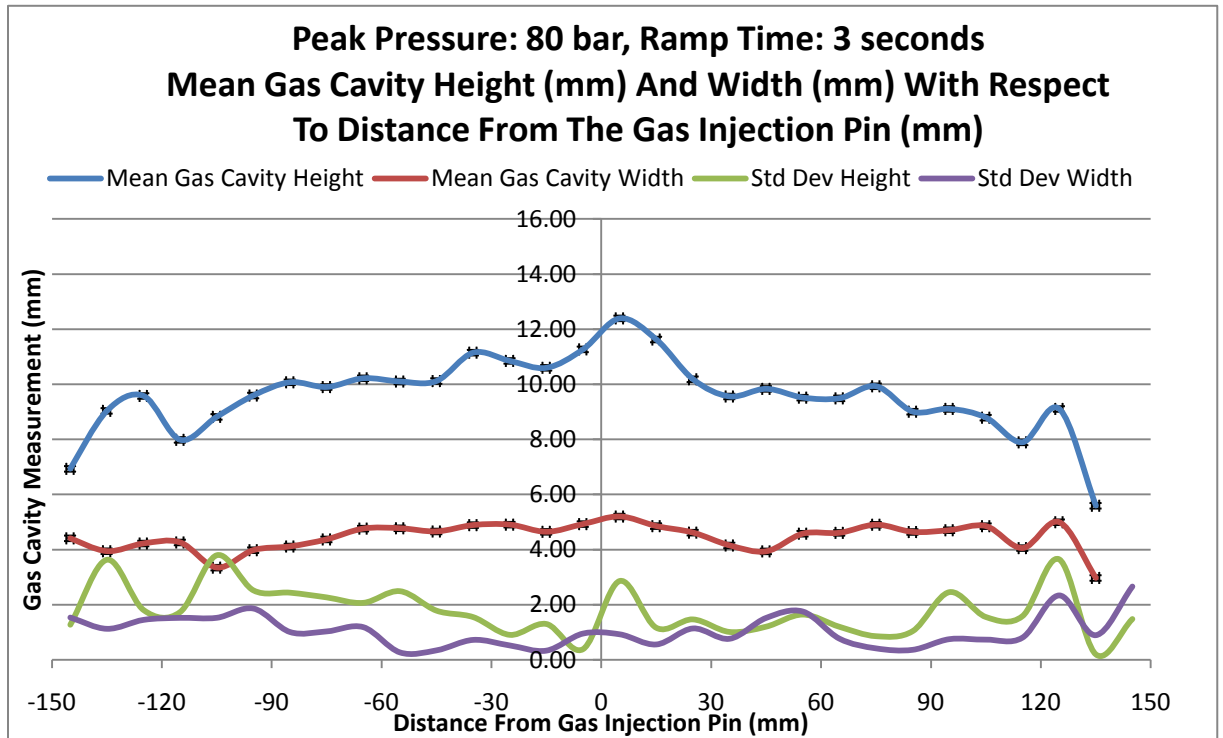


Figure 10.36 - Graph Showing the gas cavity dimensions for mouldings with a peak gas pressure of 80 bar and ramp time of 3 seconds. The error for measurements is  $\pm 0.1$ mm.

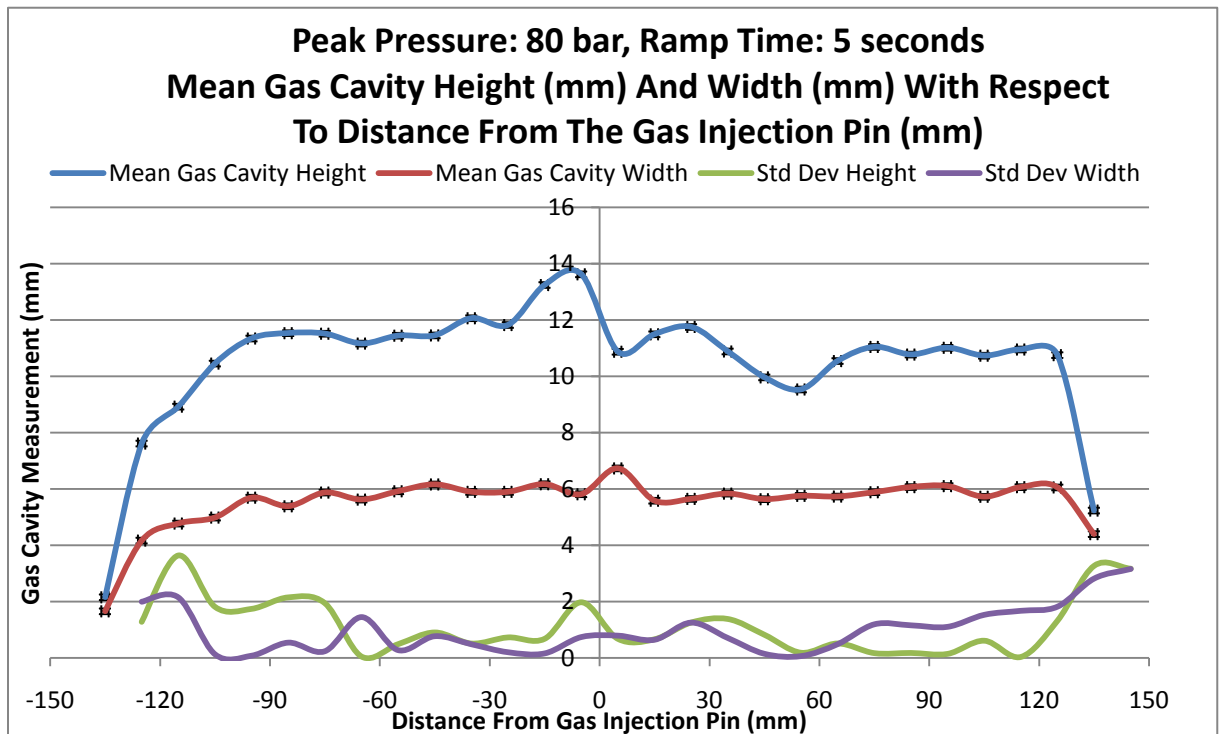


Figure 10.37 - Graph Showing the gas cavity dimensions for mouldings with a peak gas pressure of 80 bar and ramp time of 5 seconds. The error for measurements is  $\pm 0.1$ mm.

### 10.4.3. Gas Ramp in Re-GMT Discussion and Conclusions

The gas ramp study appears to show that as the ramp rate increases, the cavity length increases. The cavity volume does not change with gas pressure or gas ramp time, suggesting that a parameter outside the scope of this gas ramp study had a larger affect on the cavity volume. The ramp rate also appears to produce a smoother, more consistent cavity wall thickness.

## 11. Moulding Features

### 11.1. Compression Flow of GMT

During the GasComp cycle, the material would experience three moulding stages; consolidation, flow due to compression moulding and flow due to the gas pressure. Conventional compression moulding is carried out with hot tools and is considered as an isothermal process, which causes squeeze flow. However, as cold mould tools with hot material were used throughout the majority of this research, a non-isothermal flow is assumed. A compression moulding study with glass reinforced polypropylene carried out by Wakeman *et al.* [54] stated that during the non-isothermal compression moulding GMT the skin of the material in contact with the mould cools, with the onset of fountain flow. Further studies by Diest and Maier [102] on the fibre orientation in flat circular GMT parts state that the parts contained three distinct layers through the thickness of the part. Firstly a thin layer of frozen material near the mould tool surface contained minimal flow orientation, then a layer with high flow orientation and shear deformation and finally a central layer with some extensional and flow orientation. The study also found that during the compression

moulding of multiple GMT blanks, the outer blanks remained in place, while the inner blanks were squeezed into the flow region. After which the material will progress in a fountain flow manner during the compression moulding cycle.

Figure 11.2 shows a cold rib tool GMT moulding at 60 bar over 1 second, with oven temperature of 200°C, with the position along the rib of Figure 11.3 in an area that experienced compression moulding. Figure 11.3 shows the three distinct layers as described by Diest and Maier. A frozen layer is visible at the top and bottom of the rib, with a central area showing a small orientation to the flow. The shear layer is visible between central layer and frozen layer where the fibres have aligned to the flow direction.



Figure 11.1 - A cold rib tool GMT moulding at 60 bar over 1 second, with oven temperature of 200°C

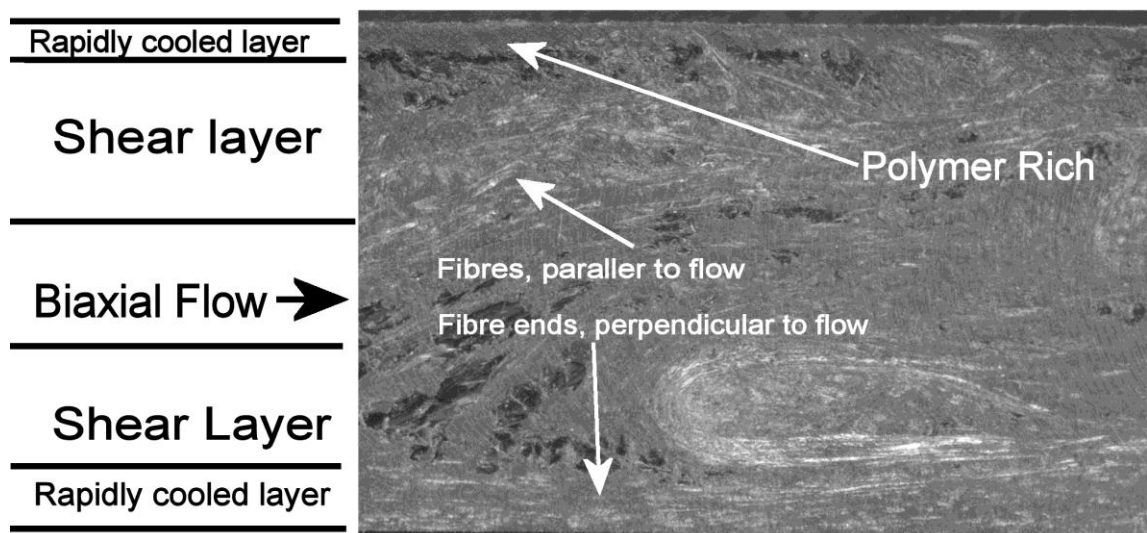
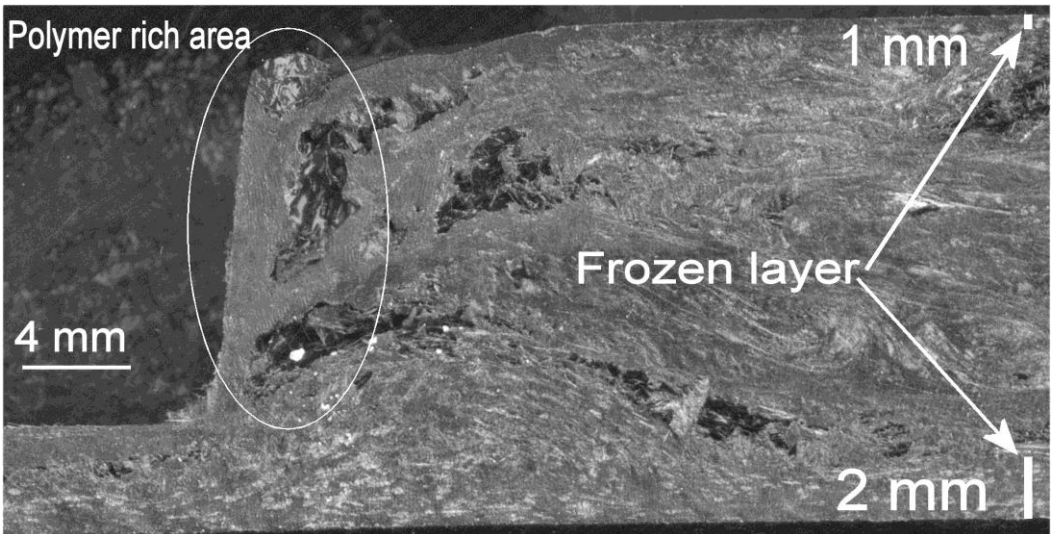


Figure 11.2 - Close up of GMT moulding showing frozen layers, shear layers and central flow layers through a GMT moulding

A hot tool moulding and cold tool moulding were taken from the GMT parameter study, to examine the effect of a hot and cold tool on the thickness of the frozen surface layer. Figure 11.3 and Figure 11.4 show the frozen skin on a rib tool moulding with a cold and hot mould tool respectively. The skin in contact with the bottom of the tool is significantly larger than the skin at the top of the tool. This is because the hot material is placed in the bottom of the mould tool and so is in contact for a short period before the upper half of the mould tool is closed and encounters the upper surface. The difference in the thickness of the frozen layer, between the hot and cold mould tools, is not significant. Approximate measurements of the frozen layers in a hot and cold mouldings showed that the hot mould tool contain a thinner frozen layer of 1.9mm and upper frozen layer of 0.9mm, where as the cold mould tool has a lower frozen layer of 2.1mm and upper frozen layer of 1mm.



**Figure 11.3 - Image of a cold rib tool GMT moulding, showing the frozen skin layer and polymer rich area in front of the gas cavity**

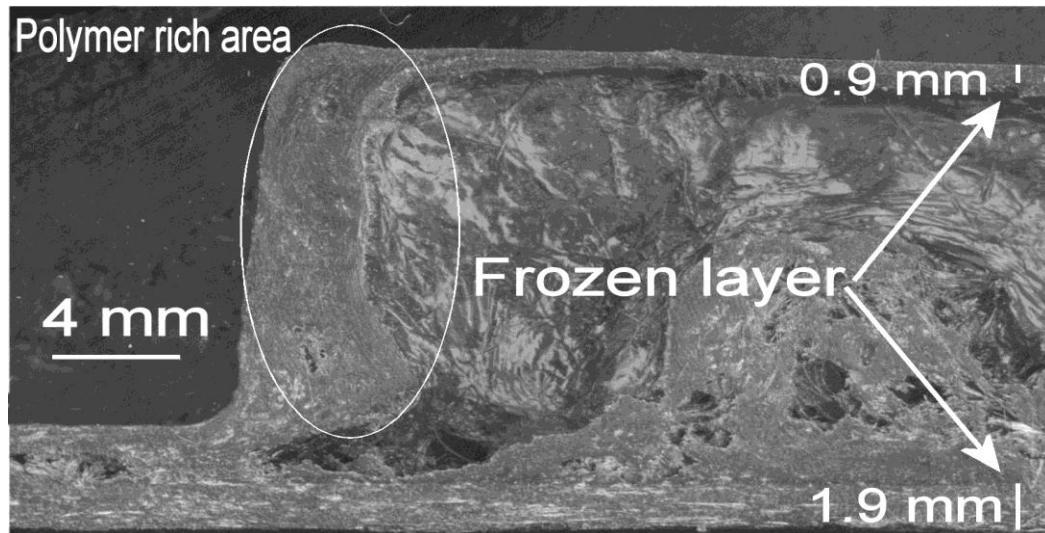
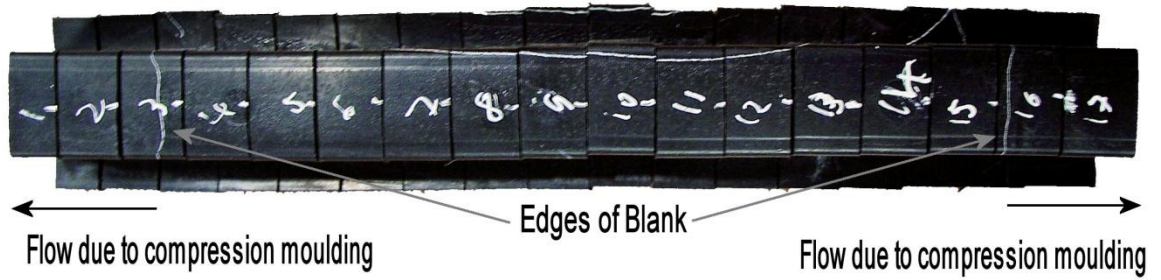


Figure 11.4 - Image of a hot rib tool GMT moulding, showing the frozen skin layer and polymer rich area in front of the gas cavity

The polymer rich areas indicated in Figure 11.3 Figure 11.4, indicates that the polymer was stripped from the glass by the gas flow front , and deposited at the end of the rib. The component processed in a cold tool shows that the material froze off quickly, where as the hot tool had a larger cavity at the end of the rib.

## 11.2. Compression Flow of Re-GMT

The flow through the top flange of a Re-GMT cold rib tool moulding processed with a 60 bar gas pressure over 1 second was investigated through microscopy. The moulding was cut into 20mm sections (Figure 11.5) and using the technique described by section 9.1 Microscopy, with sections, one, five, nine, thirteen and seventeen, polished and examined under an optical microscope. These sections were chosen as they were the sections in the centre of the blank, near the end of the blank and at the end of the rib and so the end of the flow due to compression moulding.



**Figure 11.5 - Moulding showing section positions and edge of the blank and subsequent compression moulding flow**

Figure 11.6, Figure 11.7 and Figure 11.8 shows the direction and position that was examined by microscopy in sections, nine, five and one.



**Figure 11.6 - Photo of section 9 with the examined section highlighted**

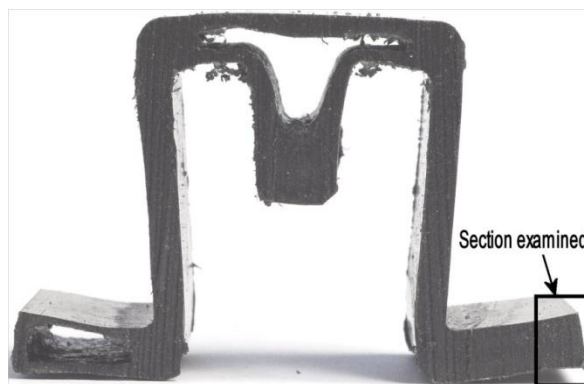


**Figure 11.7 - Photo of section 5 with the examined section highlighted**

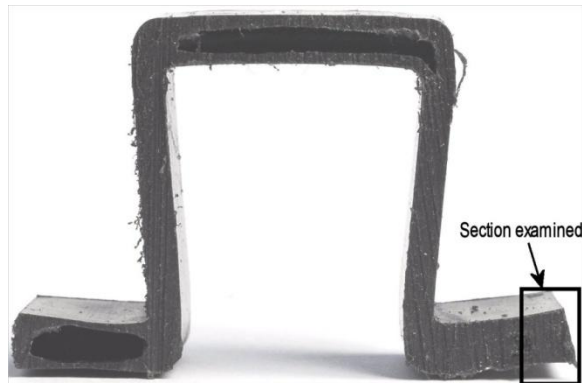


**Figure 11.8 - Photo of section 1 with the examined section highlighted**

Figure 11.9, Figure 11.10 and Figure 11.11 show micrographs of the central rib at sections nine, five and one, respectively. The small white dots and lines shown in the photos are the glass fibres and the large white dots and filler particulates. The material flow at the end of the top flange in the central section, nine, is complicated. The material was placed on the top flange and so there was only a small flow to fill the flange. Once the flange was full, the material started to flow along the length of the moulding. The glass fibre orientation distinctly changes at the end of the rib compared to the centre sections of the moulding. The glass fibres in the centre sections (Figure 11.9 and Figure 11.10) of the moulding are aligned to the direction of the flow which is towards the reader. The glass fibres in the end section (Figure 11.11) have rotated and lie perpendicular to the glass fibres in the other sections. This shows that the flow changes direction as the material reaches the rib. The number of white lines is also reduced, indicating that the concentration of glass fibres has reduced.

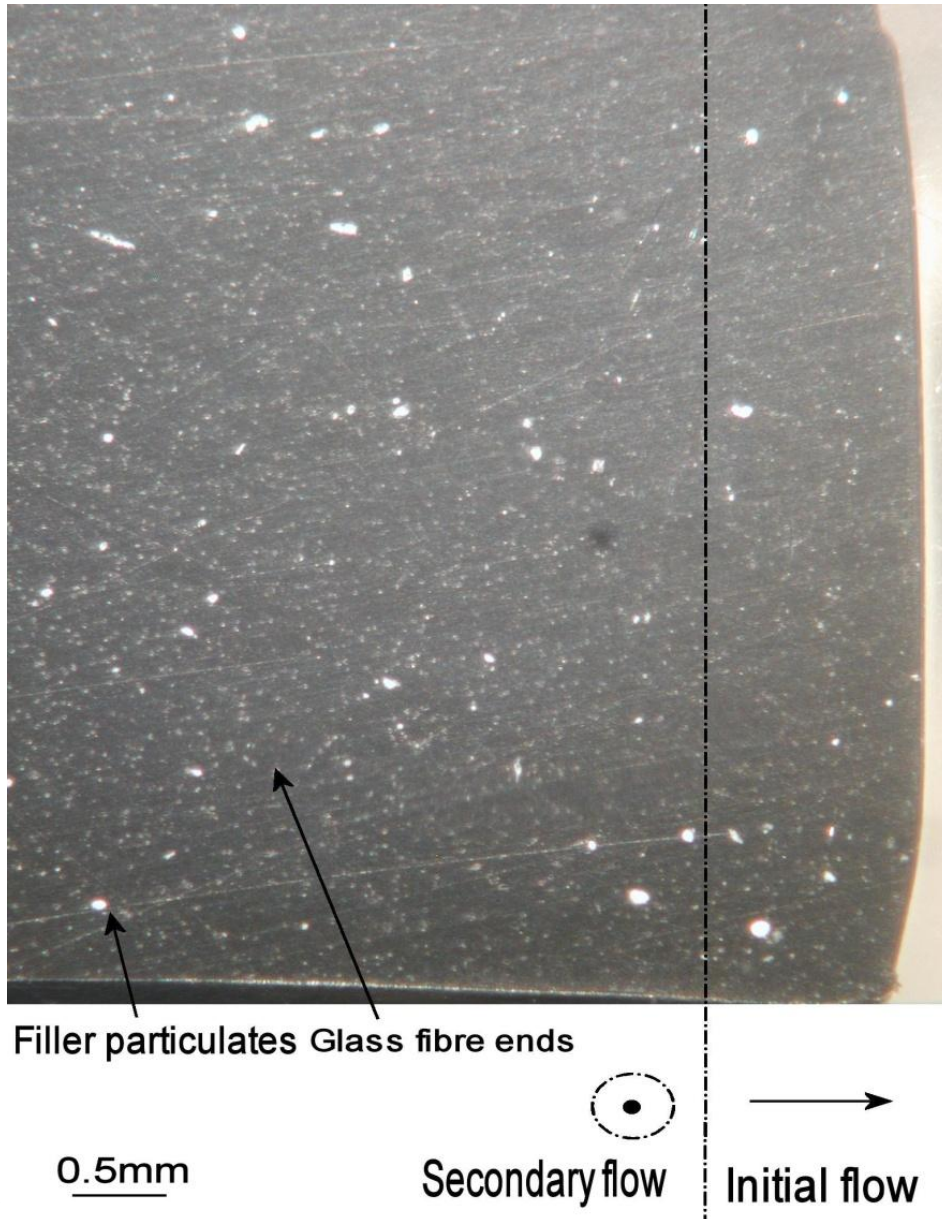
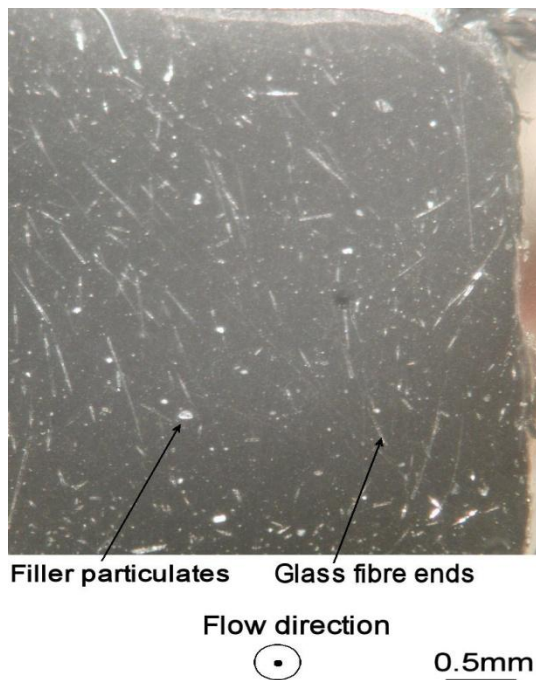


Figure 11.9 – Micrograph showing glass orientation at end of top flange of section 9, small white dots denote glass fibre ends, larger white dots denote filler particulates. The flow path is towards the reader.



**Figure 11.10 - Micrograph showing glass orientation at end of top flange of section 5, small white dots denote glass fibre ends, larger white dots denote filler particulates. The flow path is towards the reader.**



**Figure 11.11 - Micrograph showing glass orientation at end of top flange of section 1, small white dots glass fibre ends, white lines denote glass fibres rotated to perpendicular to rib direction, larger white dots denote filler particulates. The flow path is towards the reader.**

### 11.3. Re-GMT Flow Due to Gas Pressure

The material flow due to the gas pressure and the progression of the gas cavity was investigated through microscopy and photographic analysis. This was done by examining the gas cavity created in the Re-GMT moulding as described in section 11.2 Compression Flow of Re-GMT. Figure 11.13 shows that there is only a small degree of concentrated fibres around the cavity, where as Figure 11.14 indicates that there is no significant change in fibre alignment or concentration due to the gas cavity.

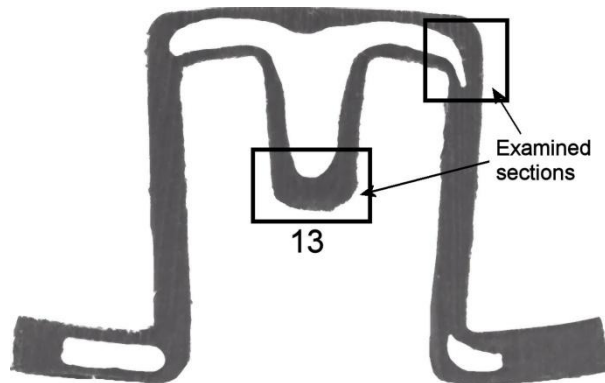


Figure 11.12- Image of slice 13 and the positions of the examined sections

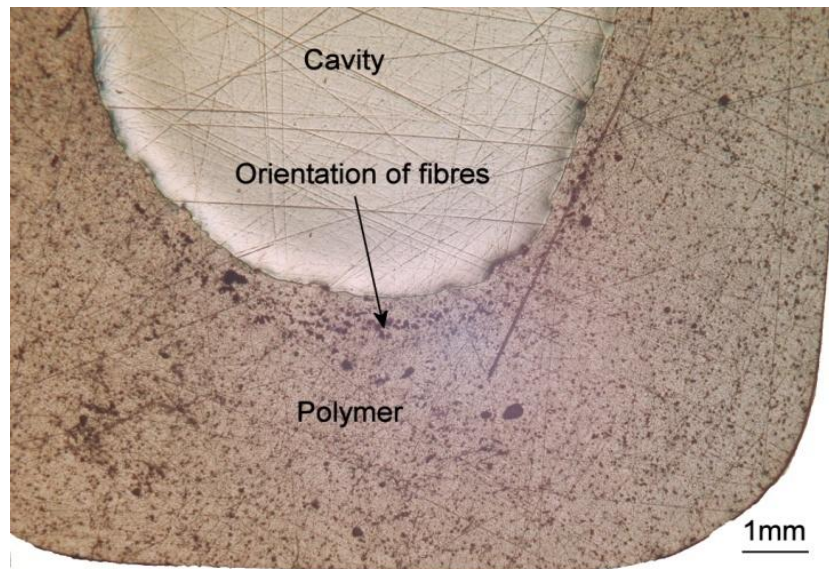
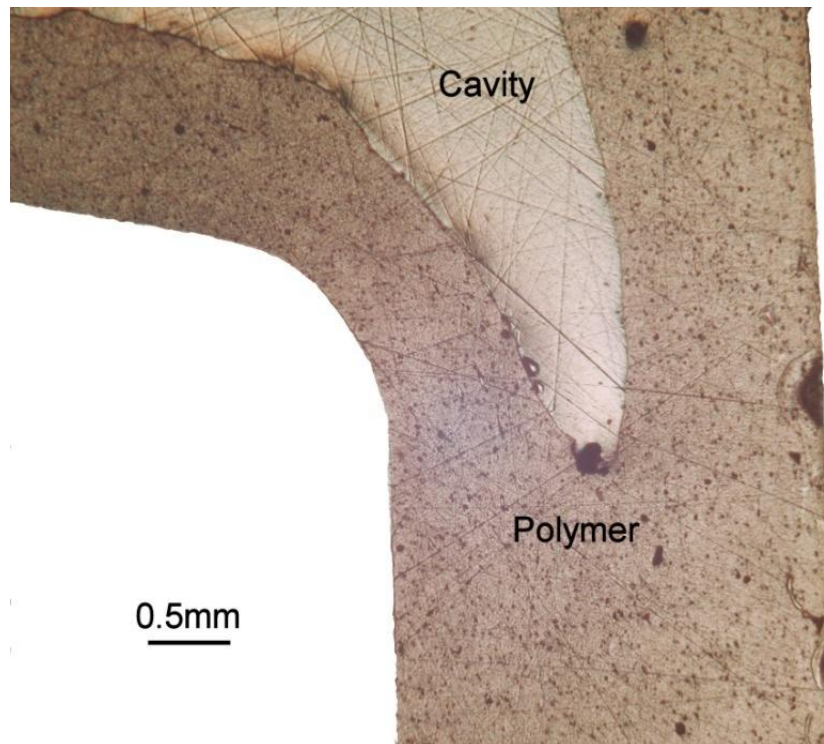
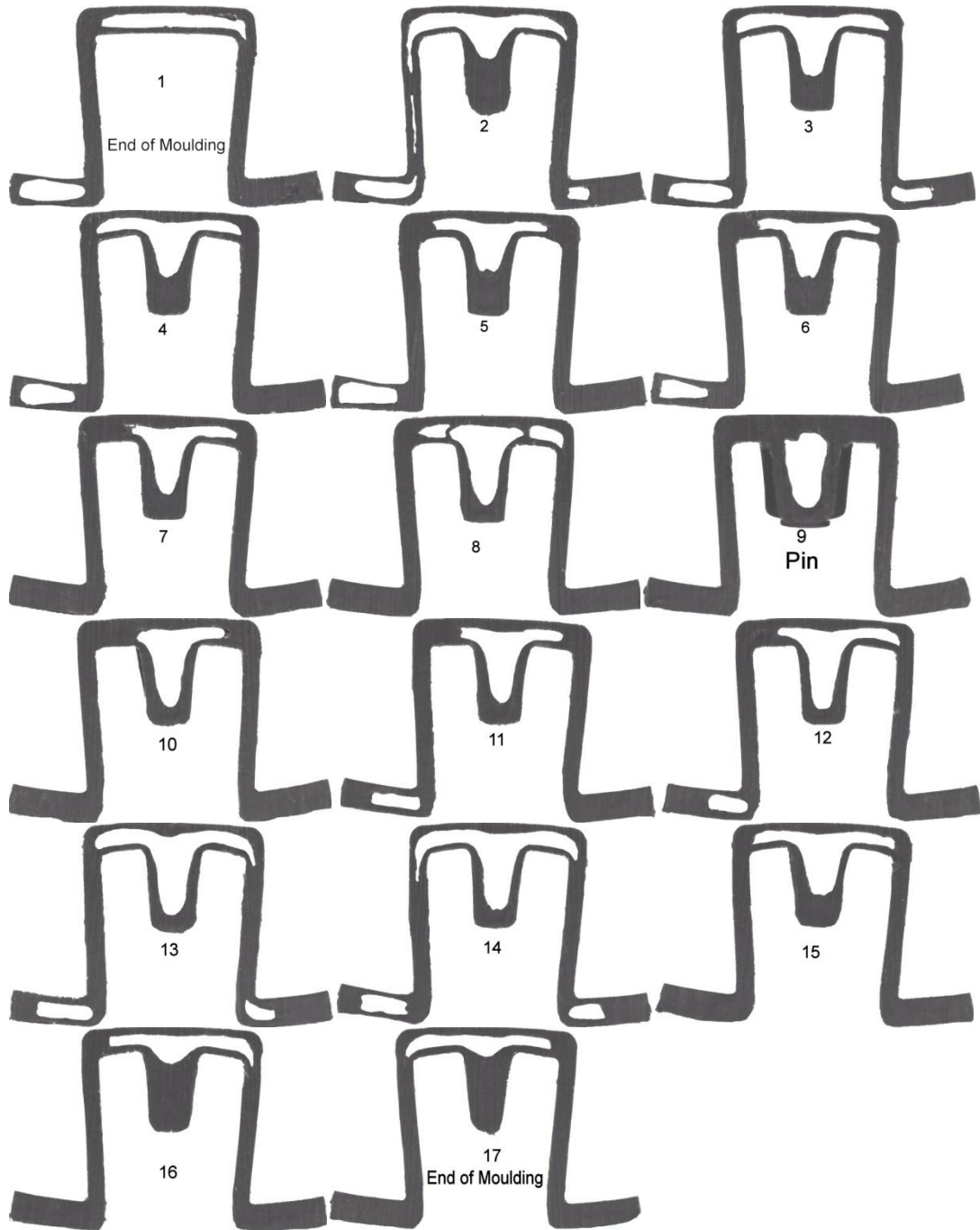


Figure 11.13 - Micrograph of cavity formation around the rib



**Figure 11.14 - Micrograph of gas cavity beginning to finger up the sidewall**

Photos were taken of each of the sections in a single direction and processed to highlight the cavity shapes using a photo-processing package. All 17 sections are displayed in Figure 11.15. The progression of the cavity can be seen to rapidly core out a significant portion of the rib, with some extent of fingering, before gradually reducing in size as it reaches the end of the rib. Section 2 shows how the gas fingered up into the top flange before expanding back towards the centre of the moulding. The same fingering effect can be seen at the opposite end of the moulding at section 14, where the gas expands in both directions along the top flange. Section 1 also shows that the gas was able to significantly core out the bottom flange.



**Figure 11.15 - Photos of sections 1-17 showing cavity shape progression in a rib moulding moulded with 60 bar peak pressure over 1 second**

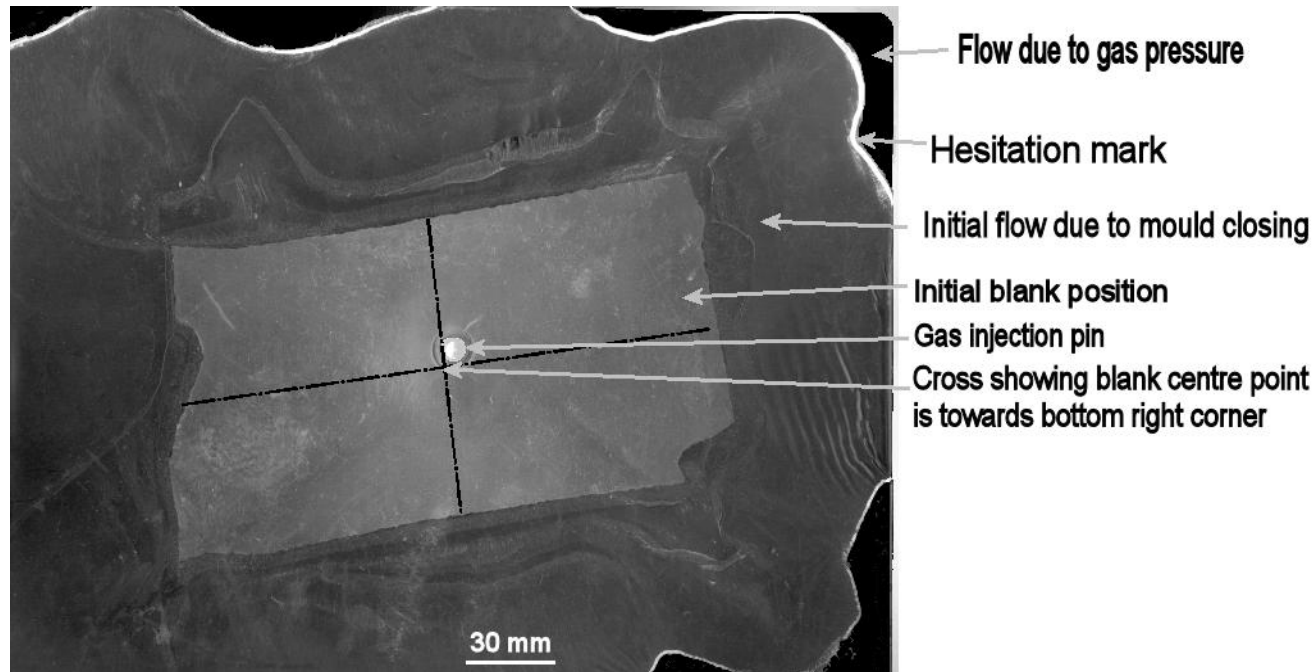
## 11.4. Gas Flow Mechanics

The gas will always follow the path of least resistance and this can change as the material flows and cools. The factors that decide the path of least resistance are:

- Polymer flow length
- Cross sectional area of cavity
- Polymer temperature

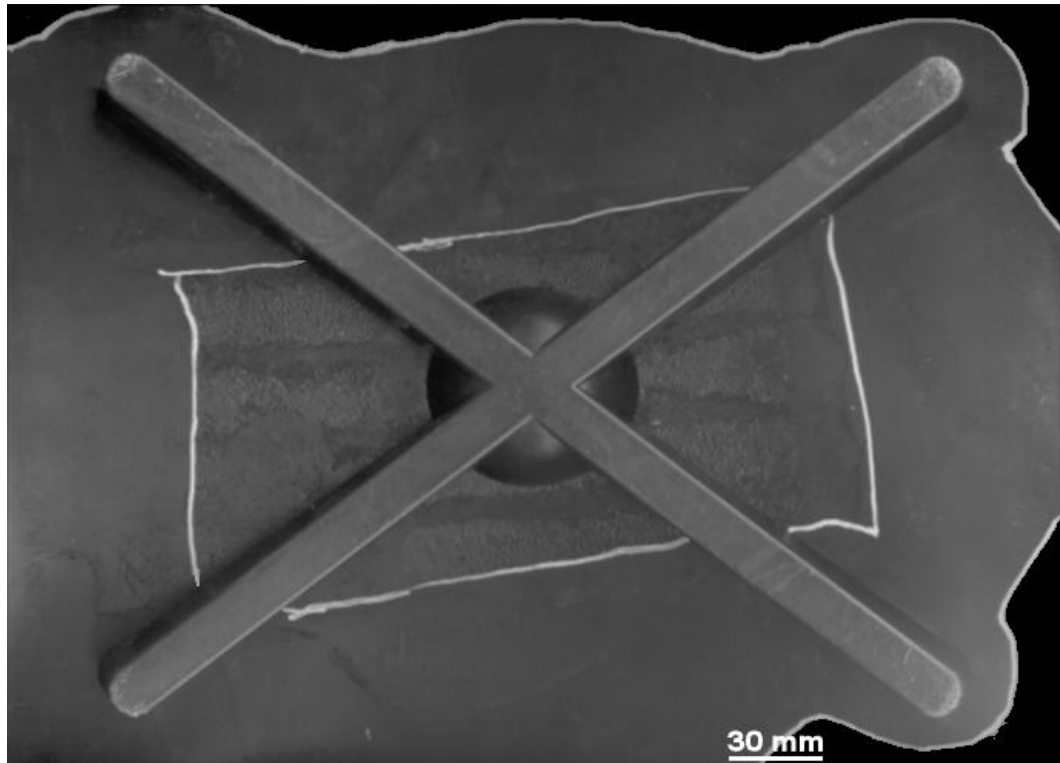
Once the gas has reached the end of one flow path the gas pressure will then push the gas down an alternative flow path. The initial path could be decided by slight changes in the material characteristics such as blank positioning and localised increase of glass concentration, as the cross sectional area of the cavity and polymer temperature are uniform at the start of the cycle. The placement of the blanks in the mould would have the largest affect in the initial path of the gas by altering the flow length relative to the location of the gas injection pin. If the blank is offset to one side of the pin then this will have an increased resistance to flow due to the larger volume of material. The side with less material would have the lower resistance and so the gas would have a preference to travel in that direction first. This is evident in Figure 11.16 where the original position of the blank has been highlighted and the resultant material flow due to the gas is shown in black after the white line. The blank position is highlighted further in the centre of the image. The blank has been placed off centre and is closer to the bottom left corner. The bottom left corner of the moulding does not show any signs of flow due to the gas. The top right edge that is furthest away from the blank position shows a large volume of material movement due to the gas. The material flow due to the compression moulding is

evenly spread from the blank position and is shown between the blank and white line. The non-uniform shape of the blank is a result of the stacking process, which has resulted in small folds in the blank.



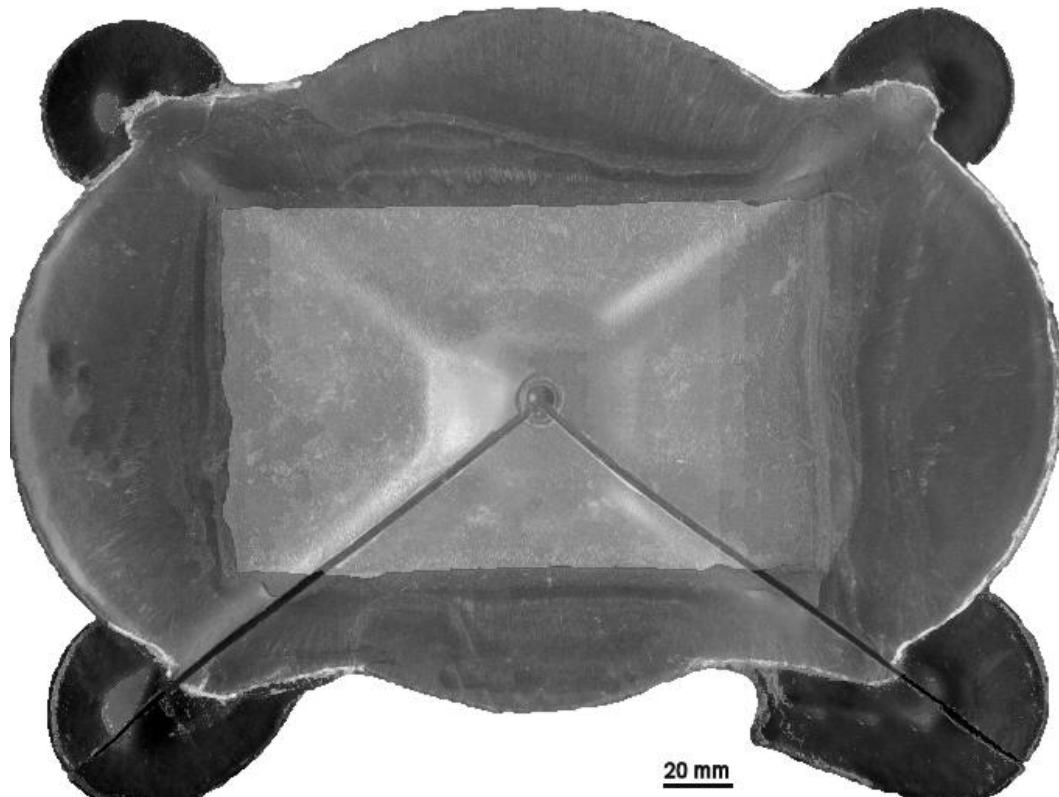
**Figure 11.16 - Image showing top side of a Re-GMT star tool moulding, processed with 100 bar over 0.1 second with a delay time of 0.5 seconds, showing the various stages of material flow and blank position.**

Figure 11.17 shows bottom side and material flow with respect to the ribs, of the same moulding shown in Figure 11.16. The flow pattern shows material being pushed from the centre blank position, denoted by the inner white lines, along the four ribs and then spreads outwards in a biaxial extension like manner. Figure 11.17 shows this radial flow pattern due to compression moulding. The material flow due to the gas is shown in black, after the hesitation mark, denoted by the outer white line.



**Figure 11.17 - Image showing rib side of Re-GMT moulding, processed with 100 bar over 0.1 second with a delay time of 0.5 seconds, showing blank placement effect on material flow**

A radial flow pattern is also evidently caused by the gas flow as shown in Figure 11.18. The white lines at the corner of the mouldings indicate the hesitation mark with the material flow due to gas injection shown in black. Some flow preference is shown at the bottom of the moulding due to the blank being placed marginally higher than centre. This shows that the flow pattern is essentially symmetrical when the blank is placed in the centre of the mould tool.



**Figure 11.18 - Radial flow pattern due to gas injection, processed with 100 bar over 4 second with a delay time of 0.5 seconds, showing the progressive flow phases during the moulding cycle**

This flow preference is again shown when the rib tool is used in Figure 11.19 and Figure 11.20. The shorter cavity was located at the end where the top flanges on both sides were full. A close up of this moulding shows several gas mechanisms and a complex gas flow involving several stages are shown in Figure 11.21. The features that appear in this moulding indicate that the gas took several paths at different time intervals in the injection. The gas injection profile used in this mould had a delay time of 1 second and a peak gas pressure of 120 bar over 1 second ramp rate. The polymer was assumed to have stopped flowing under compression before the injection of gas.

1. The gas flows into the rib creating a cavity
2. The gas ceases to flow into the right hand side, possibly due to localised fibre damming and extends the left hand side
3. Flow ceases in the left hand rib
4. Flow restarts into the right hand side rib breaking through the frozen wall created by the cooler gas. This breakthrough is evident by the shape of material at the break through point
5. Flow ceases in the right hand side rib
6. Flow starts up the side flange to the top flange where it bursts through the material
7. Continuing gas pressure partially packs out the part as the part cools.

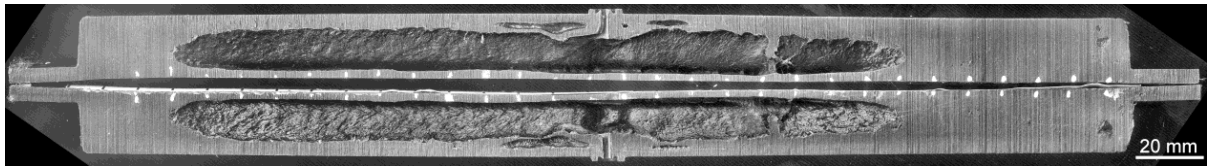


**Figure 11.19 - Image of a Re-GMT rib tool moulding, processed with a peak gas pressure of 120 bar over 1 second ramp rate**

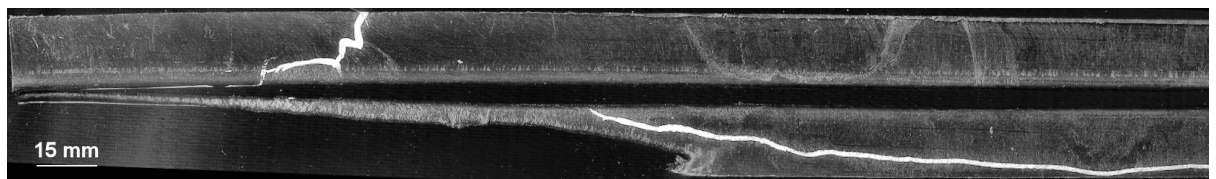


**Figure 11.20 - Image of top flange of a Re-GMT Moulding 2 processed with a peak gas pressure of 120 bar over 1 second ramp rate**

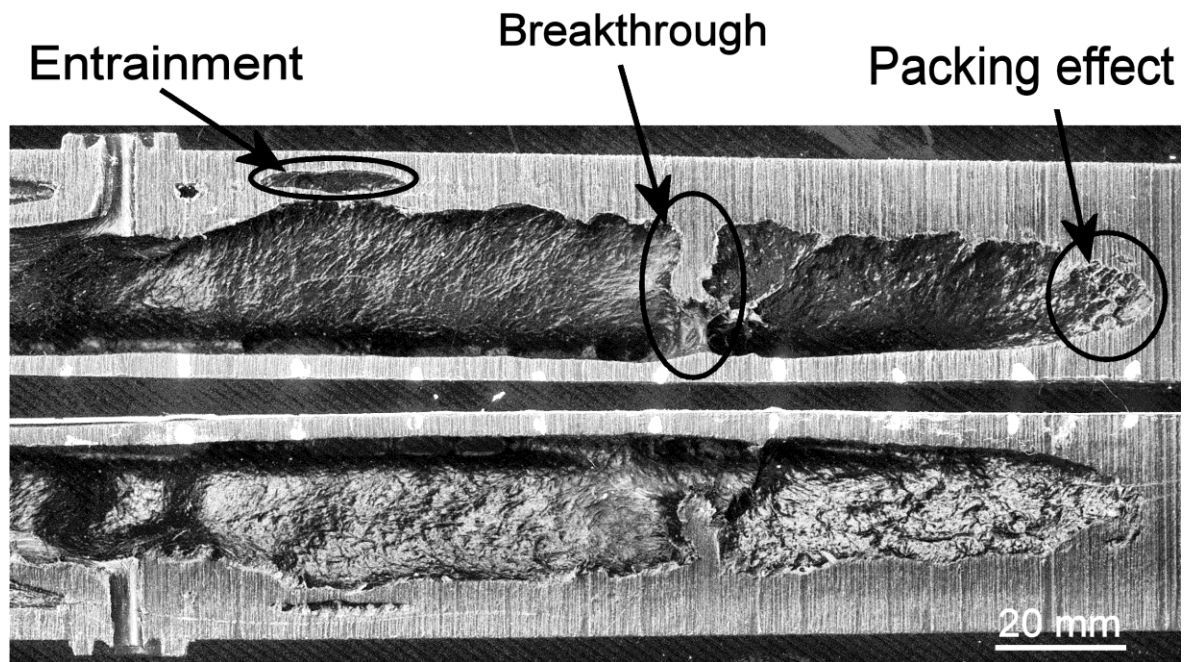


Figure 11.21 - Close up of gas flow features; polymer breakthrough and entrainment

The secondary flow front back into the frozen rib on the right hand side is not a common feature in other mouldings, as the gas would tend to finger up the side walls. This would indicate that the high gas pressure is the cause of this breakthrough.

Another feature that is present in this moulding (Figure 11.21) is entrainment. This is where high shear rate cause causes Rheological instabilities on the surface of the polymer that eventually close over, trapping the gas inside. Entrainment is more frequent at gas pressures above 80 bar.

Figure 11.22 shows the symmetrical gas flow when the blank placement is in the centre of the mould tool. There is also a symmetrical packing effect at both ends of the rib.

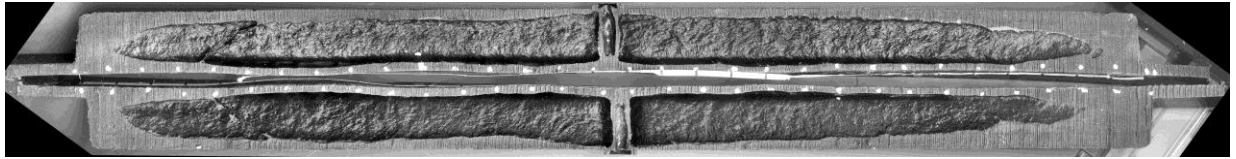


Figure 11.22 - Photo showing symmetrical gas flow in a rib tool moulding

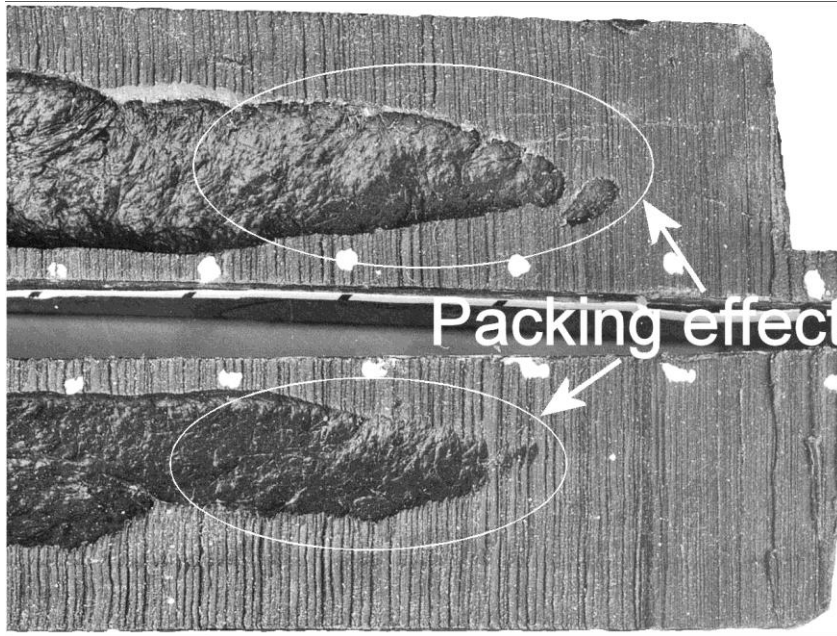


Figure 11.23 - Image showing packing effect on symmetrical gas flow

## 11.5. Hesitation Mark

Hesitation marks are present in GAIM mouldings and denote the transition between the flow due to the primary polymer injection process and gas injection. To investigate the presence of these marks on mouldings produced in the research, a small cross section from a rib tool moulding was polished and examined under an optical microscope. A micrograph was taken of a top flange that had not fully filled of a gas injected moulding, in the same position and plane as Figure 11.11. Figure 11.24 shows the cross section through the thickness of the top flange, with the locations of the upper and lower hesitation marks. There are no marks or features

through the thickness where the polymer was still molten as it was pushed through by the gas. This proves that the marks evident on the surface are hesitation marks.

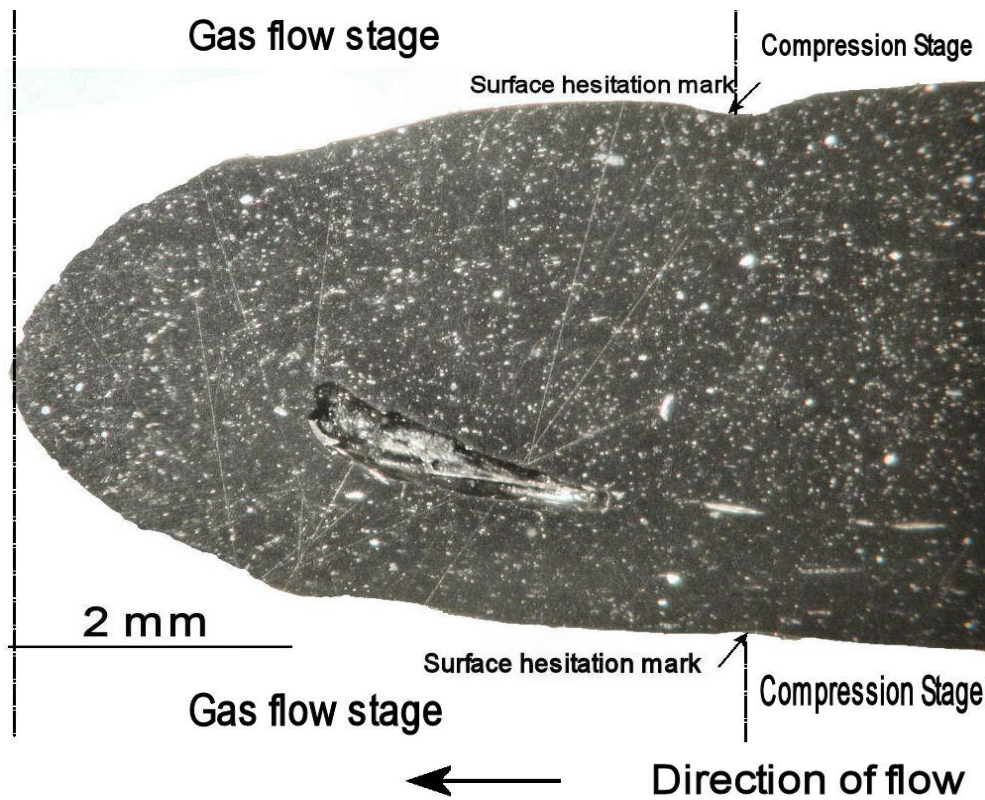


Figure 11.24 - Micrograph showing that no features are present between the upper and lower hesitation marks present on the surface, through the thickness of the top flange.

Studies were carried out during the research to reduce or eliminate the appearance of hesitation marks. In GAIM, this is done by keeping the time delay between the end of the polymer injection and the injection of gas to a minimum. This will smooth the transition between two flows. To replicate this action, the gas injection was initiated as the pin was encountering the molten material, causing the gas to flow with the compression moulding cycle. This technique had a limited success with the appearances of the marks being reduced, although they were not eliminated, although the gas escaping around the gas seal around the pin did increase. This indicates that a small delay is required to establish a strong seal.

## 11.6. Shrinkage

Literature shows that the GAIM reduces part shrinkage compared to conventional injection moulding by reducing the RWT, which increases the cooling rate of the material. An investigation was carried out to compare the shrinkage between conventional compression moulding and GasComp. The part length was used to calculate the extent of shrinkage. Since the length of the rib tool was fully 350.5mm, this would be the maximum potential length of a fully moulded part, with any reduction in length caused by shrinkage (assuming full shots). The cavity length and part length were compared in Figure 11.25. The thick horizontal red line at 347.6mm part length denotes the average part length of a conventionally compression moulded parts. As no gas was injected to fill the part, a full shot size was required to produce a full part required for an accurate comparison. This caused the material to over fill the mould tool causing the material to experience the full compressive force of the moulding machine, rather than the force being transferred to the moulding stops. The material would then experience a packing force, causing the thickness of the part to shrink, stabilising the length of the part as it cooled. Any resultant shrinkage would come from crystallisation from cooling outside of the mould where the compressive force on the part no longer has an effect. The parts with no injected gas contained **significantly** more material than parts with injected gas. It was found that a cavity length that was over 80 percent of the rib length was required to give a part that was longer than a part with no injection gas. A moulded part containing a cavity length of 276mm and a part length of 347.7mm showed a 10 percent weight reduction. The graph shows that a part containing a cavity length shorter than 247mm would have a part length shorter than a conventionally compression moulded

part. The graph shows that the cavity length increases linearly with part length. The large variation in part length vs cavity length is due to different shot sizes and processing parameters.

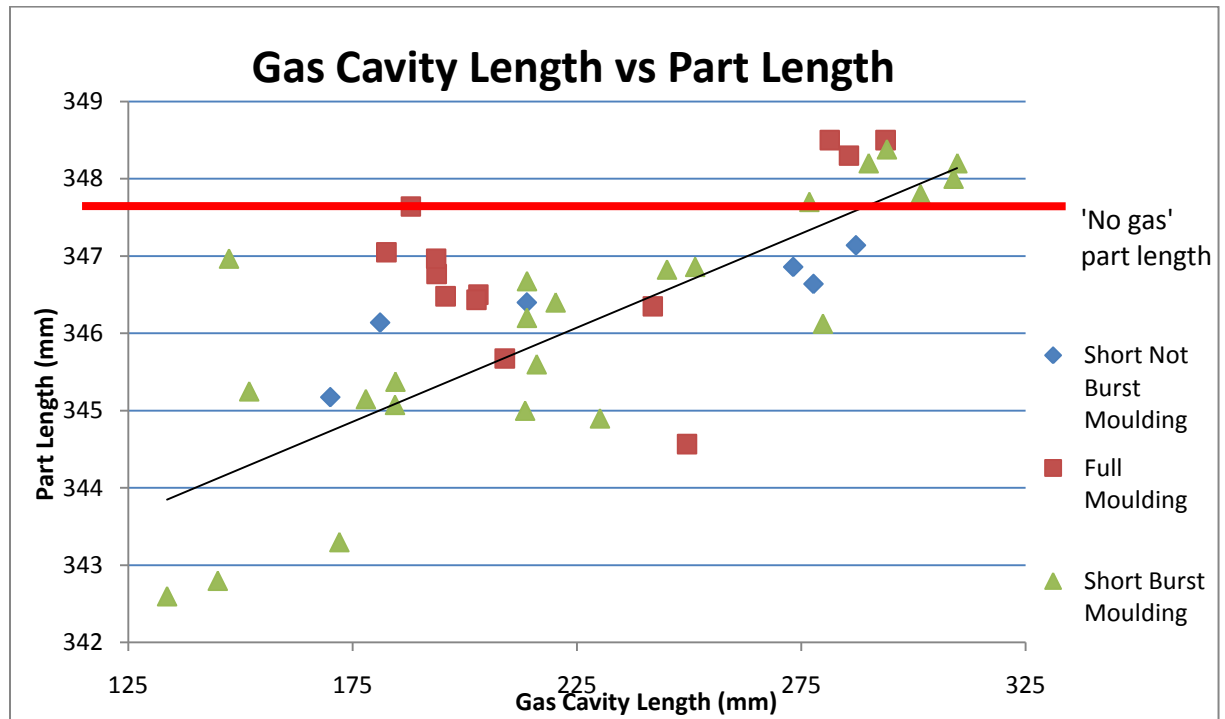
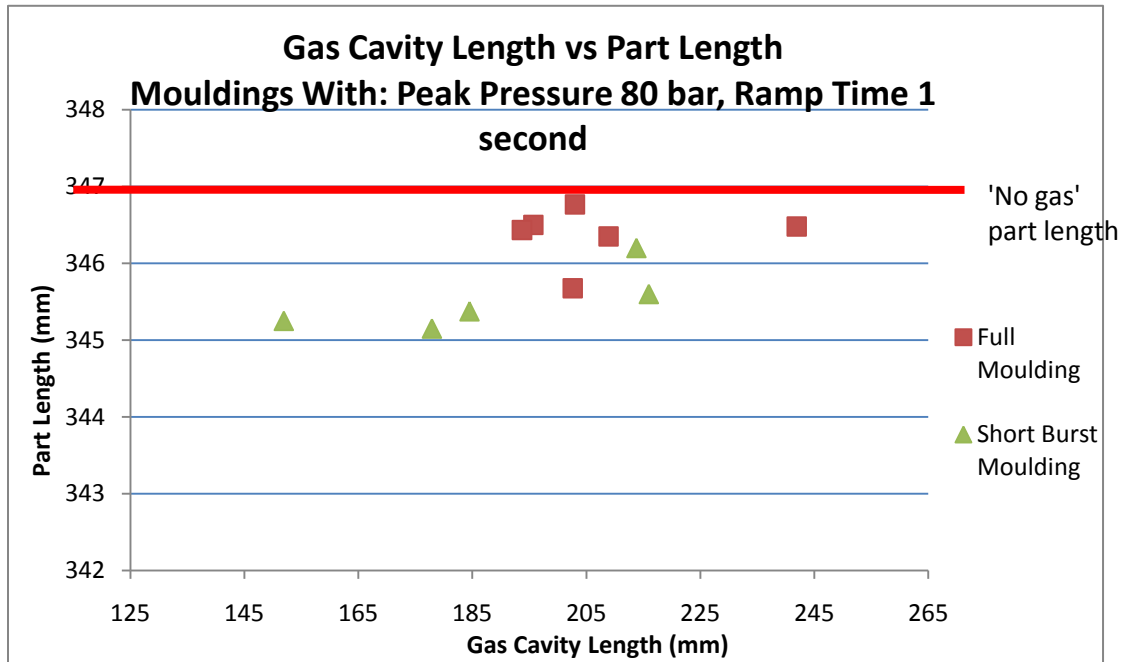


Figure 11.25 - Gas cavity length vs part length graph, with a 'no gas length line', denoted by thick red line. Part length tends to increase as cavity length increases denoted by dashed arrow. The error for Gas cavity length and Part length is  $\pm 0.1$ mm.



**Figure 11.26 - Graph showing the gas cavity length vs part length in mouldings processed with a peak pressure of 80 bar over 1 second ramp time. The error for Gas cavity length and Part length is  $\pm 0.1$ mm.**

The cooling time has a direct influence on the crystalline structure of the material. The quicker the material is cooled, the less time the material has to form an ordered crystalline structure. As GAIM proves, a part with a reduced wall thickness and injected with cool nitrogen gas would cool quicker than solid material.

An observation was noted that cored out ribs had a visibly reduced sink marks, and in some cases showing no visible marks at all. These marks were however not measured during the course of this research. Optical techniques such as microscopy depth of view measurements or computer co-ordinate measurements could be used to establish the extent of shrinkage.

## 11.7. Weight Reduction

The largest reduction of weight produced by Re-GMT with the rib tool was 17.4 percent, which contained a cavity length of 279mm with an average wall thickness of 3.1mm. The longest cavity length achieved was 309mm showing that the cavity extended past the rib and into the bottom flange.

The star tool showed that a larger weight reduction was possible with an increased rib cross section area. The star moulding produced with a 0.5 delay time (10.3 Effect of Gas Injection Delay Time) had a 30 percent reduction in weight. As Figure 10.20 shows, the ribs have not been completely cored out, showing that a greater reduction is possible. A full Re-GMT star tool moulding has a mass of 441g, a full moulding was produced using only 274g of material giving a 45 percent reduction in weight. Figure 11.27 shows a representative CAD model of a sectioned star tool with a wall thickness of 3mm. The model shows that the star tool was cored out to its full potential, indicating that the process would be capable of greater reductions in part weight.

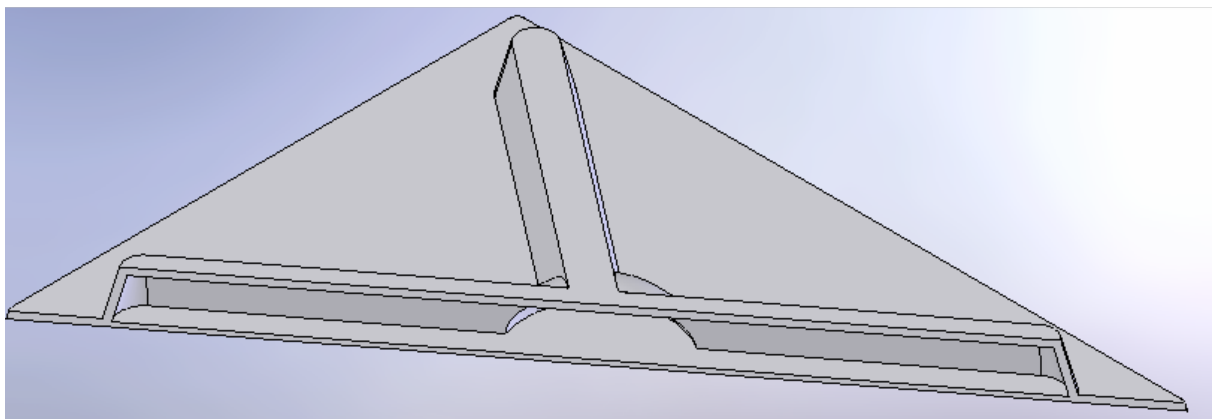


Figure 11.27 – A sectioned CAD model of Re-GMT star part with a mass of 274g

## 12. Summary of Discussion Points

The theoretical and experimental work carried out in the study of the innovative process GasComp, produced several major findings. GasComp uses gas injection to assist in the flow of compression moulding, using a novel mould tool design containing a horizontal clamping face. The process has been proved to produce a gas cavity inside a full part, giving a weight reduction of up to 45 percent. The summary of these findings include the proposed material requirements to produce a successful cavity using GasComp. The presented findings also include the effects of the processing parameters on the gas cavity and the features present in the moulded parts.

### 12.1. GMT Parameter Scoping Study

The outcome of the GMT parameter scoping study shows that a cavity can be produced GMT with a wide range of gas pressures and tool and oven temperatures. This parameter scoping study suggests that the oven temperature had a significant effect on the formation of a smooth walled cavity, where as the gas pressure and tool temperature settings investigated in this study did not.

The GMT mouldings produced by the parameter study contained sections of both fibre/polymer separation and smooth walled cavities were produced. The overall conclusion of the study is that a GMT with a 34 percent glass fibre content and a long fibre length of up to 25mm was not suitable for use with GasComp

## 12.2. Suitability of GMT, Re-GMT and LFT for GasComp

Further studies of additional materials with differing glass contents and glass fibre architecture were carried out in the course of the research. The research showed that the rheology and glass fibre architecture of the material were the most significant factor in the creation of a successful gas cavity. Re-GMT consistently produced a uniform cavity when processed with the correct processing parameters. Re-GMT had an MFR (200°C, 2.16 kg) of 1.35 g/10mins and contained a dispersed short glass fibre architecture. Successful mouldings produced with LFT, had a MFR (200°C, 2.16 kg) of around 11 g/10 mins with a pseudo aligned, glass filament architecture. This indicates that a material suitable for this process would have a MFR between 11 g/10 mins and 1 g/10 mins, with a low glass fibres entanglement. The glass fibres must not have a knitted or needled architecture in order for the process to be successful.

The success with LFT proved that the process worked with long fibres at a glass fibre content of up to 22 percent. The structural properties of LFT and the weight savings of up to 20 percent produced by the process, along with the associated benefits, could give rise to real industrial and commercial applications.

As studies in GAIM prove, as the gas flows in a glass-reinforced polymer, the gas will either push the material aside and create a cavity, or create a glass fibre rich area by separating the polymer from the glass fibres. It was found in this research, that the highly needled glass architecture of GMT prevented the gas from pushing the glass fibres aside. The gas tended to finger along the glass fibre mat to the end of the rib where the material had frozen and the tightly packed mat had broken down due to

the compression flow. The gas was then able to push the material aside and create a small cavity towards the direction of the gas pin.

### **12.3. Effect of Processing Parameters on Re-GMT**

The processing parameter with the largest effect on the cavity volume was the gas injection delay time. The cavity volume decreased with increasing delay time, with the largest decrease occurring between 0.5 seconds and 1.5 seconds. This is due to the material beginning to cool as soon as it touches the cold mould tool surface. The longer the material is in contact with the mould tool surface before the gas is injected, the less molten material is available to flow due to the gas pressure. The cavity volume did not significantly change between 1.5 seconds and 2.5 seconds, suggesting the cooling effect had reached a plateau. This finding is consistent with studies on the effects of processing parameters in GAIM [85].

The effect of Figure 12.1 through Figure 12.4 show Re-GMT rib tool mouldings produced with varying peak gas pressures and ramp rates. The cavity length tended to increase as the gas ramp time increased. This is illustrated in Figure 12.1 through Figure 12.4, showing the two mouldings processed with a 5 second ramp rate had significantly longer cavities than the two mouldings processed with a ramp rate of 1 second. The gas appeared to remain contained in the central rib for longer than at lower ramp rates. The effect of the gas pressure and gas ramp time on the cavity volume of the part was not apparent. The large variation in cavity volumes suggested that other processing parameters, such as shot size and blank positioning had a greater effect.

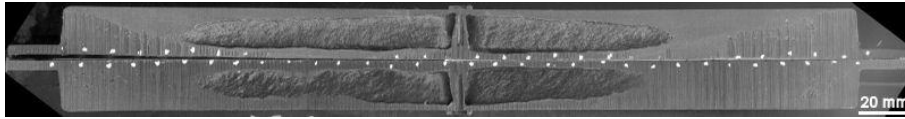


Figure 12.1 - Moulding produced with 60 bar over 1 seconds with a delay time of 1 second

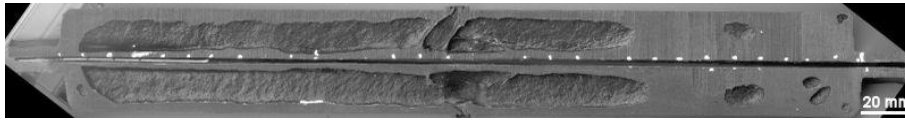


Figure 12.2- Moulding produced with 80 bar over 1 seconds with a delay time of 1 second

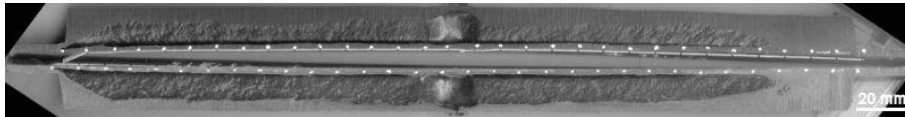


Figure 12.3- Moulding produced with 60 bar over 5 seconds with a delay time of 1 second

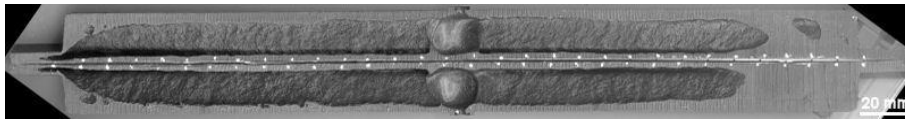


Figure 12.4 - Moulding produced with 80 bar over 5 seconds with a delay time of 1 second

The tool temperature increase carried out in this research showed a marginal decrease in the thickness of the frozen skin layer. This is consistent with studies produced in GAIM, which show that the residual wall thickness, marginally decreases with increasing tool temperature. These studies found however that other parameters, such as the gas injection delay time and gas ramp time had a larger effect on the RWT.

## 12.4. Tool and Pin Design

The mould tools designed and manufactured during the course of this research, proved that the process is versatile and can produce large volume cavities. To achieve the required consolidation, GMT is traditionally moulded using a positive plug mould tool with a vertical shear edge. The novel approach of moulding GMT with a

flash mould tool with a horizontal shear edge as used in this research, proved to be successful. This kind of tool design significantly reduced the mould tool complexity and wear that it would experience; potentially increasing the life of the mould tool. The required clamping force was also reduced as the material consolidation was produced by the internal gas pressure rather than the force of the compression moulding press. The process also showed that existing GMT mould tools, with addition of moulding stops, could be quickly adapted for use with gas injection.

The star tool proved that multiple gas flow paths of 150mm in length with a cross sectional area of 4cm<sup>2</sup> could be achieved, giving a significant weight reduction of up to 45 percent. The large mass of material around the pin designed to reduce freezing, proved successful with the gas coring out the hemisphere of material whilst coring out the ribs. Material freezing around the pin could not however be completely eliminated.

The array of pins designed and used during the course of the research, showed that the gas injection hole is critical in ensuring the correct delivery of gas into the molten material. A gas injection hole, with a depth of 0.25mm proved to provide a sufficient gas flow with minimal polymer ingress. Above this depth, the material was able to ingress into the hole and freeze, blocking the injection of gas. Although the gas pressure generally broke through the blockage, it was not always possible to do so.

## **12.5. Moulding Features**

The presence of packing effects, gas flow preference and gas fingering were observed with the unexpected discovery of entrainment. The gas cavities show the

presence of packing effects, where the gas pressure has caused secondary penetration as the material cooled.

The gas flow mechanisms showed that the gas would choose an initial path of least resistance, before expanding additional flow paths until the gas burst through the material and escaped to atmosphere, or the material had frozen sufficiently enough for it to contain the gas in the moulding. This initial path was influenced by the blank position in relation to the gas pin, with the gas expanding the areas with the least material. If the blank location was central, then the gas simultaneously took multiple flow paths. Figure 12.5 shows a close up of the uniform radial material flow created by the gas coring out the rib.

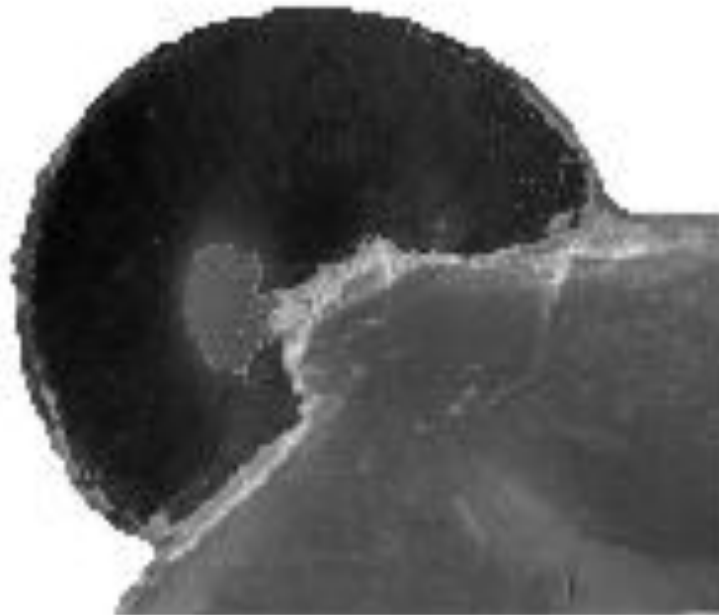


**Figure 12.5 – Biaxial material flow due to gas pressure**

Entrainment could have been caused by the rheological instabilities on the material surface caused by the gas flow. These instabilities cause wave like formations that eventually close over, trapping the gas inside.

# 13. Conclusions

In this research work, a new glass fibre reinforced thermoplastic moulding process was presented, where gas injection was used in conjunction with compression moulding to produce gas injection of glass reinforced thermoplastic components. Injected gas was used to core out a glass reinforced material during a conventional compression moulding cycle. The aims of the process were to create an internal cavity in the moulding, reducing the volume of material required to produce a moulding, significantly reducing the component weight. The GasComp process aimed to give additional benefits of reduced cooling time, increased dimensional stability and reduced wear on GMT mould tools. All of these benefits and aims were realised during the course of the research. The conclusions of the research are presented below;

1. A material with a dispersed fibre architecture and MFR of 1 g/10mins proved to be the most suitable, compared to the LFT and GMT tested in this research.
2. LFT is possible to be processed successfully, and this material can only be processed using GasComp in the creation an internal cavity, which cannot be achieved using GAIM, giving the GasComp process a unique capability.
3. A short gas injection delay time produces a larger cavity volume value.
4. As the gas ramp time increased, the cavity length increased.
5. Novel flash, horizontal clamping edge mould tool design used in the creation of glass fibre reinforced polypropylene parts. The removal of a shear edge, dramatically reduced the wear on the tool.

6. Gas injection hole of 0.25mm proved to be a good compromise of high gas flow and restricted polymer ingress.
7. Up to 45 percent weight reduction was attainable with this process with the star tool design.
8. Dimensional stability was proven to be improved over a solid component, when a high cavity volume was formed, due to a thinner wall thickness.
9. For an ideal component (thin, even wall thickness with a high reduction in weight), it is assumed through thermodynamic laws, that a reduction in thermal mass would decrease cooling time, when compared to a solid part of the same dimensions.

# 14. Recommendations for Further Work

Considering the work carried out the during this project; the following recommendations for further work can be made:

- The mould tools produced in this research were reaching the limit of cavity volume producible with a single injection point, before the material had frozen off. An investigation could be carried out into the use of multiple gas injection points and the ability to produce larger cavity volumes on larger components.
- The physical properties of the parts produced in this research such as strength and stiffness were not characterised. A component moulding trial and subsequent mechanical testing would show how a component is affected by the process.
- An optical and scanning electron microscope investigation into the crystalline structure of the material would show the effect of the cooling rate. By sampling material at specific areas along the gas cavity and along the material flow, this could be used to show the effect of the gas on the cooling rate and further insight into the gas flow mechanics.
- Limited material resources during the course of this project, restricted the ability to establish the point after which the material becomes unsuitable for use with GasComp. Development of materials with a dispersed and low fibre entanglement architecture, but with increased glass content, would show the upper limits of the material that can be used with GasComp. This development would be especially valuable for commercial ventures where the increased strength associated with higher glass content is important.

## 15. References

1. Painter, P.C. and M.M. Coleman, *Essentials of polymer science and engineering* 2008, Lancaster, Pa :: DEStech Publications, Inc.
2. Kalpakjian, S. and S.R. Schmid, *Polymers: Structure, General Properties, and Applications*, in *Manufacturing engineering and technology*, V. O'Brien, Editor. 2001, Prentice Hall: Upper Saddle River, N.J. p. 177-202.
3. Sperling, L.H., *Introduction to Physical Polymer Science*. 4th ed. 2005, New York: Wiley-Interscience. 880.
4. Cartwright, A., *Materials*, in *The University Of Warwick Engineering Data Book*, The University Of Warwick, Editor. 2006, The University Of Warwick: Coventry. p. 27-54.
5. Gardner, P., *Eigenfunction expansions with continuous spectrum, hydrogen atom, and Van der Waals forces*, ed. M. University of Warwick. Dept. of. 2007, Coventry, UK: University of Warwick. Dept. of, Mathematics.
6. Chanda, M. and S.K. Roy, *Plastics technology handbook*, in *Plastics engineering 72*. 2006, Taylor & Francis Group: Boca Raton, FL.
7. Sharples, A., *Introduction to polymer crystallization*. 1966, London: Edward Arnold Ltd.
8. Törnqvist, R., P. Sunderland, and J.-A.E. Månson, *Determination of the rheological properties of thermoplastic composites for compression flow molding*. *Polymer Composites*, 2000. **21**(5): p. 779-788.
9. Davis, B., et al., *Compression Molding*. 2003, Munich: Hanser Publications. 196.
10. Pukanszky, B., *Particulate filled polypropylene: structure and properties*, in *Polypropylene: Structure, Blends and Composites*, J. Karger-Kocsis, Editor. 1995, Chapman & Hall: London. p. 1-70.
11. Rotheron, P.R., *Filler use to grow*. *Plastics, Additives and Compounding*, 2005. **7**(2): p. 13-13.
12. Fujiyama, M. and T. Wakino, *Structures and properties of injection moldings of crystallization nucleator-added polypropylenes. I. Structure-property relationships*. *Journal of Applied Polymer Science*, 1991. **42**(10): p. 2739-47.

13. Samsudin, M.S.F., et al., *Effect of filler treatments on rheological behavior of calcium carbonate and talc-filled polypropylene hybrid composites*. Journal of Applied Polymer Science, 2006. **102**(6): p. 5421-5426.
14. Kalpakjian, S. and S.R. Schmid, *Composite Materials: Structure, General Properties, and Applications*, in *Manufacturing engineering and technology*, V. O'Brien, Editor. 2001, Prentice Hall: Upper Saddle River, N.J. p. 203-220.
15. Gibson, A.G., *Processing and properties of reinforced polypropylenes*, in *Polypropylene: Structure, Blends and Composites*, J. Karger-Kocsis, Editor. 1995, Chapman & Hall: London. p. 71-112.
16. Mlekusch, B., *Thermoelastic properties of short-fibre-reinforced thermoplastics*. Composites Science and Technology, 1999. **59**(6): p. 911-923.
17. Mallick, P.K., *Fiber-reinforced composites : materials, manufacturing, and design* C.R.C. Press, Editor. 2008, CRC Press: Boca Raton, FL.
18. Metzner, A.B., *Rheology of Suspensions in Polymeric Liquids*. Journal of Rheology, 1985. **29**(6): p. 739-775.
19. Ghosh, T., M. Grmela, and P.J. Carreau, *Rheology of short fiber filled thermoplastics*. Polymer Composites, 1995. **16**(2): p. 144-153.
20. Thomason, J.L., *The influence of fibre length and concentration on the properties of glass fibre reinforced polypropylene: 5. Injection moulded long and short fibre PP*. Composites Part A: Applied Science and Manufacturing, 2002. **33**(12): p. 1641-1652.
21. Short, W.T. and E.J. Wenzel. *Effects of residual fiber length on the mechanical properties of long fiber reinforced polypropylene from various processes*. 2007. Cincinnati, OH, United States: Society of Plastics Engineers, Brookfield, CT 06804-0403, United States.
22. Dai, X.Y. and P.J. Bates, *Mechanical properties of short -and long-glass-fibre-reinforced polypropylene compounds*, in *ANTEC 2005 Plastics: Annual Technical Conference*. 2005, Society of Plastics Engineers. p. pp. 1520-1524.
23. Thomason, J.L. and M.A. Vluc, *The influence of fibre length and concentration on the properties of glass fibre-reinforced polypropylene: 4. Impact properties*. Composites - Part A: Applied Science and Manufacturing, 1997. **28**(3): p. 277-288.
24. Thomason, J.L. and W.M. Groenewoud, *The influence of fibre length and concentration on the properties of glass fibre reinforced polypropylene: 2. Thermal properties*. Composites - Part A: Applied Science and Manufacturing, 1996. **27**(7): p. 555-565.

25. Ceresana Research, *Market Study: Polypropylene (UC-805)*. 2008: Konstanz, Germany.
26. Ceresana Research. *Trends in polypropylene production and uses*. 2008 [cited; Available from: <http://www.engineeringtalk.com/news/cev/cev103.html>].
27. Hoffman, J.M. *Smart pioneers first full polypropylene body panels*. 2007 November 21, 2007 [cited 2009 30/01]; Available from: <http://machinedesign.com/article/smart-pioneers-first-full-polypropylene-body-panels-1121>.
28. Thomason, J.L., et al., *The influence of fibre length and concentration on the properties of glass fibre-reinforced polypropylene: Part 3. Strength and strain at failure*. *Composites - Part A: Applied Science and Manufacturing*, 1996. **27**(11): p. 1075-1084.
29. Berglund, L.A. and M.L. Ericson, *Glass mat reinforced polypropylene*, in *Polypropylene: Structure, Blends and Composites*, J. Karger-Kocsis, Editor. 1995, Chapman & Hall: London. p. 204-205.
30. Hartness, T., et al., *The characterization of low cost fiber reinforced thermoplastic composites produced by the DRIFT(TM) process*. *Composites Part A: Applied Science and Manufacturing*, 2001. **32**(8): p. 1155-1160.
31. MEPS LTD. *MEPS - World carbon steel prices - with individual product forecasts (\$US/tonne)*. 2008 01/11/08 [cited 2008 12/2008]; Available from: [http://www.meps.co.uk/World\\_Carbon\\_Price.htm](http://www.meps.co.uk/World_Carbon_Price.htm).
32. Limited, T.L.M.E. *Primary Aluminium 2008* [cited 2008 12/2008]; Available from: <http://www.lme.co.uk/aluminium.asp>.
33. Do, M.-L. *Improved aerodynamics and weight-saving for BMW M3 with SymaLITE® underbody shields from Quadrant Plastics Composites*. 2008 [cited 2009 15/01/2009]; Available from: <http://www.quadrantcomposites.com/pdf/qpcpr006e0208%20bmw%203%20series%20underbody%20shielding.pdf>.
34. Malnati, P., *Reinforced Thermoplastics: LFRT/GMT Roundup*. *Composite Technologies*, 2007. **2007**(October).
35. Schemme, M., *LFT - development status and perspectives*. *Reinforced Plastics*, 2008. **52**(1): p. 32-34, 36-39.
36. Bigg, D.M., *Manufacturing methods for long fibre reinforced polypropylene sheets and laminates*, in *Polypropylene: Structure, Blends and Composites*, J. Karger-Kocsis, Editor. 1995, Chapman & Hall: London. p. 263-292.

37. Karsten, F., et al., *Plastics moulding containing reinforced fillings*, in *United States Patent and Trademark Office*, U.S.P.a.T. Office, Editor. 1989, BAYER AG: Leverkusen, Germany.
38. Karsten, F., et al., *Process and apparatus for manufacturing a component moulded from reinforced plastic*, in *European Patent Application*, E.P. Application, Editor. 1989, BAYER AG: Leverkusen, Germany.
39. Truckenmüller, F. and H.G. Fritz, *Injection molding of long fiber-reinforced thermoplastics: A comparison of extruded and pultruded materials with direct addition of roving strands*. *Polymer Engineering & Science*, 1991. **31**(18): p. 1316-1329.
40. Brandrup, J., *Preparation of Feedstock for Petrochemical Recycling - Requirements Imposed on Plastic Waste*, in *Recycling and recovery of plastics* J. Brandrup, Editor. 1996, Hanser: Cincinnati, OH :. p. 393-411.
41. Kaminsky, W. and H. Sinn, *Pyrolytic Processes for Recycling Plastics*, in *Recycling and recovery of plastics* J. Brandrup, Editor. 1996, Hanser: Cincinnati, OH. p. 434-443.
42. Dirks, E., *Energy Recovery from Plastic Wastes in Waste Incineration Plants*. *Recycling and recovery of plastics*, ed. J. Brandrup. 1996, Cincinnati, OH: Hanser.
43. Jones, F.R., *Handbook of polymer-fibre composites*. Polymer science and technology series. 1994, Harlow: Longman Scientific & Technical. xiv,418p.
44. Online, W. *Plastics Recycling*. 2006 02/06 [cited 2009 March]; Available from: [http://www.wasteonline.org.uk/resources/InformationSheets/Plastics.htm#\\_Hows](http://www.wasteonline.org.uk/resources/InformationSheets/Plastics.htm#_Hows).
45. Muccio, E.A., *Plastics processing technology / Edward A. Muccio*. 1994, Materials Park, OH :: ASM International.
46. Brandrup, J., et al., *Recycling and recovery of plastics* ed. J. Brandrup. 1996, Cincinnati, OH :: Hanser.
47. Piñero-Hernanz, R., et al., *Chemical recycling of carbon fibre composites using alcohols under subcritical and supercritical conditions*. *The Journal of Supercritical Fluids*, 2008. **46**(1): p. 83-92.
48. European Parliament, C., *Directive 2000/53/EC of the European Parliament and of the Council of 18 September 2000 on end-of life vehicles*. 2000, The European Parliament and the Council of the European Union. p. 9.
49. Ward, I.M. and P.J. Hine, *Novel composites by hot compaction of fibers*. *Polymer Engineering & Science*, 1997. **37**(11): p. 1809-1814.

50. Lafone, E., *Big Advances in self-reinforced polypropylene for manufacturing*, E. Lafone, Editor. 2005, Foresight Vehicle: Birmingham.
51. Vehicle, F., *Big Advances in Self-Reinforced Polypropylene for Manufacture*, E. Lafone and D. Wallace, Editors. 2005, Foresight Vehicle: Alcester, Warwickshire. p. 4.
52. Mike and P. Brady, *Composites on the move*. Reinforced Plastics, 2008. **52**(10): p. 41-44.
53. Kalpakjian, S. and S.R. Schmid, *Forming and Shaping Plastics and Composite Materials*, in *Manufacturing engineering and technology*, V. O'Brien, Editor. 2001, Prentice Hall: Upper Saddle River, N.J. p. 480-511.
54. Wakeman, M.D., et al., *Compression moulding of glass and polypropylene composites for optimised macro- and micro-mechanical properties II. Glass-mat-reinforced thermoplastics*. Composites Science and Technology, 1999. **59**(5): p. 709-726.
55. Stevenson, J.F., *Innovation in polymer processing : molding*. 1996, Munich: Hanser. 504.
56. Painter, P.C. and M.M. Coleman, *Processing*, in *Essentials of polymer science and engineering*. 2008, DEStech Publications, Inc.: Lancaster, Pa :. p. 473-514.
57. Liang, J.Z. and J.N. Ness, *The calculation of cooling time in injection moulding*. Journal of Materials Processing Technology, 1996. **57**(1-2): p. 62-64.
58. Závadský, E., J. Karniš, and V. Pechoč, *The time, temperature and shear dependence of the viscosity of polypropylene and its influence upon the extrusion process*. Rheologica Acta, 1982. **21**(4): p. 470-474.
59. Staff, P.E., *Rapid Temperature Cycling*, in *Plastic Engineering*. 2007, SPE. p. 12.
60. Cox, H.W. and C.C. Mentzer, *Injection molding: The effect of fill time on properties*. Polymer Engineering & Science, 1986. **26**(7): p. 488-498.
61. Crowson, R.J., A.J. Scott, and D.W. Saunders, *Rheology of short glass fiber-reinforced thermoplastics and its application to injection molding. III. Use of a high shear rate capillary rheometer in the injection molding shear rate range*. Polymer Engineering & Science, 1981. **21**(12): p. 748-754.
62. Mavridis, H., A.N. Hrymak, and J. Vlachopoulos, *Finite element simulation of fountain flow in injection molding*. Polymer Engineering & Science, 1986. **26**(7): p. 449-454.

63. Acheson, D.J., *Elementary fluid dynamics*. Oxford applied mathematics and computing science series. 1990, Oxford: Clarendon. ix,397p.
64. Townsend, A.A.R., *The Structure of Turbulent Shear Flow*. 2nd ed. 1980, Cambridge: Cambridge University Press.
65. *Hesitation*. C-MOLD Documentation Library 2006 20/12/2006 [cited 2009; Available from: <http://www.scudc.scu.edu/cmdoc/sysadm/sysadmtoc.fm.html>].
66. Vaxman, A., et al., *Short fiber reinforced thermoplastics. II. Interrelation between fiber orientation and rheological properties of glass fiber-reinforced Noryl*. Polymer Composites, 1989. **10**(2): p. 84-91.
67. Kamal, M.R., A.T. Mutel, and L.A. Utracki, *Elongational behavior of short glass fiber reinforced polypropylene melts*. Polymer Composites, 1984. **5**(4): p. 289-298.
68. Miles, J.N., N.K. Murty, and G.F. Modlen, *The viscosity of fiber suspensions at low fiber volume fractions*. Polymer Engineering & Science, 1981. **21**(17): p. 1171-1172.
69. Young, R.T., M.A. McLeod, and D.G. Baird, *Extensional processing behavior of thermoplastics reinforced with a melt processable glass*. Polymer Composites, 2000. **21**(6): p. 900-917.
70. Vaxman, A., et al., *Short fiber reinforced thermoplastics. I. Rheological properties of glass fiber reinforced Noryl*. Polymer Composites, 1989. **10**(2): p. 78-83.
71. Vaxman, A., et al., *Short-fiber-reinforced thermoplastics. Part III: Effect of fiber length on rheological properties and fiber orientation*. Polymer Composites, 1989. **10**(6): p. 454-462.
72. Thomasset, J., et al., *Rheological properties of long glass fiber filled polypropylene*. Journal of Non-Newtonian Fluid Mechanics, 2005. **125**(1): p. 25-34.
73. Crowson, R.J. and M.J. Folkes, *Rheology of short glass fiber-reinforced thermoplastics and its application to injection molding. II. The effect of material parameters*. Polymer Engineering & Science, 1980. **20**(14): p. 934-940.
74. Crowson, R.J., M.J. Folkes, and P.F. Bright, *Rheology of short glass fiber-reinforced thermoplastics and its application to injection molding I. Fiber motion and viscosity measurement*. Polymer Engineering & Science, 1980. **20**(14): p. 925-933.

75. Folgar, F. and C.L. Tucker, III, *Orientation Behavior of Fibers in Concentrated Suspensions*. Journal of Reinforced Plastics and Composites, 1984. **3**(2): p. 98-119.
76. Franzén, B., et al., *Fibre degradation during processing of short fibre reinforced thermoplastics*. Composites, 1989. **20**(1): p. 65-76.
77. Vu-Khanh, T., et al., *The effects of injection molding on the mechanical behavior of long-fiber reinforced PBT/PET blends*. Composites Science and Technology, 1991. **40**(4): p. 423-435.
78. Schwendemann, D., *New developments in co-rotating twin-screw extrusion for production of long glass fiber composites*, in *SPE ANTEC Conference 2002*. 2002, Society of Plastic Engineers: San Francisco, CA, USA.
79. Utracki, L.A. and A. Luciani, *Rheology of polypropylene*, in *Polypropylene : an A-Z reference*, J. Karger-Kocsis, Editor. 1999, Kluwer: Dordrecht ; London :. p. 715-720.
80. ERNST, F., *Method for injection molding of hollow shaped bodies from thermoplastic resins*, in *European Patent Office*, E.P. Office, Editor. 1978, ROEHM GMBH.
81. Shin, J.-W. and A.I. Isayev, *Experimental study of gas penetration in gas-assisted injection molding*. Journal of Injection Molding Technology, 2002. **6**(4): p. 314-330.
82. Lu, X., et al., *Study of 'gas fingering' behavior in gas-assisted injection molding*. Polymer Engineering and Science, 1999. **39**(1): p. 62-77.
83. Goodship, V., *Interfacial instabilities : implications for multi-material moulding*, ed. E. University of Warwick. Dept. of. 2001, Coventry, UK: University of Warwick. Dept. of, Engineering.
84. He, Q., et al., *Free Surface Instability and Gas Entrainment during Blast Furnace Drainage*. Developments in Chemical Engineering and Mineral Processing, 2006. **14**(1-2): p. 249-258.
85. Parvez, M.A., et al., *Gas-assisted injection molding: The effects of process variables and gas channel geometry*. Journal of Materials Processing Technology, 2002. **121**(1): p. 27-35.
86. Yang, S.Y. and S.J. Liou, *Development of moldability diagrams for gas-assisted injection molding*. Advances in Polymer Technology, 1995. **14**(3): p. 197-205.

87. Zhou, H. and D. Li, *Filling simulation and gas penetration modeling for gas-assisted injection molding*. Applied Mathematical Modelling, 2003. **27**(11): p. 849-860.
88. Zhao, J., et al., *Statistical Experiment Study of Gas-Assisted Injection Molding Process*, in *ANTEC 1998 Plastics: Plastics on My Mind*,. 1998, Society of Plastic Engineers Inc: Atlanta, Georgia, USA. p. 454-459
89. Fu, S.-Y., et al., *Correction of the measurement of fiber length of short fiber reinforced thermoplastics*. Composites Part A: Applied Science and Manufacturing, 2002. **33**(11): p. 1549-1555.
90. Becker, O., K. Koelling, and T. Altan, *Gas-Assisted Injection Molding of Glass Fiber Reinforced Thermoplastics*, in *Journal of Injection Moulding Technology*. 1997, Engineering Research Center for Net Shape Manufacturing, The Ohio State University: Columbus, Ohio 43210-1271.
91. Thomas, R., *Process for gas assisted and water assisted injection molding*. 2003, Alliance Gas Systems, Inc.: US. p. 3.
92. Magalhães, R., *Cryogenic gas-assisted injection moulding*, in *School Of Engineering*. 2002, University Of Warwick: Coventry, UK. p. 431 p.
93. Knights, M. (2002) *Feature Article: Water Injection Molding Makes Hollow Parts Faster, Lighter*. **Volume**,
94. Giles, H.F.J., *Compression Molding Tooling for Thermoplastic Composites*, in *ANTEC 2001*. 2001, Society of Plastic Engineers: Dallas, TX, USA.
95. Davis, S.M. and K.P. McAlea, *Stamping rheology of glass mat reinforced thermoplastic composites*. Polymer Composites, 1990. **11**(6): p. 368-378.
96. Kotsikos, G., et al., *Squeeze flow testing of glass mat thermoplastic material*. Composites Part A: Applied Science and Manufacturing, 1996. **27**(12): p. 1195-1200.
97. Leterrier, Y. and C. G'Sell, *Multilayer plug flow modeling of the fast stamping process for a polypropylene/glass fiber composite*. Polymer Composites, 1996. **17**(2): p. 231-241.
98. Nilsson, G., M.L. Ericson, and J.A. Holmberg, *Flow induced fiber orientation in compression molded glass mat thermoplastics*. Polymer Composites, 2000. **21**(6): p. 1007-1013.
99. Bushko, W.C. and V.K. Stokes, *Random glass mat reinforced thermoplastic composites. Part V: Statistical characterization of the tensile modulus*. Polymer Composites, 1992. **13**(4): p. 295-308.

100. Nuel, L. and M.M. Denn, *Effect of processing and particulate fillers on the rheology of a nematic polymer melt*. Rheologica Acta, 1991. **30**(1): p. 65-70.
101. Systèmes, D. *Solidworks : 3D CAD Design Software*. 2009 [cited 2009 27/07/2009]; Available from: <http://www.solidworks.com/>.
102. Diest, K. and M. Maier. *Experimental evaluation and numerical simulation of fibre orientation during compression moulding of GMT*. in *Proceedings tenth international conference on composite materials*. 1995. Canada: Woodhead Publishing LTD.